Institute of Geophysics
Polish Academy of Sciences

PUBLICATIONS
OF THE INSTITUTE OF GEOPHYSICS
POLISH ACADEMY OF SCIENCES

Geophysical Data Bases, Processing and Instrumentation

453 (E-14)

BOOK OF ABSTRACTS

XLII International School of Hydraulics
FRESHWATER SYSTEM HEALTH:
A HYDRAULIC PERSPECTIVE

Radocza, Poland, 20–23 May 2025

Editors:
Monika Kalinowska, Magdalena Mrokowska, and Paweł M. Rowiński

Warsaw 2025 (Issue 2)

INSTITUTE OF GEOPHYSICS
POLISH ACADEMY OF SCIENCES

PUBLICATIONS
OF THE INSTITUTE OF GEOPHYSICS
POLISH ACADEMY OF SCIENCES

Geophysical Data Bases, Processing and Instrumentation

453 (E-14)

BOOK OF ABSTRACTS

XLII International School of Hydraulics
FRESHWATER SYSTEM HEALTH:
A HYDRAULIC PERSPECTIVE

Radocza, Poland, 20–23 May 2025

Editors:
Monika Kalinowska, Magdalena Mrokowska, and Paweł M. Rowiński

Warsaw 2025

Published by the Institute of Geophysics, Polish Academy of Sciences

ISBN 978-83-66254-25-1 ISSN-2544-428x eISSN-2299-8020
DOI: 10.25171/InstGeoph_PAS_Publs-2025-022

Photo on the front cover by Anna Łoboda

Editorial Office
Instytut Geofizyki Polskiej Akademii Nauk
ul. Księcia Janusza 64, 01-452 Warszawa

C O N T E N T S

Publications of the Institute of Geophysics, Polish Academy of Sciences
Geophysical Data Bases, Processing and Instrumentation
vol. 453 (E-14), 2025, pp. 3–3
DOI: 10.25171/InstGeoph_PAS_Publs-2025-023
XLII International School of Hydraulics, Radocza, Poland, 20–23 May 2025

Preface

The 42nd International School of Hydraulics, titled "Freshwater System Health: A Hydraulic Perspective", held on May 20–23, 2025, in Radocza near Kraków, continued a series of events focused on broadly understood hydraulics. The conference covered the fundamentals of hydraulics in the context of understanding and managing the health of rivers, lakes, and other aquatic ecosystems. It highlighted new and challenging topics in both applied and basic research. ISH2025 aimed to foster a fruitful exchange of knowledge, ideas, and experiences in various fields of hydro-environment research. It also served as a platform for intellectual growth, collaboration, and innovation, helping to build new connections and strengthen existing ones. ISH2025 sought not only to provide answers and explore new ideas, but also to offer a global forum for scholars, decision-makers, and enterprises sharing a common interest in the field.

It is a great privilege for us to present the proceedings of ISH2025 to the authors and delegates of the event. The proceedings contain abstracts and extended abstracts of all presentations delivered during the meeting. Please note that selected full papers will be published in a separate volume. We hope you find this collection useful and inspiring.

In summary, ISH2025 included four keynote lectures, two invited lectures, and around 40 presentations, attracting a diverse range of contributors and presenters from nine countries across three continents. This diversity is a testament to the international reach of our School, fostering interdisciplinary collaboration, intellectual growth, and exchange. This School is a joint initiative of the Institute of Geophysics, Polish Academy of Sciences, and the newly established Committee of Water Science and Water Management of the Polish Academy of Sciences. It is organized under the auspices of the International Association for Hydro-Environment Engineering and Research (IAHR), in partnership with State Water Holding Polish Waters.

We would like to express our gratitude to all authors and participants, the members of the scientific committee, and especially the organizing team for making this School possible. We also extend our appreciation to all reviewers who helped us maintain the high quality of the manuscripts included in the proceedings. We look forward to continuing our collaboration in the future.

Monika B. Kalinowska
Paweł M. Rowiński
School Chairs

Publications of the Institute of Geophysics, Polish Academy of Sciences
Geophysical Data Bases, Processing and Instrumentation
vol. 453 (E-14), 2025, pp. 5–5
DOI: 10.25171/InstGeoph_PAS_Publs-2025-024
XLII International School of Hydraulics, Radocza, Poland, 20–23 May 2025

Are We Getting Dry? A Satellite-based Analysis of Water Conditions in the Vistula River

Michael NONES

Institute of Geophysics, Polish Academy of Sciences, Warsaw, Poland

✉ mnones@igf.edu.pl

The present study takes advantage of Google Earth Engine and the JRC Yearly Water Classification History dataset to depict temporal changes in permanent water conditions (i.e., river channel always covered by water) along the reach of the Vistula River from Dęblin to Włocławek. The JRC dataset contains maps of the location and temporal distribution of surface water from 1984 to 2021, as well as statistics on the extent and change of those water surfaces. Results show that, along the investigated reach, a decrease in permanent water conditions is visible starting from the late 1990s, which is somehow not fully correlated to the slight decrease in flow discharge observed at the Dęblin gauging station. Indeed, the observed significant decrease of the surface occupied by permanent water is likely due also to other natural and anthropogenic divers, such as global warming and increased population density. Despite being only a preliminary analysis of permanent water conditions in a selected reach of the Vistula River, the present analysis shows the potential of remote sensing for depicting changes in the availability of flowing water across multiple spatiotemporal scales.

Publications of the Institute of Geophysics, Polish Academy of Sciences
Geophysical Data Bases, Processing and Instrumentation
vol. 453 (E-14), 2025, pp. 7–10
DOI: 10.25171/InstGeoph_PAS_Publs-2025-025
XLII International School of Hydraulics, Radocza, Poland, 20–23 May 2025

Wind Surge Modeling in the Vistula Lagoon using HEC-RAS 2D – Today's and Tomorrow's Perspective

Michał SZYDŁOWSKI

Gdańsk University of Technology, Faculty of Civil and Environmental Engineering, Gdańsk, Poland

✉ mszyd@pg.edu.pl

A b s t r a c t

This conference paper describes numerical simulations of water flow in the Vistula Lagoon using the HEC-RAS 2D (version 6.6) hydrodynamic model. The model was validated by comparing its results with previous simulations and field measurements conducted by the Polish Institute of Meteorology and Water Management (IMGW-PIB). Preliminary findings on the impact of climate change are also discussed, highlighting how an increase in wind speed over the lagoon may elevate water levels in the Żuławy Elbląskie region and subsequently heighten flood hazard from the Vistula Lagoon waters.

1. STUDY AREA

The Vistula Lagoon, part of the Gulf of Gdańsk in the Baltic Sea (Fig. 1), is a shallow water basin stretching 90.7 km in length and averaging 8.9 km in width. It has an average depth of 2.75 m and is separated from the Gulf by the 65 km long Vistula Spit. Its only natural connection to the sea is through the Strait of Baltiysk, located in the Russian section of the lagoon. In 2022, a navigable canal with a lock was built in the Polish section, providing an additional link to the Gulf (Cieśliński et al. 2024). Water circulation in the lagoon is influenced by wind and fluctuations in the Gulf of Gdańsk sea level. Prolonged north or northeast winds can cause water to accumulate in the Polish part of the lagoon, raising levels by over 1.0 m above sea level (m asl) and threatening the low-lying Żuławy Elbląskie region (Szydłowski et al. 2019).

2. HEC-RAS 2D HYDRODYNAMIC MODELING

The primary objective of this study was to assess the feasibility of using the HEC-RAS 2D (version 6.6) model (Brunner 2021) to simulate wind surges in the lagoon. To achieve this, the flow area was represented using a rectangular numerical grid with a mesh size of 100 × 100 m. In the computational options of the HEC-RAS program, the dynamic wave model, described in the manual as Shallow Water Equations with a Eulerian-Lagrangian approach to solving for

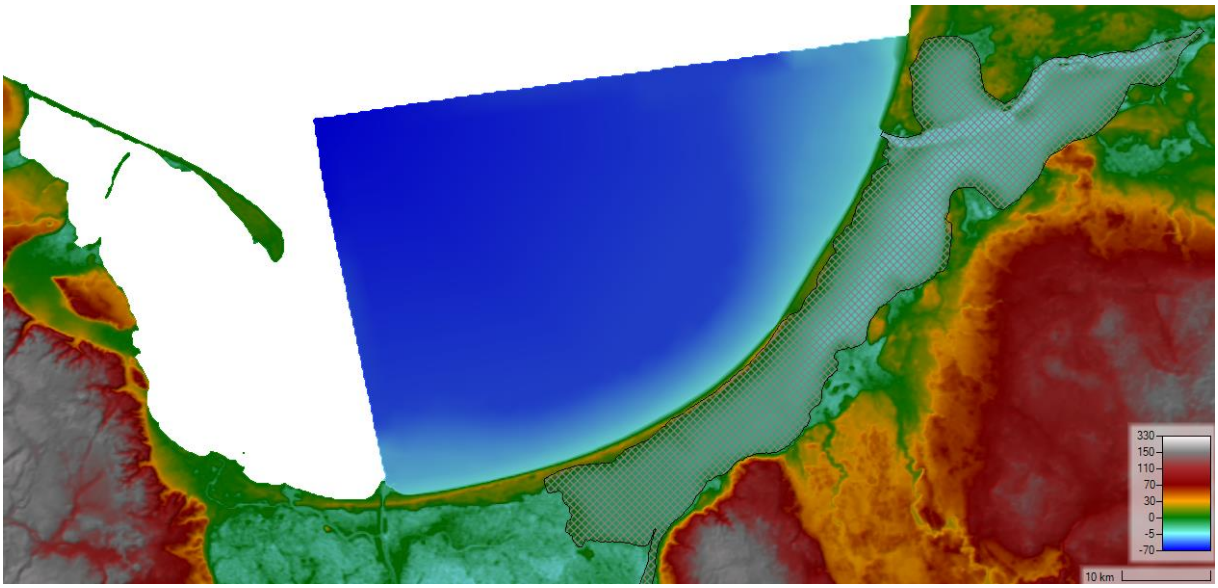

Fig. 1. Gulf of Gdańsk and Vistula Lagoon DEM (color scale) and HEC-RAS 2D numerical mesh.

advection (SWE-ELM), was selected as the mathematical model of the lagoon's hydrodynamics. The wind shear stress was modelled using Hsu (1988) concept, lagoon's bottom friction was given as a constant value of Manning's roughness coefficient 0.025 $m^{-1/3}$ s and turbulent viscosity was neglected.

Model validation was performed by replicating the simulation described by Szydłowski et al. (2019), which analyzed the historical flood event in the southwestern part of the lagoon in January 2019. The boundary conditions for this simulation included data on sea-level variations in the Gulf of Gdańsk and wind parameters recorded at IMGW-PIB stations from January 1 to 6, 2019.

The comparison between observed water stage data (IMGW-PIB) and the computational results obtained using the original model and HEC-RAS (Fig. 2) confirmed that the latter provides reliable simulations of wind surges in the Vistula Lagoon. Statistical measures describing the calculation errors relative to the observations were consistent. For the original model and HEC-RAS, respectively, the results were as follows: bias of –0.099 and –0.105 m, mean absolute error of 0.113 and 0.109 m, root mean square error of 0.128 and 0.124 m, standard deviation of 0.129 and 0.125 m, and a correlation coefficient of 0.986 and 0.934. Moreover, the Nash-Sutcliffe Efficiency (NSE) values, exceeding 0.93 for both models, confirm their high reliability,

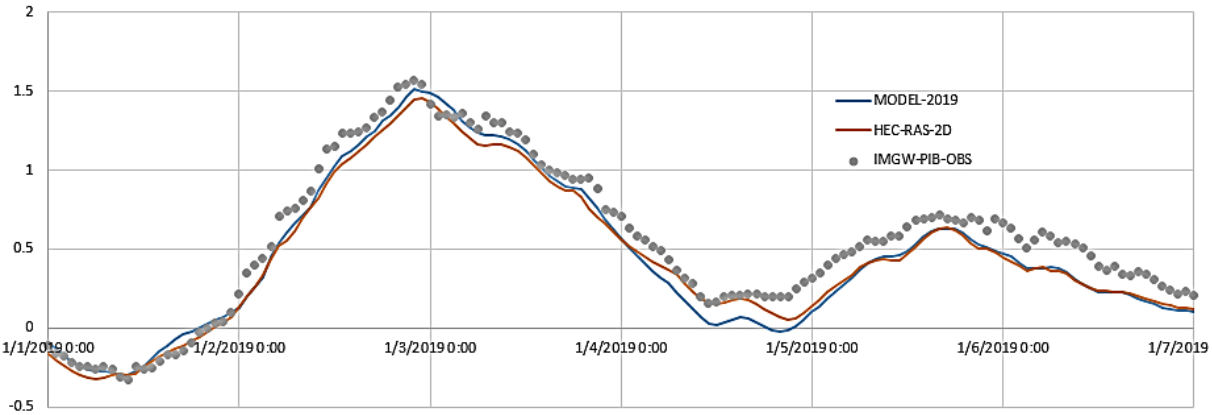

Fig. 2. Observed and calculated water level (m asl) at Polish end of the Vistula Lagoon (Nowakowo).

as NSE values above 0.9 denote an excellent fit between modelled and observed data. However, a slight systematic underestimation of water levels is observed in both models, as reflected in the bias values, which are negative and of similar magnitude. This suggests that while the models capture the overall trend effectively, they tend to predict water surface elevations marginally lower than the actual measurements.

3. CLIMATE CHANGE IMPACT ON FLOOD HAZARD IN ŻUŁAWY ELBLĄSKIE

According to IPCC reports, "The rise in mean sea level will increase the frequency of extreme sea level events in most locations around the globe". Although the Baltic Sea is unique in having very small, almost imperceptible tides, and the Danish Straits limit the ocean's influence, the strong impact of wind surges on flood risk in the low-lying areas of Żuławy makes it reasonable to consider the wind factor in the context of climate change.

Simulations of surges were conducted for extreme wind speeds from the NE direction, assuming an initial zero sea level and constant wind speed. The calculated water stage elevations at the southwestern end of the Vistula Lagoon are presented in Table 1.

Table 1
Water accumulation in the Polish part
of the Vistula Lagoon depending on the wind speed

Speed of NE wind (ms^{-1})	12	20	25	30	35
Water stage elevation (m asl)	0.55	1.40	2.19	3.12	3.69

Considering that water levels in this region reached approximately 1.0 m asl in 1986, 1.6 m asl in 2019, and nearly 2.0 m asl during the absolute maximum in 2009, it is evident that flood risk in Żuławy Elbląskie will increase with ongoing climate change. This underscores the urgent need for intensive adaptation measures to address the forecasted changes.

4. CONCLUSIONS AND LIMITATIONS

- The HEC-RAS 2D model effectively simulates wind surges in the Vistula Lagoon, with validation results confirming high reliability, though with a slight systematic underestimation of water levels.
- Climate change-induced increases in wind speed will likely exacerbate flood hazard in the Żuławy Elbląskie region, highlighting the need for proactive adaptation measures.
- The study provides a basis for further research on flood risk management and mitigation strategies, emphasizing the importance of considering wind-driven surges in future planning.
- The sensitivity of the HEC-RAS model to the formulation of wind shear stress, bed friction and turbulent viscosity was not tested, which may influence local flow dynamics and impact the accuracy of surge simulations.
- The study assumes constant and uniform in space wind speeds in simulations, which may not fully reflect the variability and complexity of real-world meteorological conditions.
- The boundary conditions did not incorporate projected long-term sea level rise due to climate change, which could exacerbate future flood hazards.

References

Brunner, G.W. (2021), HEC-RAS River Analysis System, 2D Hydraulic reference manual, Version 6.0, US Army Corps of Engineers—Hydrologic Engineering Center.

Cieśliński, R., I. Chlost, and M. Szydłowski (2024), Impact of new, navigable canal through the Vistula Spit on the hydrologic balance of the Vistula Lagoon (Baltic Sea), *J. Marine Syst.* **241**, 103908, DOI: 10.1016/j.jmarsys.2023.103908.

Hsu, S.A. (1988), *Coastal Meteorology*, Academic Press Inc., New York.

Szydłowski, M., T. Kolerski, and P. Zima (2019), Impact of the artificial strait in the Vistula Spit on the hydrodynamics of the Vistula Lagoon (Baltic Sea), *Water* **11**, 5, 990, DOI: 10.3390/w11050990.

Publications of the Institute of Geophysics, Polish Academy of Sciences
Geophysical Data Bases, Processing and Instrumentation
vol. 453 (E-14), 2025, pp. 11–14
DOI: 10.25171/InstGeoph_PAS_Publs-2025-026
XLII International School of Hydraulics, Radocza, Poland, 20–23 May 2025

Impact of Land Topography on Runoff and Soil Erosion: An Experimental Approach

Xuhua HUANG[1], Yiwei GUO[2], and Michael NONES[3]

[1]Jiangxi Academy Science and Engineering, Nanchang, China
✉ 13755674959@163.com

[2]Institute of Geophysics, Polish Academy of Sciences, Warsaw, Poland
✉ yguo@igf.edu.pl

[3]Institute of Geophysics, Polish Academy of Sciences, Warsaw, Poland
✉ mnones@igf.edu.pl

Abstract

Soil erosion is causing major concerns across the world, as the loss of soil jeopardises not only environmental sustainability, but also land productivity, eventually leading to reduced resources for populations that heavily rely on land. However, how runoff drives soil erosion and the impact of different land coverages on this is not yet well understood, also because of the lack of data acquired in controlled conditions. To fill this gap, experiments were performed in the Yan Gou runoff observation site (China) by controlling runoff volume, sediment transport, soil loss, and soil water content in five square plots, each with an area of 100 m^2, covered by different vegetation and having different topography. The results presented here focus only on plots covered by citrus but have different slopes, to decouple the effects of vegetation coverage and soil topography. Assuming a constant hydrological forcing (i.e., fixed precipitation), it was observed that plots with down-slop ridge drive a larger runoff, as expected, which implies that more sediments are mobilized causing higher soil loss. At the same time, this loss of soil influences the content of water differently, which changes more significantly in the horizontal plot than in the inclined one. Comparing all plots, it was noticed that standard terraces are the most effective method to conserve soil, reducing the runoff and keeping the content of water more constant over time.

Keywords: Yangou watershed, cross-slope tillage, down-slope tillage, typical terrace.

1. METHODS

1.1 Study area and experimental environment

Located in the south of De'an County (Fig. 1B and C), the Yangon Small watershed (YGSW) has a total area of 27.1 km^2 and an elevation of 45–75 m. The YGSW belongs to the red soil hilly region of South China, and the total area subjected to soil erosion is 9.8 km^2.

A total of 16 runoff observation runoff plots have been constructed within the YGSW (Fig. 1D), and the observations from 5 of them are used in this study. To investigate the impact of different vegetation coverage on soil erosion, the five plots are covered with trifolium repens + citrus tree, cross-slope tillage + citrus tree, down-slope tillage + citrus tree, and typical terrace + citrus tree (hereinafter referred to as trifolium repens, cross-slope tillage, down-slope tillage, and typical terrace), and bare land used as reference conditions.

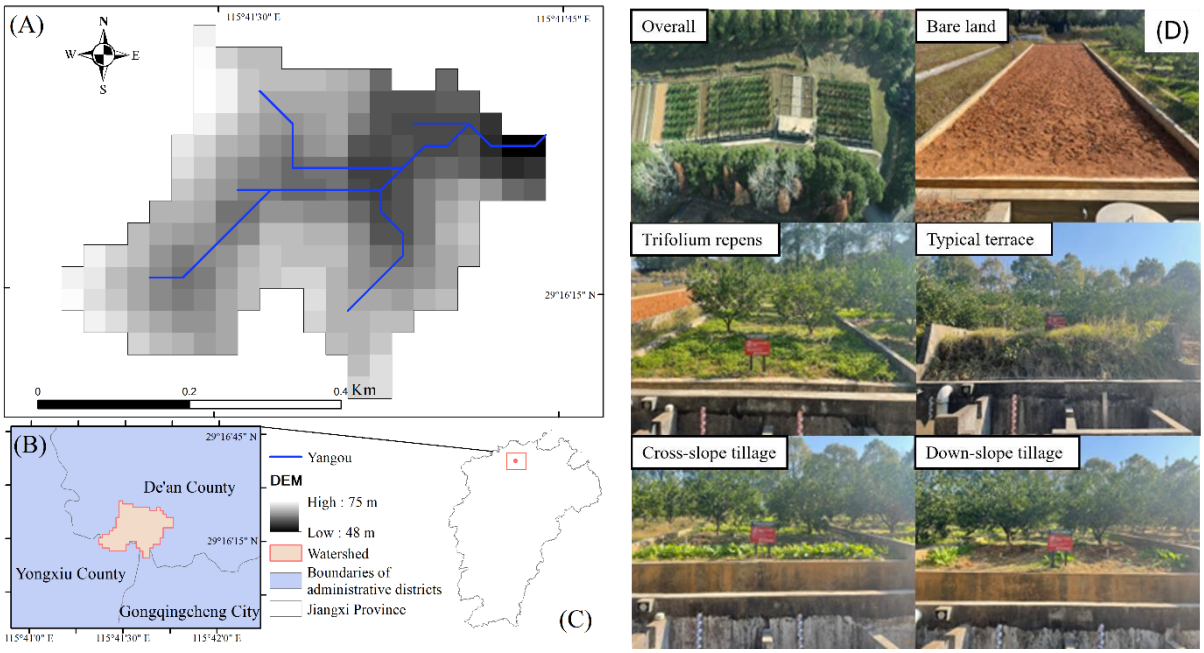

Fig. 1. Location of the study area (YGSW) and the experimental environment. Note that (A) is the DEM of the YGSW, (B) and (C) are its location in the Jiangxi Province, and (D) is the picture of the whole experimental field and each runoff plot.

2.2 Date collection and processing

144 rainfall events have been recorded from 2018.12.31 to 2022.07.20, and 12 rainstorm events, whose precipitation exceeded 50 mm in 24 hours, are analyzed in this study (Table 1).

Table 1

Analysed rainfall events

Rainfall events no.		1	2	3	4	5	6	7	8	9	10	11	12
Data	Year	2019				2020				2021			2021
	Month and day	3.1	3.20	7.4	7.12	5.29	6.2	7.7	7.29	5.10	5.15	7.17	4.12

2. RESULTS AND CONCLUSIONS

The precipitation of 12 selected rainstorms and the generated runoff and sediment after every rainfall event of runoff plots with different vegetation cover are illustrated in Fig. 2A. Figure 2B shows the reduction rate of runoff and sediment of every plot with different coverages.

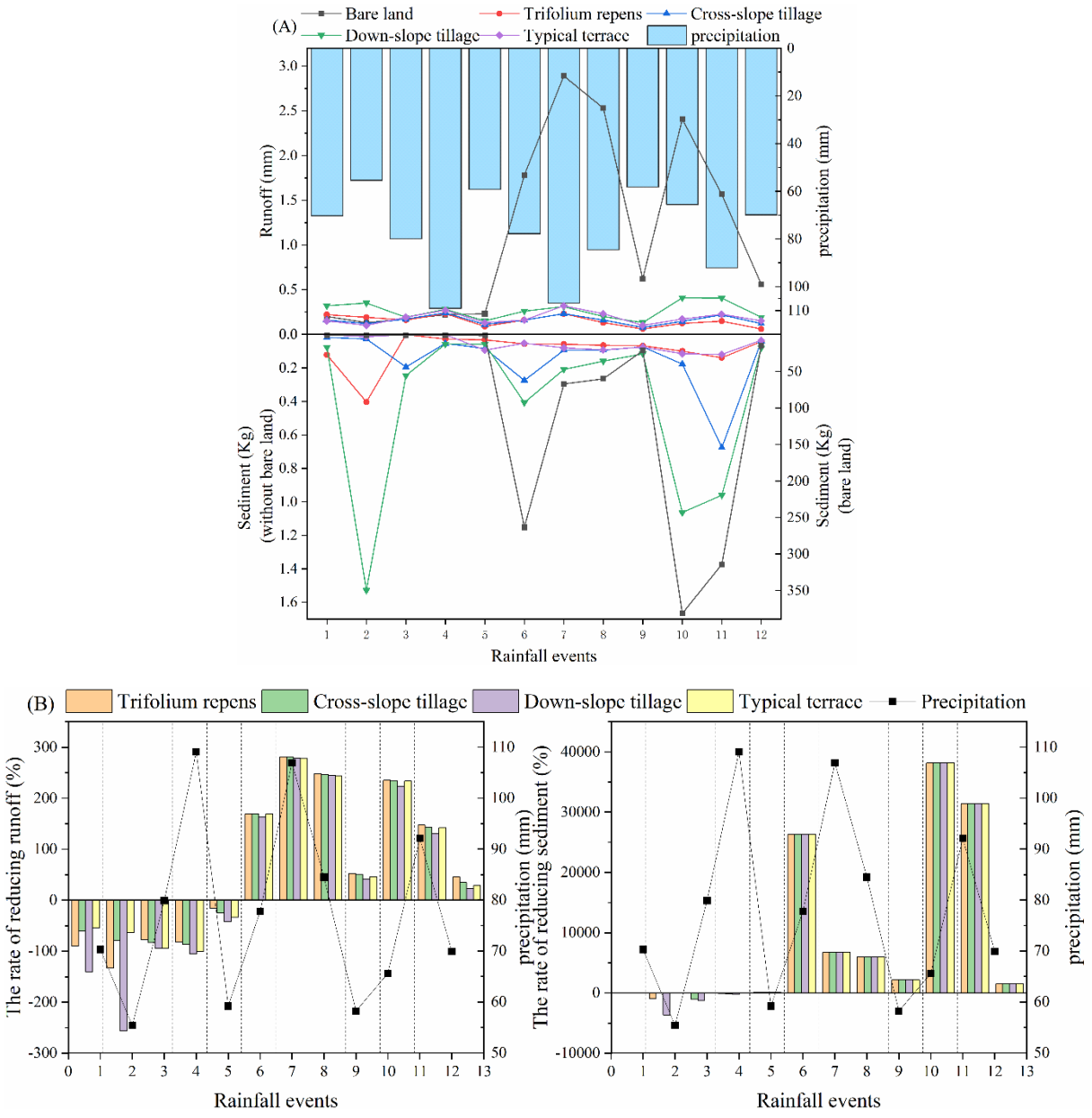

Fig. 2: (A) Rainfall event, runoff yield, and sediment produced after each rainfall event; (B) Reduction rate of flow generation and sediment production of different vegetation cover under different rainfall events.

The results are shown as follows:

1. The produced runoff and sediment of the bare land is the highest, especially the sediment generation, with the lowest value of 50 kg, indicating that the vegetation inhibits sediment and runoff production.

2. The plot for down-slope tillage produced more runoff than plots used for other practices. For the sediment generation, that of the plots for down-slope tillage is the highest and that of plot for cross-slope tillage ranks second.

3. The reduction rates of runoff and sediment of all plots after the rainfall events of 2019 are negative, meaning that all practices did not reduce flow and sediment. After 2019, the trifolium repens performed better in terms of reducing runoff, while down-slope tillage did not perform properly. On the other part, the performance of the four vegetation cover methods in reducing sediment production was rather similar.

Acknowledgements. This research was funded by NCN National Science Centre Poland – call PRELUDIUM BIS-3, Grant Number 2021/43/O/ST10/00539.

Publications of the Institute of Geophysics, Polish Academy of Sciences
Geophysical Data Bases, Processing and Instrumentation
vol. 453 (E-14), 2025, pp. 15–18
DOI: 10.25171/InstGeoph_PAS_Publs-2025-027
XLII International School of Hydraulics, Radocza, Poland, 20–23 May 2025

Numerical Simulation of Earth Dam Erosion due to Overtopping Using a One-dimensional Model

Mikołaj URBANIAK

Wrocław University of Science and Technology, Wrocław, Poland

✉ mikolaj.urbaniak@pwr.edu.pl

Abstract

The increasing frequency of extreme weather events, driven by climate change, poses significant challenges to hydraulic structures such as earth dams. These structures are increasingly exposed to sudden inflows of large water volumes, which can exceed their discharge capacities. When overtopping occurs, the resulting erosion of the earth dam can lead to catastrophic releases of retained water, endangering downstream areas. In Poland, two such disasters have taken place in recent years: in 2010 in Niedów and in 2024 in Stronie Śląskie. These events emphasize the critical need for advanced computational tools to model erosion processes and enhance the safety of areas located downstream. This study presents the application of a one-dimensional numerical model based on the physics of erosion phenomena. The simulation results were validated through experimental studies conducted at Wrocław University of Science and Technology, where physical models of earth embankment erosion were tested. The comparative analysis demonstrates the robustness of numerical approaches in a predicting erosion dynamics. The findings underscore the vital role of integrating numerical simulations and laboratory experiments to improve the predictive capabilities of dam safety assessments in the context of a changing climate.

1. INTRODUCTION

The increasing frequency of extreme weather events driven by climate change has intensified the risk of catastrophic failures in hydraulic structures such as earth dams. Events like the overtopping of the Niedów Dam in 2010 and the washout of the Stronie Śląskie Dam in 2024 highlight the vulnerability of these structures to intense rainfall and the devastating consequences for downstream areas. These incidents emphasize the critical need for advanced tools to predict and mitigate the risks associated with dam breaches.

This study applies a one-dimensional numerical model calibrated against laboratory experiments. The model captures the breach development and resulting outflow hydrograph during overtopping scenarios. By combining experimental data with numerical simulations, this study provides a practical framework for enhancing dam safety amidst increasingly frequent extreme weather events.

2. LABORATORY EXPERIMENTS CARRIED OUT

Laboratory experiments were conducted at the Wrocław University of Science and Technology to investigate the erosion mechanisms of a homogeneous earth embankment under overtopping conditions. The embankment, constructed from noncohesive sand with a height of 0.50 m, was tested in a controlled setting using a reservoir with a capacity of 14.4 m³. The experiments aimed to simulate real-world overtopping scenarios and analyze the breach development process. Four distinct phases of erosion were identified: the initiation phase, vertical erosion, lateral erosion, and reservoir emptying. These phases were consistently observed across three trials, with lateral erosion showing the highest variability (Urbaniak et al. 2024).

3. CALCULATIONS ACCORDING TO NUMERICL MODEL

The model described by Macchione (2008) offers a physically-based numerical framework for predicting dam breaches caused by overtopping. It captures both the temporal evolution of the breach geometry and the resulting outflow hydrograph. According to this approach, the breach initially develops in a vertical direction with a triangular cross-section until its base reaches the foundation level. Subsequent lateral erosion causes the breach to expand, eventually forming a trapezoidal shape. This process aligns with breach morphologies observed in both experimental

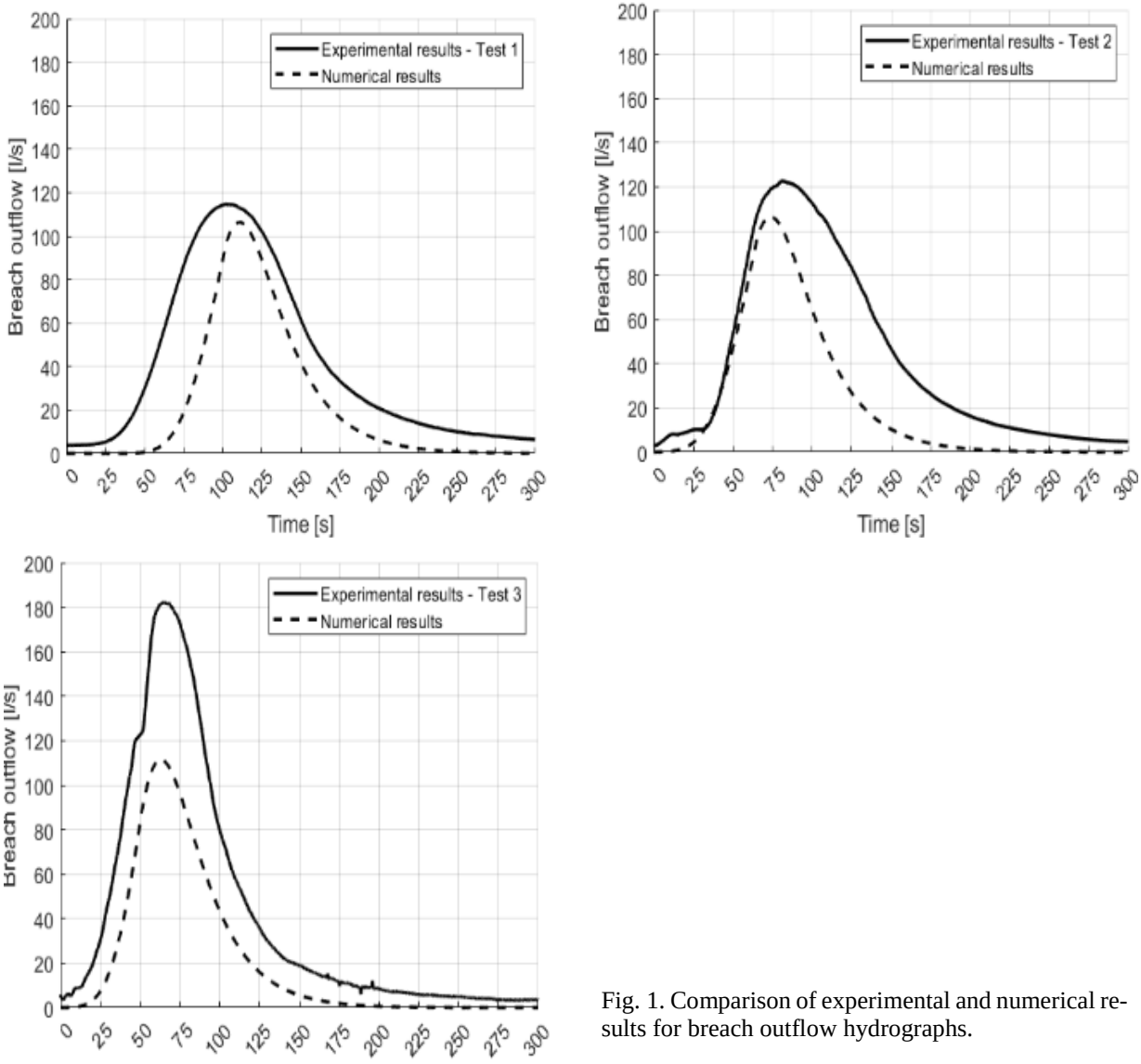

Fig. 1. Comparison of experimental and numerical results for breach outflow hydrographs.

and real-world scenarios. The model incorporates critical flow conditions through the breach to calculate discharge, using formulations specific to triangular and trapezoidal cross-sections. The volumetric sediment load per unit width is determined using the Meyer-Peter Müller formula, assuming that critical shear stress is negligible compared to the mean shear stress.

The model relies on system of coupled differential equations describing breach growth and the corresponding outflow hydrograph. The evolution of breach width and depth is governed by sediment transport equations, which depend on hydraulic shear forces acting on the erodible material.

The implementation of the model produced a hydrograph illustrating the temporal evolution of discharge during a breach event (Fig. 1). The results captured the rapid rise to peak discharge, followed by a gradual decline, reflecting the progressive widening and deepening of the breach. These numerical simulations were calibrated against laboratory test results conducted earlier in this study, ensuring that the model accurately represents observed erosion processes. Hydrographs that best correspond to the results of the laboratory tests are presented in Fig. 1.

4. SUMMARY AND CONCLUSION

The comparison between experimental and numerical results, as summarized in Table 1, highlights the strengths and limitations of the numerical model in predicting key breach characteristics. The peak discharge values (Q_p) from the numerical model closely align with experimental results in Tests 1 and 2, with errors of –7.20% and –13.27%, respectively. However, in Test 3, the model significantly underestimates Q_p by –37.94%. This discrepancy may be attributed to the increased variability observed in the lateral erosion phase during the experiments, which is challenging to capture with the current one-dimensional framework.

In terms of the time to peak discharge (T_p), the numerical model demonstrates reasonable accuracy, with errors ranging from +8.80% in Test 1 to –13.95% in Test 2. For Test 3, the predicted T_p is slightly higher than the experimental value +6.25%, indicating the model's capacity to approximate the temporal progression of the breach despite inherent simplifications.

Table 1

Comparison of experimental (Exp.) and numerical (Num.) results for peak discharge Q_p and time to peak discharge T_p across three tests

	Test 1		Test 2		Test 3	
	Exp.	Num.	Exp.	Num.	Exp.	Num.
Q_p [ls^{-1}]	114.65	106.39	122.67	106.39	182.17	113.05
T_p [s]	102	111	86	74	64	68

Overall, the results underscore the importance of calibrating numerical models with experimental data to improve their predictive accuracy. The discrepancies observed in Test 3 suggest the need for further refinement, particularly in representing the dynamic interactions of hydraulic forces and erosion processes during the lateral erosion phase. Nonetheless, the close agreement in Tests 1 and 2 validates the robustness of the model and its utility in assessing dam breach scenarios under varying conditions. These findings highlight the necessity for continued advancement of numerical methodologies to better capture complex erosion mechanisms and enhance predictive capabilities. Furthermore, additional experimental studies are crucial for providing high-quality data to support model calibration and validation, ultimately ensuring the reliability of such tools in real-world applications.

References

Macchione, F. (2008), Model for predicting floods due to earthen dam breaching. I: Formulation and evaluation, *J. Hydraul. Eng*. **134**, 12, DOI: 10.1061/ASCE0733-94292008134:121688.

Urbaniak, M., K. Zamiar, and S. Kostecki (2024), Understanding geotechnical embankment washout due to overtopping: insights from physical tests, *Stud. Geotech. Mech*. **46**, 4, 328–336, DOI: 10.2478/sgem-2024-0025.

Publications of the Institute of Geophysics, Polish Academy of Sciences
Geophysical Data Bases, Processing and Instrumentation
vol. 453 (E-14), 2025, pp. 19–22
DOI: 10.25171/InstGeoph_PAS_Publs-2025-028
XLII International School of Hydraulics, Radocza, Poland, 20–23 May 2025

Flume Investigation of Hydraulics of Nature-like Patchy Vegetation

Hafiza Aisha KHALID, Kaisa VÄSTILÄ, and Juha JÄRVELÄ

Aalto University, School of Engineering, Espoo, Finland

✉ hafizaaisha.khalid@aalto.fi; kaisa.vastila@aalto.fi; juha.jarvela@aalto.fi

Abstract

Spatial distribution of riparian vegetation is a critical factor altering flow hydrodynamics and transport processes in rivers. Distribution of riparian vegetation in the form of distinct patches is typical for riverbanks and floodplains, but scarcely investigated from the viewpoint of its hydraulic impacts. The present study aims to investigate reconfiguration of the riparian vegetation patches in relation to the mean flow conditions. Experiments were conducted over a range of mean flow velocities (0.1 to 0.6 m/s) and under low relative submergences ($h/h_d \approx$ 1 and 2). The results showed a substantial increase in the patch reconfiguration and flow resistance with the increase in velocities. The extent of these phenomena depends on the patch density and shape.

1. INTRODUCTION

The significance of vegetation growing on riverbed, banks, and on floodplains is widely recognized by river managers (Jakubínský et al. 2021). The application of this vegetation to manage the quantity and quality of flow is considered as a vital tool for sustainable river management (Rowiński et al. 2018).

Riparian vegetation typically forms in patchy distributions (Bae et al. 2024), which contribute to spatial variations in hydraulic resistance. These variations are influenced by the arrangement, size, and shape of the patches (Luhar and Nepf 2013). Beyond its natural distribution, the management of vegetation in patchy patterns offers a cost-effective, sustainable, and aesthetically beneficial approach to manage the flood risk in streams and rivers (Bae et al. 2024). Therefore, accurate quantification of flow resistance in areas with patchy vegetation is essential for optimizing the conservation of riparian habitats.

The present study reports the ongoing development, as part of a larger research project focused on the investigation of influence of patchy riparian vegetation on hydraulic resistance. The patchiness was characterized using leaf area index (LAI) and blockage factors. Laborato-

ry experiments were carried out with six different patch setups to study the relative significance of static and dynamic reconfiguration of the woody patches in explaining the hydraulic resistance.

2. FLUME EXPERIMENTS

The experiments were conducted at the Aalto Environmental Hydraulics Lab in the 16 m long flow channel having width and depth of 60 and 80 cm, respectively. A vegetated reach of about 7 m was constructed, consisting of 14 patches, each made using 22 cm tall flexible wo-ody plants. Two reach scale plant densities (LAI = leaf area/ground area ≈ 1 and 2.4) and three different patch shapes were formed to obtain the six different patch setups (L3W4, L4W4, L9W2, L9W3, L5W2, and L6W2). For each setup, the number of plants varied between the patch setups, but per patch was constant across the reach. The vegetated reach also had 35 mm tall understory grasses.

Twelve hydraulic conditions were investigated with flow rates varying between 11–140 l/s. The hydraulic conditions were varied by testing two different submergences ($h/h_d \approx 1$ and 2) and six flow velocities for each patch setup, ranging from 0.1 to 0.6 m/s. The water depths were adjusted with the weir located at the end of the channel. The flume bed was tilted to establish steady quasi-uniform flow conditions. The water depths were measured at six different locations along the reach using the high accuracy pressure sensors (0.1% of full-scale value, corresponding to 1 mm accuracy at full scale) to obtain bulk friction factors *f*.

The friction factors of the foliated woody patches were derived by subtracting *f'* of the grasses from the bulk friction ($f'' = f - f'$), assuming the linear superposition principle (Västilä and Järvelä 2014). The *f'* of the grasses was derived separately by running experiments with only grasses.

Patch blockage parameters were determined using the patch areas at two different planes. Planform (i.e. bird's eye view) ($A_{b,p}$) and cross-sectional (B_A) areas were measured at static and dynamic conditions through image analysis using open-source software imageJ. Here, static and dynamic refer to no-flow in dry conditions and velocity-dependent reconfigured areas, respectively.

3. RESULTS

Figure 1 shows the static and dynamic measurement of vegetation patch areas with relation to measured vegetative friction factors *f''*. The results are further categorized as per two investigated submergence levels. The markers for data points are varied for different patch shapes as shown in the legend. Here, the cross-section projection areas (B_A) of the vegetation patches represent the vegetation blockage within the representative cross-section but not the number of vegetation patches occupied at the reach scale. The dynamic planform projection areas ($A_{b,p}$) changed by 23% on average, as compared to static values for various patch setups. On the other hand, the cross-sectional projection areas (B_A) changed on an average by 37%, with higher changes observed at higher velocities and comparatively lower deflections at high sub-mergence levels. This can be attributed to the fact that, at $h/h_d = 1$ all the flow bypasses within the vegetation column, and there is no free flow on top of the patches.

The extent of reconfiguration reflected in the changes in $A_{b,p}$ and B_A varied across different density and shapes of patches. The longer patches with low density (L9W3 and L9W2) showed the highest decrease in areas, results in minimal resistance, allowing the flow to move freely while causing the patches to flex or bend in response. Overall, both areas explaining the blockage properties of patches are dependent on velocity-induced reconfiguration, and this "dynamic" velocity-dependency of areas explains variability of *f''*.

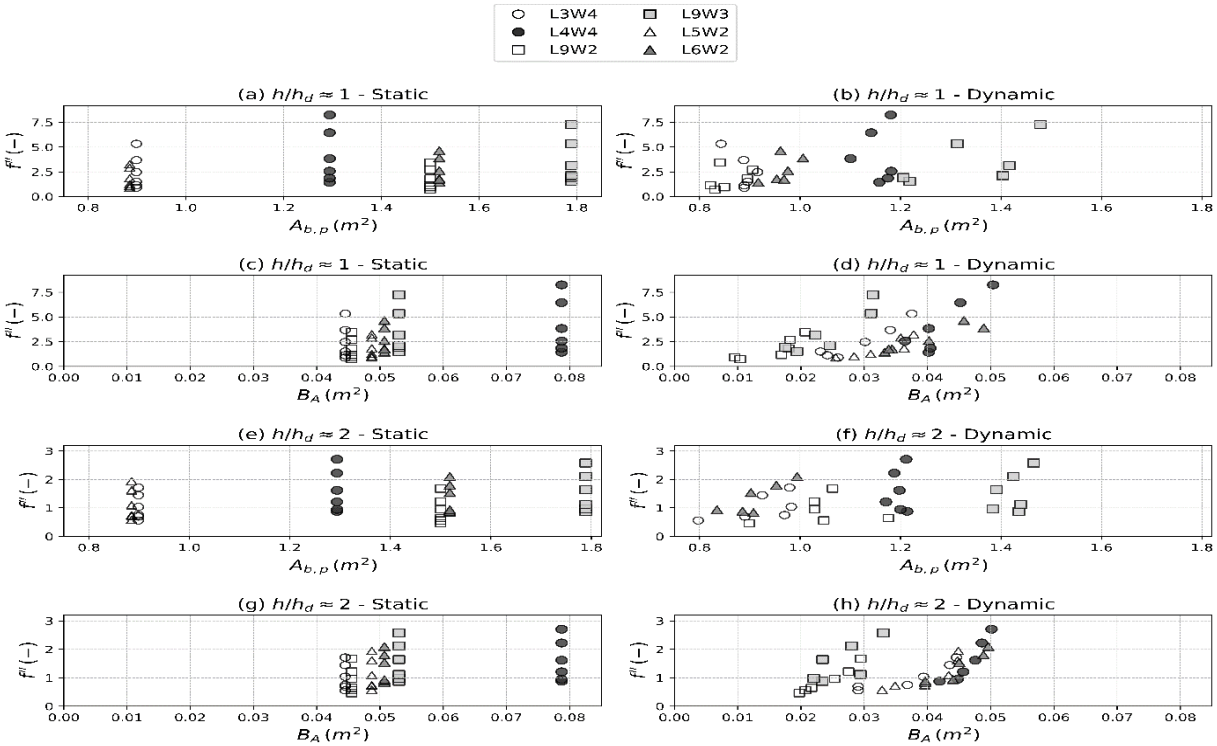

Fig. 1. Vegetated resistance *f''* caused by woody vegetation patches as a function of static and dynamic planform $A_{b,p}$ and cross-sectional B_A areas categorized by the two investigated hydraulic submergences h/h_d = 1 and 2. Patch designs for reach scale LAI 1.0: L3W4, L9W2, and L5W2. Patch designs with reach scale LAI 2.4: L4W4, L9W3, and L6W2. Name of the layouts are given with reference to number of rows and columns of plants in one patch.

4. CONCLUDING REMARKS

The observed patch reconfiguration explained through patch projection areas was found to be sensitive to the flow velocities, patch shape, while its sensitivity to submergence level is comparatively lower. These areas will further be converted to the non-dimensional analyses using blockage factors to incorporate the patch characteristics in hydraulic modelling.

Further investigations are under way, including relative analyses of static and dynamic blockage factors and patch shapes in determination of hydraulic resistance of patchy vegetation.

References

Bae, I., U. Ji, J. Järvelä, and K. Västilä (2024), Blockage effect of emergent riparian vegetation patches on river flow, *J. Hydrol*. **635**, 131197, DOI: 10.1016/j.jhydrol.2024.131197.

Jakubínský, J., M. Prokopová, P. Raška, L. Salvati, N. Bezak, O. Cudlín, P. Cudlín, J. Purkyt, P. Vezza, C. Camporeale, J. Daněk, M. Pástor, and T. Lepeška (2021), Managing floodplains using nature-based solutions to support multiple ecosystem functions and services, *WIREs Water* **8**, 5, e1545, DOI: 10.1002/wat2.1545.

Luhar, M., and H.M. Nepf (2013), From the blade scale to the reach scale: A characterization of aquatic vegetative drag, *Adv. Water Resour*. **51**, 305–316, DOI: 10.1016/j.advwatres.2012.02.002.

Rowiński, P.M., K. Västilä, J. Aberle, J. Järvelä, and M.B. Kalinowska (2018), How vegetation can aid in coping with river management challenges: A brief review, *Ecohydrol. Hydrobiol*. **18**, 4, 345–354, DOI: 10.1016/j.ecohyd.2018.07.003.

Västilä, K., and J. Järvelä (2014), Modeling the flow resistance of woody vegetation using physically based properties of the foliage and stem, *Water Resour. Res*. **50**, 1, 229–245, DOI: 10.1002/2013WR013819.

Publications of the Institute of Geophysics, Polish Academy of Sciences
Geophysical Data Bases, Processing and Instrumentation
vol. 453 (E-14), 2025, pp. 23–23
DOI: 10.25171/InstGeoph_PAS_Publs-2025-029
XLII International School of Hydraulics, Radocza, Poland, 20–23 May 2025

Flow Resistance due to Stream Meandering: An Evaluation of Existing Methods and Implications for Streamflow Estimations

Cristopher Alexander GAMBOA MONGE✉ and Ana Maria FERREIRA DA SILVA

Department of Civil Engineering, Queen's University, Kingston, Ontario, Canada

✉ c.gamboamonge@queensu.ca

Abstract

Resistance to flow governs flow and sediment transport capacities in rivers and streams and is a critical factor in hydraulic and environmental engineering applications, including projects dealing with flood management, stream restoration and re-naturalization, establishment of environmental flows to sustain aquatic ecosystems, and mitigation of climate change. Flow resistance arises from factors such as bed granular roughness, bed forms, and channel bends. This work focuses exclusively on flow resistance caused by stream meandering. Despite its practical significance, the topic has been the focus of very few studies in the past and at present it is not known whether the methods proposed so far to determine meandering flow resistance yield realistic results. This study aims to fill this gap by analyzing and evaluating two of the existing methods, selected because they appear as the most popular by far and are rooted on the physics of the phenomenon. To this end, a dataset consisting of all laboratory experiments conducted in sine-generated streams over the past 60 years was gathered. The existing methods were used to determine flow velocities. By comparing these to their measured counterparts, it was found that both methods systematically underestimate flow resistance due to stream meandering, leading to significant overestimations of streamflow. This work highlights the need to develop substantially more accurate methods for the prediction of energy losses due to stream meandering.

Publications of the Institute of Geophysics, Polish Academy of Sciences
Geophysical Data Bases, Processing and Instrumentation
vol. 453 (E-14), 2025, pp. 25–25
DOI: 10.25171/InstGeoph_PAS_Publs-2025-030
XLII International School of Hydraulics, Radocza, Poland, 20–23 May 2025

An Experimental Setup for Thermal Jets Dispersion Analysis

Rui ALEIXO, Jarosław BIEGOWSKI, Małgorzata ROBAKIEWICZ,
and Piotr SZMYTKIEWICZ

Institute of Hydro-Engineering of the Polish Academy of Sciences, Gdańsk, Poland

✉ rui.aleixo@ibwpan.gda.pl; jarbieg@ibwpan.gda.pl; marob@ibwpan.gda.pl;
p.szmytkiewicz@ibwpan.gda.pl

A b s t r a c t

Thermal powerplants for energy production often pump water from a colder source (e.g. river or lake) into their refrigeration circuit to later release it in a form of a jet or plume into the aquatic environment. Since the released water is at a higher temperature than the surrounding environment, it will contribute to its warming, thus potentially causing environmental damage like the increase of algae and eutrophication. This paper presents an experimental setup designed to model the dispersion of jets and plumes, capable of measuring both the velocities and temperatures of the jet and ambient. This experimental setup integrates a temperature-controlled tank, a water reservoir, a pump and a flowmeter. The water pumped from the temperaturecontrolled tank into the reservoir by means of a nozzle placed at the bottom. This nozzle can be easily changed and adapted to different geometry and configurations. A laser is used to light the reservoir and the jet section. Imaging acquisition techniques are then used to capture the jet trajectory, and its velocity can be determined by means of Particle Image Velocimetry. Finally, the simplicity of the proposed setup allows it to be easily upscaled.

Publications of the Institute of Geophysics, Polish Academy of Sciences
Geophysical Data Bases, Processing and Instrumentation
vol. 453 (E-14), 2025, pp. 27–30
DOI: 10.25171/InstGeoph_PAS_Publs-2025-031
XLII International School of Hydraulics, Radocza, Poland, 20–23 May 2025

Calibration and Validation of 3D Numerical Models of a Straight Channel with Leaky Barriers

Oscar HERRERA-GRANADOS[1] and Pedro MARTIN-MORETA[2]

[1]Wrocław University of Science and Technology, Wrocław, Poland
✉ Oscar.Herrera-Granados@pwr.edu.pl

[2]Brunel University London, London, United Kingdom
✉ Pedro.Martin-Moreta@brunel.ac.uk

A b s t r a c t

In this contribution, two 3D numerical models are tested using laboratory records to properly calibrate and validate these models. 1D numerical techniques are also used for this purpose. Mesh sensitivity analyses, different roughness coefficients, and Acoustic Doppler Velocimetry (ADV) records were applied to increase the reliability of the 3D model results. Thanks to these analyses, the output of the models can be used for design purposes to properly assign the geometry of leaky barriers in real world cases to enhance flood resilience above all in urban areas.

1. INTRODUCTION

Natural Flood Management (NFM) is a concept that refers to the mitigation measures that use processes to restore flow regimes and help increase the attenuation of flood events in a natural way. Leaky barriers dams are one of those techniques. The purpose of this kind of structure is to allow water flow without causing backwater during normal conditions, but to attenuate the formation of higher flood waves in case of heavy rainfall. The last described situation can be achieved with a proper configuration (leaky barrier adequate dimensions) of the dam logs.

However, the design of these dams is still complex to understand from a hydraulic point of view. Novel experiments are being carried out to analyze the flow behavior through this kind of infrastructure in a rectangular channel. The flow behavior through these structures can be also researched using state-of-the-art numerical tools such as computational fluid dynamics (CFD) models using the same geometry as in the laboratory for a wide range of scenarios. Moreover, to obtain reliable results, a proper calibration and validation procedure shall be carried out. Therefore, setting up a reliable model is the main purpose of this contribution.

1.1 Available experimental data

Data from two experimental flumes were available for this research: a) the data from the experiments carried out at the Brunel University London (Martin-Moreta et al. 2025) and the data

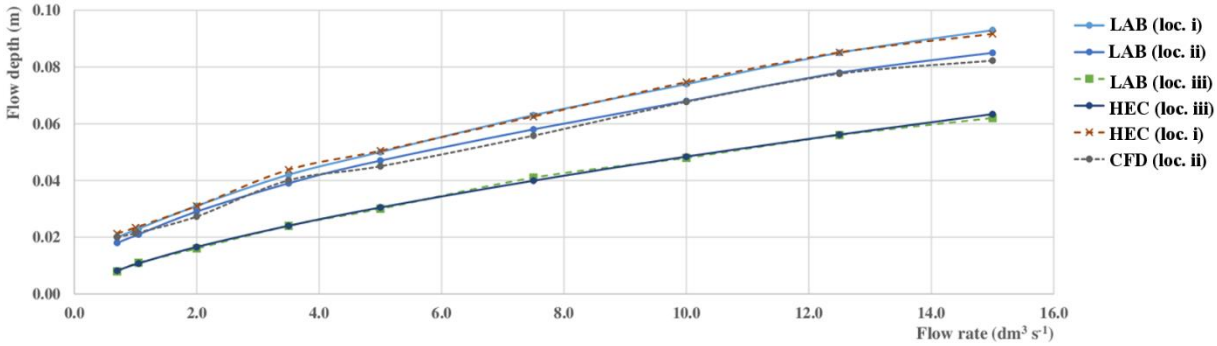

Fig. 1. Rating curves that were registered (at Brunel University London) and that were calculated using 1D and 3D modeling using HEC-RAS (1D) and Flow3D.

available from the experimental research at the Wrocław University of Science and Technology – WrUST (see Fig. 1) in South Poland. For both cases a three-log leaky barrier was analyzed. For the case of the experiments that were carried out in London, the general purpose was to establish the flume's roughness coefficient that will assure the accurate approximation of the velocity field profiles using 3D modeling (and for calibration using the records registered at WrUST). For this analysis, the rating curve of the experimental flume was recorded and numerically analyzed using 1D techniques (HEC-RAS) as well as the Flow 3D RANS closure (k-ε) without the leaky dams. As depicted in Fig. 1, the rating curve was registered and calculated at four different locations: i) at the beginning of the flume; ii) at the location of the leaky barriers (without them), and iii) at the outlet.

As appreciated in Fig. 1, the records from the experiments best fit the 1D and 3D numerical results with the roughness value equal to k_s = 0.0013 mm. As stated in Table 1, the results of the models in comparison with the measured rating curves present good agreement. Once the determination of the roughness was obtained, another run was compared with the leaky barriers and to validate whether the model is reliable using the well-known k-ε mathematical approach.

2. NUMERICAL MODELLING

The Reynolds' Average Navier Stokes (RANS) equations represent an adequate technique to analyse 3D flows for engineering because not all the turbulent scales are resolved (Herrera-Granados 2021) and provided time averaged reliable results (such as the time-averaged profile

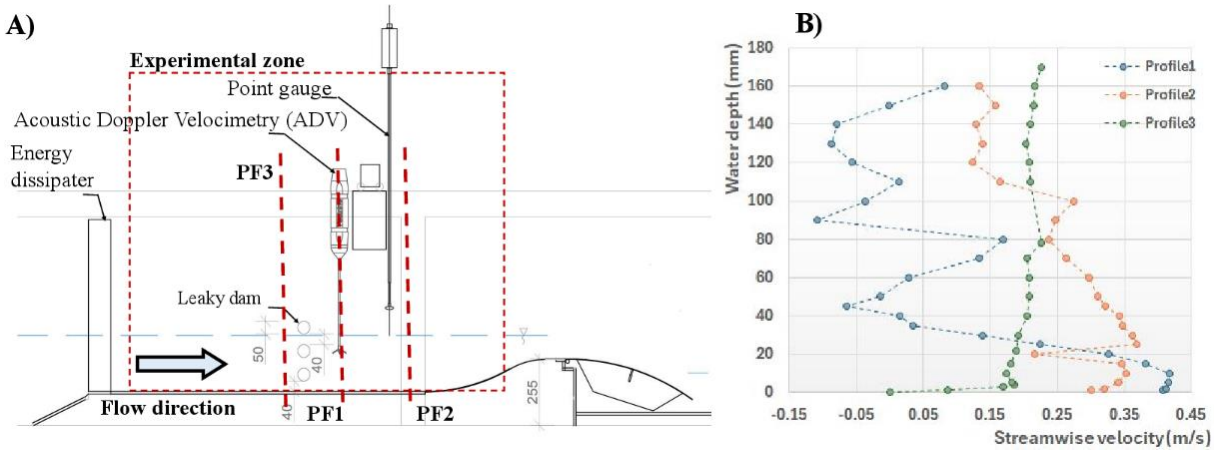

Fig. 2. Experimental set-up at the WrUST laboratory: A) scheme of the experimental set-up and location of the record measurements, B) records for Q_1 at PF1, PF2 (downstream), and PF3 (upstream).

of the velocity). Therefore, the k-ε and k-ω approaches were used for this part of the analysis. The commercial software Flow 3D (developed by Flow Science) was used for the analysis.

2.1 Numerical set-up and model run

The time averaged velocity profiles for two flow rates ($Q_1 = 0.0203$ m^{3}s^{-1} and $Q_2 = 0.0361$ m^{3}s^{-1}) at three different locations (PF1, PF2, and PF3) were recorded at the Wrocław University of Science and Technology. The time averaged velocity profiles for Q_1 are depicted in Fig. 2B.

2.2 Output, calibration, and validation of the models

The most widely used calibration procedure is optimization of the model performance, which means that the model output is compared to the observed data. This can be done using a trial-error procedure or changing the parameters that are introduced as data in the model (Herrera-Granados 2022). The velocity profiles (streamwise) registered at the lab were compared with the output of the simulated values of the two CFD (see Fig. 3), which were very similar using both mathematical approaches. However, after doing a mesh sensitivity analysis, the k-ε provided a slightly smaller error. The Root Mean Square Error (RMSE) for all the models were calculated as summarized in Table 1. Once the authors archived a good agreement for the velocity profiles for Q_1, the validation procedure was carried out for Q_2.

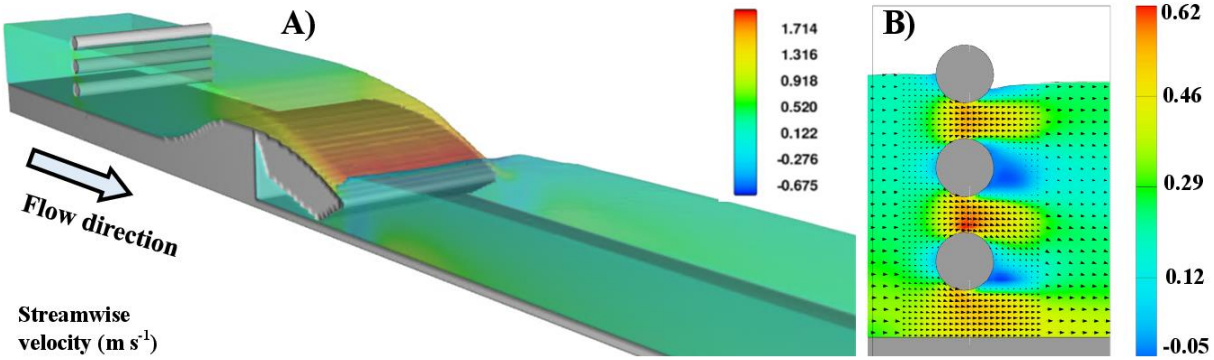

Fig. 3: A) CFD visual output for Q_2, and B) velocity field close to the leaky barriers.

Table 1
Comparison of the CFD output with the experimental results

Calibration and validation comparison between simulation results and experimental records			
Situation (simulation ID)	Purpose	Max error (%)	RMSE (–)
Brunel no-logs (1)	Determination of roughness	7.02	0.40
Brunel smooth (2)	Calibration of roughness	9.23	0.50
WrUST Q_1 (3)	Roughness calibration (PL)	8.41	0.49
WrUST Q_2 (4)	Velocity profile calibration	6.78	0.42
WrUST Q_3 (5)	Velocity profile validation	6.60	0.20

3. CONCLUSIONS AND FURTHER RESEARCH

As the calibration and validation procedures were achieved as described in this contribution, the simulation of different scenarios is to be carried out. Thanks to this model, different schemes for 3-logs leaky barriers are to be analyzed and it can contribute to a better understanding of them. As stated in Table 1, the RMSE are small enough to consider the model as reliable.

References

Herrera-Granados, O. (2021), Numerical analysis of flow behavior in a rectangular channel with submerged weirs, *Water* **13**, 10, 1396, DOI: 10.3390/w13101396.

Herrera-Granados, O. (2022), Theoretical background and application of numerical modeling to surface water resources. **In:** M. Zakwan, A. Wahid, M. Niazkar, and U. Chatterejee (eds.), *Water Resource Modeling and Computational Technologies*, Current Directions in Water Scarcity Research Series, Vol. 7, Elsevier, Amsterdam, 319–340, DOI: 10.1016/B978-0-323-91910-4.00019-4.

Martin-Moreta, P., O. Herrera-Granados, R. Bourne, T. Curwel, D. Ramsbottom, R. Body, and M. Roca-Collel (2025), Experimental coefficient of discharge for Leaky Wood Dams in clear water conditions, *CIWEM J. Flood Risk Manag*. (under review).

Publications of the Institute of Geophysics, Polish Academy of Sciences
Geophysical Data Bases, Processing and Instrumentation
vol. 453 (E-14), 2025, pp. 31–31
DOI: 10.25171/InstGeoph_PAS_Publs-2025-032
XLII International School of Hydraulics, Radocza, Poland, 20–23 May 2025

An Experimental Study on Downstream Fish Guidance Efficiency

Cumhur OZBEY[1], Serhat KUCUKALI[1,✉], Baran YOGURTCUOGLU[2], and Ahmet ALP[3]

[1]Department of Civil Engineering, Hydraulics Division, Hacettepe University, Turkey

[2]Division of Hydrobiology, Biology Department, Hacettepe University, Turkey

[3]Fisheries Department, Kahramanmaras Sutcu Imam University, Turkey

✉ kucukali78@gmail.com

A b s t r a c t

Hydropower plants restrict or completely block fish downstream migrations, which play a critical role throughout their life cycles. Recent experimental and field studies indicate that there is a need for efficient finer bar rack screens to protect multiple fish species, including the small-bodied ones, at water intakes with minimum head loss. We have experimentally investigated the hydraulic and fish guidance performance of the angled Oppermann fine screen, both with and without a guidance wall. We conducted the experiments at a 45° screen angle, with a bar spacing of 10 mm. According to the analyses, implementing a guidance wall reduces the maximum streamwise velocity gradient in the screen region. The experimental measurements revealed that the tangential velocities in front of the screen tend to increase in the presence of a guidance wall, which leads to an effective guiding current for fish in the bypass channel. The downstream guidance efficiencies for small-bodied fish species of *Alburnus escherichii* and *Alburnoides kosswigi* are presented.

Publications of the Institute of Geophysics, Polish Academy of Sciences
Geophysical Data Bases, Processing and Instrumentation
vol. 453 (E-14), 2025, pp. 33–33
DOI: 10.25171/InstGeoph_PAS_Publs-2025-033
XLII International School of Hydraulics, Radocza, Poland, 20–23 May 2025

Analysis of the 2024 Flood Events in the Upper Biała Lądecka Basin up to the Lądek Zdrój Town

Jakub IZYDORSKI✉ and Oscar HERRERA-GRANADOS

Wrocław University of Science and Technology, Faculty of Civil Engineering, Wrocław, Poland

✉ Jakub.Izydorski@pwr.edu.pl

Abstract

In this contribution, the authors developed a hydrological model based on the SCS-CN curve methodology and GIS (Geographic Information Systems) to estimate flood hydrographs in the upper parts of the Biała Lądecka River basin. The numerical models were calibrated based on the data available from the Polish Institute of Meteorology and Water Management (IMGW). The output of the model demonstrates the effect in the flood hydrograph at the town of Lądek Zdrój. The hydrological model was developed and enhanced using different hydraulic routing, transform, and loss methods. The results of these analyses can allow water stakeholders to make better decisions to diminish the negative effects of new hydrological flood events at the planning stage, occurring more often due to climate change.

Publications of the Institute of Geophysics, Polish Academy of Sciences
Geophysical Data Bases, Processing and Instrumentation
vol. 453 (E-14), 2025, pp. 35–37
DOI: 10.25171/InstGeoph_PAS_Publs-2025-034
XLII International School of Hydraulics, Radocza, Poland, 20–23 May 2025

Longitudinal Dispersion from Cylinders to Realistic Plant Forms

Doreen MACHIBYA, Finna FITRIANA, Virginia STOVIN, and Ian GUYMER

University of Sheffield, Sheffield, United Kingdom

✉ ddmachibya1@sheffield.ac.uk; ffitriana1@sheffield.ac.uk; v.stovin@sheffield.ac.uk; i.guymer@sheffield.ac.uk

Abstract

Many studies on the hydrodynamics and mixing processes due to vegetation have significantly simplified the physical characteristics of plants by representing the stem distribution, e.g. for reeds, as an array of cylinders. These studies often use single diameter cylinders, placed in regular arrays, producing unrealistic preferential flow paths. New solute tracing studies (Machibya 2024) were performed using realistic plant forms, with leaves, stems and branches. Experiments were conducted in a 12.5 m long, 300 mm wide flume and longitudinal dispersion coefficients (D_x) were determined over a range of discharges. The results confirm the linear relationship between D_x and the mean velocity, u observed in cylinder arrays. The longitudinal dispersion coefficients for the realistic plant forms were found to be an order of magnitude greater than those from studies conducted using cylinders. This illustrates and quantifies the effect of plant structure on solute mixing processes.

1. BACKGROUND

Sonnenwald *et al*. (2017) summarised longitudinal dispersion coefficient (D_x) values for real vegetation at low velocities, whilst Sonnenwald *et al*. (2019) provided estimates for D_x based on parameterisation of vegetation and flow. Corredor-Garcia *et al*. (2022, 2025) investigated the mixing processes and flow hydrodynamics within a cylinder distribution containing a range of diameters in a random spatial distribution. This new study determines the longitudinal dispersion coefficient in open channel flows containing realistic vegetation.

2. METHOD

The study was performed using realistic plastic plant forms, with leaves, stems and branches. Initial tests were conducted without vegetation, to determine the basic channel characteristics. These were followed by the installation of dense vegetation, Fig. 1, with a solid volume fraction of 0.008, over the complete channel length, Fig. 2. Uniform flow conditions were created, with a fixed flow depth of 105 mm (i.e. emergent plants), across a range of discharges up to 12 l/s.

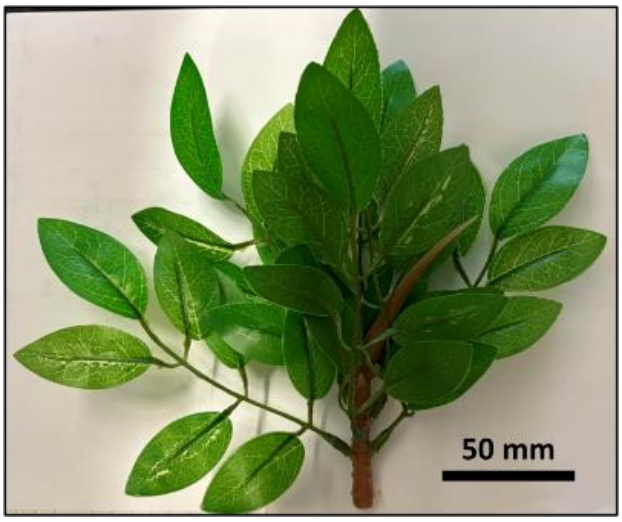

Fig. 1. Realistic "plant".

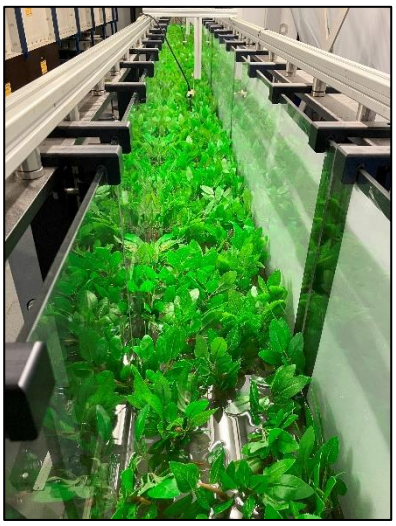

Fig. 2. Flume installation of realsitic plants.

Four Turner C7 Cyclops were evenly spaced at 3 m intervals along the flume, measuring fluorescence concentrations at the mid-width and mid-depth point. Five repeat instantaneous injections of a small volume of Rhodamine WT were made, providing data to estimate 15 values of the mean flow velocity, u (m/s) and the longitudinal dispersion coefficient, D_x (m^2/s) for each flow condition. An example of the recorded raw data is shown in Fig. 3.

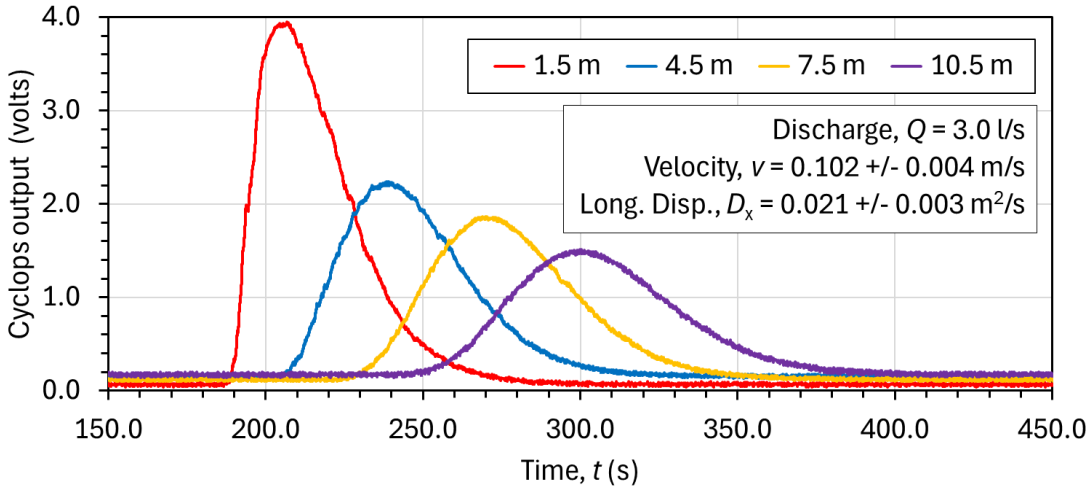

Fig. 3. Recorded temporal variation of Cyclops output.

3. RESULTS

The travel times and dispersion coefficient values were obtained by optimizing the solute routing equation using the TCPAT2 code (Sonnenwald and Guymer 2024). The results show a linear relationship between D_x and velocity, with the D_x values for the realistic plant forms an order of magnitude greater than those from previous similar studies that used cylinder arrays, Fig. 4. This emphasizes how plant structure influences mixing processes.

Normalizing D_x, using previously suggested length scales of stem diameter or stem spacing, did not agree well with previous non-dimensional values. However, normalizing D_x by a characteristic plant diameter, in this case 0.133 m, aligned these new results with earlier ones, for stem Reynolds numbers in excess of 300. This indicates that a "representative diameter" may serve as a more appropriate length scale for complex vegetation forms.

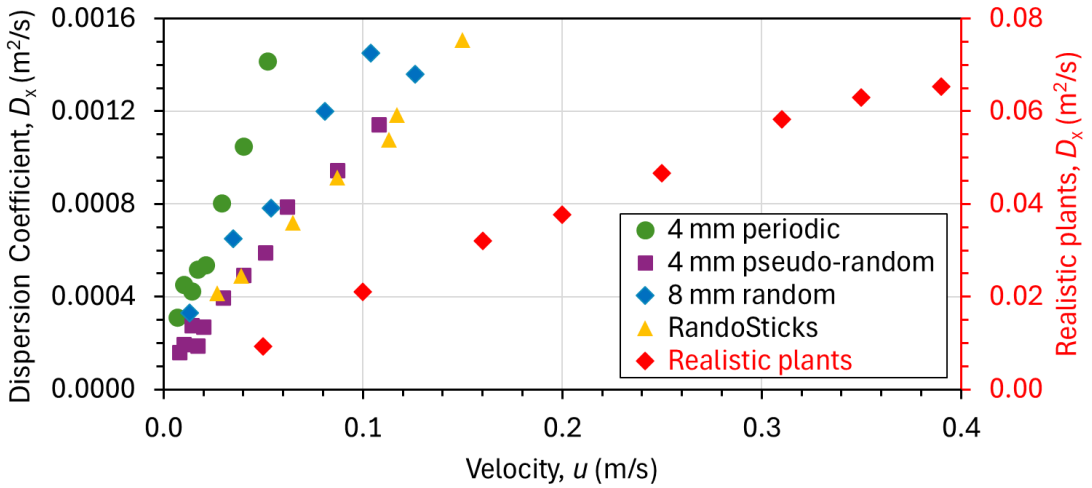

Fig. 4. Variation of Optimised Longitudinal Dispersion Coefficient, D_x with mean velocity, u, for cylindar arrays and a realistic plant form.

4. CONCLUSIONS

This study confirms that earlier simplified physical models using cylinder arrays do not accurately reflect the complex mixing processes seen in realistic vegetated flows.

References

Corredor-Garcia, J.L., V. Stovin, and I. Guymer (2022), Spatio-temporal characterisation of hydrodynamics and mixing processes in obstructed flows using optical techniques. **In:** *Proc. 39th IAHR World Congress, 19–24 June 2022, Granada, Spain*, 5140–5149, DOI: 10.3850/iahr-39wc 2521711920221035.

Corredor-Garcia, J.L., V. Stovin, and I. Guymer (2025), Hydrodynamics and length-scale distributions of a random cylinder array, *ASCE J. Hydraul. Eng.* **151**, 1, DOI: 10.1061/JHEND8.HYENG-13872.

Machibya, D. (2024), Quantifying Longitudinal Dispersion in realistic Synthetic Vegetation, MSc Dissertation, University of Sheffield.

Sonnenwald, F., and I. Guymer (2024), Temporal Concentration Profile Analysis Tool 2, The University of Sheffield, Software, available from: https://doi.org/10.15131/shef.data.26739427.v2 (accessed: 23 August 2024).

Sonnenwald, F., J.R. Hart, P. West, V.R. Stovin, and I. Guymer (2017), Transverse and longitudinal mixing in real emergent vegetation at low velocities, *Water Resour. Res.* **53**, 1, 961–978, DOI: 10.1002/2016WR019937.

Sonnenwald, F., V. Stovin, and I. Guymer (2019), A stem spacing-based non-dimensional model for predicting longitudinal dispersion in low-density emergent vegetation, *Acta Geophys.* **67**, 3, 943–949, DOI: 10.1007/s11600-018-0217-z.

Publications of the Institute of Geophysics, Polish Academy of Sciences
Geophysical Data Bases, Processing and Instrumentation
vol. 453 (E-14), 2025, pp. 39–39
DOI: 10.25171/InstGeoph_PAS_Publs-2025-035
XLII International School of Hydraulics, Radocza, Poland, 20–23 May 2025

From the Renaissance to Turbulence – A modern Look at Da Vinci's Impinging Jet Flow

Marianna BIUNGNER[1], Ludwika SZOPA[1], Stanisław WIERCZYŃSKI[1], Massimo GUERRERO[2], Jarosław BIEGOWSKI[3], and Rui ALEIXO[3]

[1]University of Gdańsk, Gdańsk, Poland
✉ m.biungner.823@studms.ug.edu.pl; l.szopa.727@studms.ug.edu.pl; s.wierczynski.887@studms.ug.edu.pl

[2]University of Bologna, Bologna, Italy
✉ massimo.guerrero@unibo.it

[3]Institute of Hydro-Engineering of the Polish Academy of Sciences, Gdańsk, Poland
✉ jaroslawbiegowski@ibwpan.gda.pl; rui.aleixo@ibwpan.gda.pl

A b s t r a c t

In Leonardo Da Vinci's body of work, its genius is also expressed in his water flows drawings. In Da Vinci drawings, different fluid flow phenomena were illustrated e.g.: the impinging jet and the flow around obstacles. Aiming at obtaining more quantitative information about the drawings of Da Vinci an experimental setup was built at the Institute of Hydro-Engineering of the Polish Academy of Sciences to reproduce the impinging jet in a basin and measure it with modern measurement techniques such as imaging techniques with high-speed cameras. Although there is no quantitative data regarding Da Vinci's drawings, several educated guesses were made to estimate a range of flows and dimensions. Using imaging techniques, it was possible to characterize the dimensions and range of the jet for different flow rates, and by means of Particle Tracking Velocimetry, it was possible to characterize the induced velocity field in the stilling basin. These measurements have practical application since the impinging jet flow is currently used in cases such as: jet energy dissipation, fluid mixing, flow aeration, and turbulence studies.

Publications of the Institute of Geophysics, Polish Academy of Sciences
Geophysical Data Bases, Processing and Instrumentation
vol. 453 (E-14), 2025, pp. 41–43
DOI: 10.25171/InstGeoph_PAS_Publs-2025-036
XLII International School of Hydraulics, Radocza, Poland, 20–23 May 2025

Methodology to Study Plastic Transport Through Vegetated Channels

Łukasz PRZYBOROWSKI[1,✉], Anna M. ŁOBODA[1], Jarosław BIEGOWSKI[2], Zuzanna CUBAN[3], Tomasz KOLERSKI[3], Dariusz GĄSIOROWSKI[3], and Małgorzata ROBAKIEWICZ[2]

[1]Institute of Geophysics of Polish Academy of Sciences, Warsaw, Poland
✉ lprzyborowski@igf.edu.pl

[2]Institute of Hydro-Engineering of Polish Academy of Sciences, Gdańsk, Poland

[3]Gdańsk University of Technology, Gdańsk, Poland

Abstract

Observing the actual behaviour of floating plastic litter in the presence of vegetation in natural conditions should provide unique insights into the details of flow-biota-plastic interactions, needed for evaluating conceptual and numerical models. Therefore, a comprehensive approach to investigating the river plastic transport processes must include a description of various physical aspects. To address this, we propose a methodology encompassing in-situ measurements in a vegetated channel coupled with physical experiments in a controlled, full-scale laboratory channel. Both approaches will be used to prepare a numerical model and evaluate simulations of plastic transport.

1. STATE OF THE PROBLEM

There are significant research gaps on the subject of plastic transport processes in rivers (Al-Zawaidah et al. 2021), where riparian vegetation plays a major role (e.g. Cesarini and Scalici 2022). To date, only a limited number of studies with physical experiments have investigated this aspect, e.g. Valyrakis et al. (2024) explored how stem density affects the trapping of differently sized plastic pieces. The variability of plastic abundance along river channels is largely stochastic. However, several other factors can significantly influence plastic transport. The three most important deterministic factors at the catchment scale are flow regime, precipitation, and wind conditions (Roebroek et al. 2021). Then, narrowing the view on the phenomena of the river plastic transport to a river reach scale, aspects of vegetation and plastic properties will come into play on top of the channel hydrodynamics.

2. DESIGNED METHODOLOGY

To study plastic transport through a vegetated channels, we designed the following methodology, focusing on three work packages (WPs, Fig. 1).

The task WP1 is to gather hydrometric data about the water level and discharge through a hydrological year in a small, vegetated urban stream. Simultaneously, monitoring of plastic litter occurrence along the channel reach will be performed to determine influx, hotspots, and spatiotemporal changes in the plastic accumulation, concerning vegetation cover. The goal of this WP is not only to compile gathered data but also to provide necessary input for building and validating a numerical model of the flow and subsequently, particle transport.

The WP2 task is to conduct laboratory experiments in a channel with real vegetation, prepared according to preliminary surveys of the investigated stream, simulating it in a 1:1 scale. A series of experiments with various water depths and velocities will be conducted during two stages of plants' vegetative cycle and representative types of plastic litter will be released in uniform batches. The goal is to observe and analyze litter paths by utilising particle tracking velocimetry. Litter travel time and identified accumulation zones in relation to channel conditions will then be compared to field surveys.

The WP3 has two goals: to build a 2D mathematical model of floating plastic transport and to reproduce in numerical simulations (like Delft 3D) both laboratory experiments and investigated channel hydrodynamics. Detailed experiments describing the real behaviour of plastic litter and field data will primarily serve as calibration/validation material for the models. Such an approach will allow us to immediately determine whether numerical simulations can reliably predict the dynamics of plastic transport and accumulation hot spots.

The results of this project will provide a more objective view of the floating plastic transport phenomenon in rivers. By combining different approaches to the problem, a new, detailed and evaluated description will be produced, with the ability to simulate and predict floating plastic transport. Understanding the locations and mechanisms of plastic accumulation within vegetated rivers will contribute to the optimization of existing and the development of novel plastic removal techniques, and to the preparation of enhanced accumulation maps, particularly in areas where remote sensing data is limited.

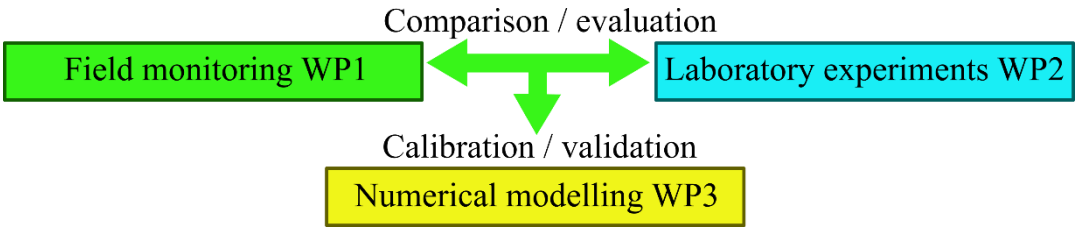

Fig. 1. Methodology scheme.

Acknowledgements. This research was funded in whole by the National Science Centre, Poland, Grant number 2023/51/D/ST10/02488.

References

Al-Zawaidah, H., D. Ravazzolo, and H. Friedrich (2021), Macroplastic in rivers: present knowledge, issues and challenges, *Environ. Sci. Process. Impacts* **23**, 4, 535–552, DOI: 10.1039/D0EM00517G.

Cesarini, G., and M. Scalici (2022), Riparian vegetation as a trap for plastic litter, *Environ. Poll.* **292**, B, 118410, DOI: 10.1016/j.envpol.2021.118410.

Roebroek, C.T.J., R. Hut, P. Vriend, W. de Winter, M. Boonstra, and T.H.M. van Emmerik (2021), Disentangling variability in riverbank macrolitter observations, *Environ. Sci. Technol*. **55**, 8, 4932–4942, DOI: 10.1021/acs.est.0c08094.

Valyrakis, M., G. Gilja, D. Liu, and G. Latessa (2024), Transport of floating plastics through the fluvial vector: The impact of riparian zones, *Water* **16**, 8, 1098, DOI: 10.3390/w16081098.

Publications of the Institute of Geophysics, Polish Academy of Sciences
Geophysical Data Bases, Processing and Instrumentation
vol. 453 (E-14), 2025, pp. 45–48
DOI: 10.25171/InstGeoph_PAS_Publs-2025-037
XLII International School of Hydraulics, Radocza, Poland, 20–23 May 2025

Investigating the Change in River Bed Morphology under the Influence of Blockage – Physical Modelling in a Curved Laboratory Channel

Zuzanna CUBAN✉, Magdalena WIŚNIEWSKA, and Tomasz KOLERSKI

Gdańsk University of Technology, Gdańsk, Poland
✉ zuzana.cuban@pg.edu.pl

A b s t r a c t

River restoration and pro-ecological design are essential in modern hydrotechnical projects, yet guidelines for the design of sinuous channels with erodible beds under blockage conditions remain lacking. This study investigates the effects of blockages – caused by ice, debris or litter – on sediment transport and river bed morphology. Experiments were conducted in a 2 m wide, 60 m long meandering channel with a sediment recirculation system. Velocity was measured using ADV and PTV and bathymetric data was collected using a FARO 3D scanner. The results show how blockages disrupt flow, increase turbulence, and intensify sediment transport, providing critical insights for designing resilient, ecologically functional river channels.

1. INTRODUCTION

The restoration of rivers and the design of pro-ecological solutions are now standard practices in the modernisation and construction of hydrotechnical structures. Numerous guidelines have been developed for the design of sinuous riverbeds in order to optimise both ecological functions (providing habitat for the development of flora and fauna) and hydraulic performance (maintaining the correct flow height, capacity, etc.) (RRC 2002, Rohde et al. 2005, Soar and Thorne 2001). However, there is still a clear need for specific guidelines for the design of sinuous channels with erodible beds to take account of blockages.

Blockages are increasingly caused not only by seasonal (e.g. ice) or local (e.g. fallen trees) obstructions, but also by an increase in litter blockages. Such litter often enters surface waters as a result of improper waste management, illegal dumping or run-off from urban areas during heavy rainfall. In this study, a blockage is defined as an accumulation of floating material that completely covers the water surface over a given area.

A blockage significantly changes the hydrodynamics of the river cross-section where it occurs. The first visible effect is an increase in the wetted perimeter and a reduction in the cross-sectional flow area below the obstruction. This results in higher average flow velocities and shifts the maximum velocity closer to the river bed. Obstructions such as ice jams, fallen trees or debris typically have irregular shapes which, when submerged, disrupt local flow patterns and create increased turbulence. The increased flow and turbulence enhance sediment transport, which is controlled by factors such as flow velocity (especially the vertical component), channel geometry, and sediment characteristics (e.g. shape, size, and concentration). Uncontrolled sediment discharge can lead to local erosion and deepening of the river bed and banks.

This study aims to advance the understanding of how blockages impact sediment transport and riverbed dynamics, providing insights critical for the ecological and hydraulic design of meandering river channels.

2. METHODOLOGY

2.1 Experimental setup

The research was conducted in a curved, meandering channel located at IBW PAN. The channel, shown in Fig. 1a, is 2 m wide and 60 m long along its axis. A reservoir at the end of the channel collects sediment, which is pumped back to the beginning of the channel, providing a constant supply of sediment during the experiments. This setup allows precise modelling of large-scale river bed formation phenomena.

The blockage was made up of 0.5 litre polypropylene plastic bottles, as shown in Fig. 1b.

2.2 Velocity measurements

Velocity measurements were made using Acoustic Doppler Velocimeters (ADV) at the cross sections shown in Fig. 1a. In each cross section, 2–5 vertical profiles were defined (depending on the bed configuration) and velocity was measured at 1 to 4 points per vertical profile.

Surface velocity was determined using Particle Tracking Velocimetry (PTV). High resolution cameras were used to record wood particles floating on the water surface. After removing camera and perspective distortions, the velocity was calculated from the film frames.

a) b)

Fig. 1: a) Photo of the laboratory channel. The measured cross sections are marked in blue. The white dashed line indicates where the blockage started; b) Photo of a blockage formed by bottles in a laboratory channel.

2.3 Bathymetry

A FARO Focus 3D scanner was used to collect full bathymetric data. Images from 25 points around the site were used to create a point cloud, resulting in a three-dimensional bathymetric map. In addition, bathymetric measurements were taken manually in all cross sections during velocity measurements.

2.4 Grain size analysis

After each series of experiments, sediment samples were collected at three locations in each cross section: the channel centreline and 20 cm from each channel wall. These samples were subjected to grain size analysis.

3. RESULTS

The placement of a blockage in the channel has caused significant changes in the channel bed morphology, as shown in Fig. 2. The presence of the blockage resulted in a reduction of the average sand layer thickness upstream of the blockage by 5 cm relative to the initial condition. During the initial conditions, sediment accumulation occurs along the inner bend of the channel, while scouring takes place along the outer bend. In contrast, with the blockage placed, sediment is eroded more uniformly across the entire width of the channel. Additionally, significant erosional changes have been observed along the outer bend at the front of the blockage, with a maximum depth of 15 cm compared to the initial state.

These changes are driven by modifications in the velocity profile and an increase in flow velocity caused by the local reduction in flow depth due to the blockage. Furthermore, the introduction of the blockage increases the surface roughness, which alters the transverse velocity direction. Under free conditions, this process leads to erosion of the outer bank and deposition of sediment on the inner bend of the meander.

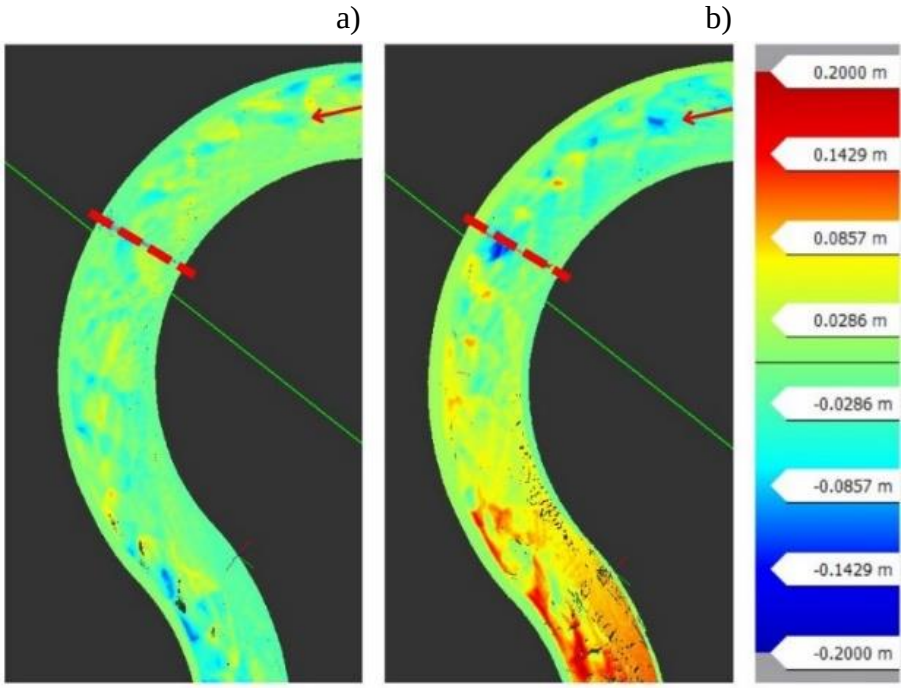

Fig. 2: a) Scan of the laboratory channel before the obstruction occurred; b) Scan of the laboratory channel after the obstruction was created using empty bottles with a constant flow maintained in the channel for 4 hours. The red dashed line indicates the grid visible in Fig. 1b, and the red arrow indicates the direction of flow.

Further research will be conducted under various flow conditions and different blockage configurations to better understand the impact of these factors on channel bed morphology and flow dynamics.

References

Rohde, S., M. Schütz, F. Kienast, and P. Englmaier (2005), River widening: An approach to restoring riparian habitats and plant species, *River Res. Appl*. **21**, 10, 1075–1094, DOI: 10.1002/rra.870.

RRC (2002), Manual of river restoration techniques, River Restoration Centre, Silsoe, U. K.

Soar, P.J., and C.R. Thorne (2001), Channel Restoration Design for Meandering Rivers, Final Report, Coastal and Hydraulics Laboratory, ERDC/CHL CR-01-1, U.S. Army Corps of Engineers, Washington, DC, 454 pp.

Publications of the Institute of Geophysics, Polish Academy of Sciences
Geophysical Data Bases, Processing and Instrumentation
vol. 453 (E-14), 2025, pp. 49–49
DOI: 10.25171/InstGeoph_PAS_Publs-2025-038
XLII International School of Hydraulics, Radocza, Poland, 20–23 May 2025

Sediment Yields Estimation under Climate Change and Land Use Impact of the Upper Catchment of the Tuul River Basin in Mongolia

Ganzorig SHARAV[1,✉], Ayurzana BADARCH[1], Gomboluudev PUREVJAV[2], and Byamba-Ochir MUNKHNAIRAMDAL[1]

[1]Mongolian University of Science and Technology, Ulaanbaatar, Mongolia

[2]Information and Research Institute of Meteorology, Hydrology and Environment, Ulaanbaatar, Mongolia

✉ ganzorig@prestige.mn

A b s t r a c t

The upper catchment of the Tuul River basin (TRB) is the most stressed watershed, containing over half of Mongolia's total population, accounting for more than 60% of the country's GDP. Although the upper catchment of the TRB is protected, recent changes in land use and climate change have had a significant impact on it, resulting in increased land degradation. This has had a negative impact on the river's ecological health and creates challenges for sustainable water management. Therefore, it is critical to assess current sediment yield as well as potential changes due to climate and land use change. In this study, we used the RUSLE model to estimate the sediment yield under current and future conditions for the upper TRB catchment. According to the current estimation, sediment yield values in the study area were as follows: 52.8% of the area exhibited 0–5.1 t/km²/year, 39.3% exhibited 5.1–17.8 t/km²/year, and 7.9% exhibited 17.8–70.5 t/km²/year. According to future precipitation trends, winter precipitation is expected to rise by up to 60.0%, spring by 25.9%, and autumn by 27.8%. In contrast, summer precipitation is expected to either decrease by up to 5.3% or increase by up to 2.3%. The effect of these climatic and expected land use changes on sediment yield by 2040 was up to a 76% increase compared to 2024 and recommendations for integrated water resource management together with the comprehensive land management made based on the findings.

Publications of the Institute of Geophysics, Polish Academy of Sciences
Geophysical Data Bases, Processing and Instrumentation
vol. 453 (E-14), 2025, pp. 51–53
DOI: 10.25171/InstGeoph_PAS_Publs-2025-039
XLII International School of Hydraulics, Radocza, Poland, 20–23 May 2025

Satellite Imagery in Hydraulic Research

Niklas EICKELBERG and Jochen ABERLE

Leichtweiß-Institute for Hydraulic Engineering and Water Resources,
Technische Universität Braunschweig, Braunschweig, Germany

✉ n.eickelberg@tu-braunschweig.de; jochen.aberle@tu-braunschweig.de

Abstract

This study, conducted in the framework of the Future Lab Water project funded by the Federal State of Lower Saxony, Germany, explores the potential of satellite imagery in hydraulic research, focusing on floodplain vegetation roughness. A Machine Learning (ML) framework will be developed to derive accurate estimates of vegetation parameters, such as Leaf Area Index (LAI) and vegetation height, from Moderate-resolution Imaging Spectroradiometer (MODIS) and ICESat-2 via high resolution Sentinel data. These parameters will be used to calculate vegetation roughness maps through formulas developed for flexible, foliated vegetation, enhancing the accuracy of flood modeling with openly accessible satellite data.

The presently ongoing Future Lab Water project is a collaborative project involving multiple research facilities in the federal state of Lower Saxony in Germany. It addresses various water-related challenges that can be enhanced using digitalization and artificial intelligence such as detection of water- and energy usage in agriculture, retrieving river morphology and vegetation characteristics by publicly provided data and black box models to estimate flood extend in real time. The present paper introduces details of a sub-project focusing on the determination of vegetation characteristics on floodplains making use of advances in remote sensing technologies that have enabled the collection of geospatial data with unprecedented accuracy.

Alongside drone imagery and aerial surveys, satellite-based imagery has become a powerful tool for scientific research and environmental monitoring. Due to the high spatial and temporal resolution, satellite data provide valuable solutions for assessing critical parameters in fluvial environments. For example, the European Earth Observation Copernicus Programme captures radar and multispectral images at resolutions of up to 10 meters per pixel with a revisit cycle of less than a week (Liang et al. 2024, Radočaj et al. 2020). Multispectral sensors like Sentinel-2 and Landsat 9 record certain spectral band widths. By analysing the spectral reflectance or the combination of multiple spectral bands with indices such as the Normalized Difference Water Index (NDWI) and the Normalized Difference Vegetation Index (NDVI), valuable information

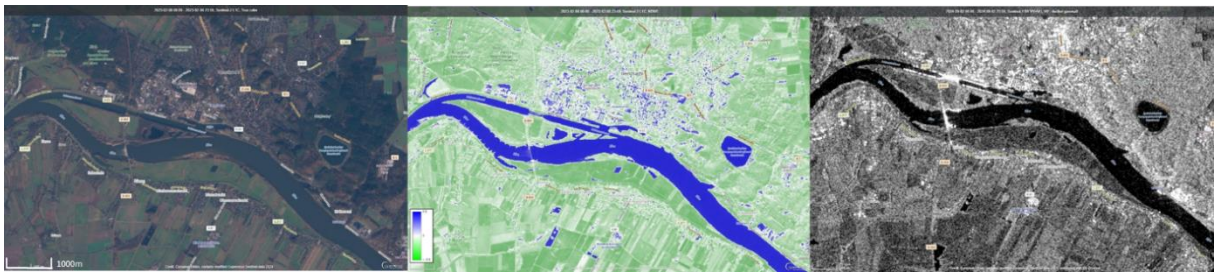

Fig. 1. Comparison of a true-color image (left), a NDWI image (middle) derived from Sentinel-2, and a SAR image (right) from Sentinel-1, showing the Elbe River at Geesthacht, Germany. Copernicus Sentinel-2 imagery was acquired on August 2, 2023, and Copernicus Sentinel-1 imagery on September 2, 2024 downloaded on September 6, 2024. Map data © OpenStreetMap contributors, licensed under the Open Database License (ODbL). Analysis and visualization were conducted in QGIS.

regarding the land cover can be derived. Active sensors, such as the Sentinel-1 Synthetic Aperture Radar (SAR) satellite, have the advantage that their signal can penetrate cloud cover and deliver valuable information also during night-time with high temporal and spatial resolution (see Fig. 1). By analysing the reflectance value, information concerning the surface roughness and the moisture of soil and vegetation can be estimated (Radočaj et al. 2020).

In the field of environmental hydraulics multiple studies have been conducted using satellite imagery data in combination with digital elevation models and artificial intelligence to, for example, estimate sediment transport rates (Kryniecka et al. 2022), extract small water bodies (Sun and Li 2024), and determine vegetation borders (Muir et al. 2024) as well as vegetation characteristics (Fortes et al. 2024), to name just a few recent applications. Especially the latter aspect is of interest for the inclusion of novel approaches for the determination of the flow resistance of flexible foliated vegetation in hydrodynamic models. In this context, Folke (2023) developed a hybrid equation for submerged flexible vegetation by combining the formulas of Järvelä (2004) and Baptist et al. (2007) and showed that it delivered the most accurate results with close proximity to the original formula of Järvelä (2004) compared to other approaches. The equation was also tested in a nature-scale hydraulic simulation with vegetation parameters derived by Airborne Laser Scanning (ALS) during the low vegetation period to create DEMs. Folke (2023) suggested to use image-based solutions to acquire data at high temporal and spatial scales in different vegetation periods to effectively model flooding scenarios and acquire validation data for the hydraulic models based on new vegetation roughness formulas to improve the accuracy in vegetation roughness and flood prediction.

So far, the application of such novel approaches in combination with remote sensing data has been limited in practice and the objective of the present FLW-sub project is therefore to determine the roughness of flexible, foliated riparian vegetation with high spatial and temporal resolution using satellite data. In order to derive required vegetation parameters, it is planned to downscale data from Moderate-resolution Imaging Spectroradiometer (MODIS) for accurate estimates of the Leaf Area Index (LAI) (e.g. Fortes et al. 2024) and ICESat-2 data for accurate vegetation heights (e.g. Xi et al. 2022) via Sentinel-2 data as well as Sentinel-1 data for the latter. This will enable the derivation of vegetation roughness maps with high temporal and spatial resolution that can be used to validate hydraulic simulations on past scenarios and to carry out simulations with, more or less, real time data. This will improve the flood prediction accuracy with benefits in the protection of infrastructure and human lives.

Acknowledgements. This project was funded by the Future Lab Water initative by the federal state of Lower Saxony, Germany.

References

Baptist, M.J., V. Babovic, J. Rodríguez Uthurburu, M. Keijzer, R.E. Uittenbogaard, A. Mynett, and A. Verwey (2007), On inducing equations for vegetation resistance, *J. Hydraul. Res.* **45**, 4, 435–450, DOI: 10.1080/00221686.2007.9521778.

Folke, F. (2023), Abbildung der Rauheitswirkung von Vorlandvegetation in der ingenieurtechnischen Anwendung, Karlsruhe: Bundesanstalt für Wasserbau, BAW Dissertationen 2625-8072, 7, available from https://hdl.handle.net/20.500.11970/112739 (accessed: 22 August 2023).

Fortes, A.A., M. Hashimoto, K. Udo, and K. Ichikawa (2024), Satellite and UAV derived seasonal vegetative roughness estimation for flood analysis, *Proc. IAHS* **386**, 203–208, DOI: 10.5194/piahs-386-203-2024.

Järvelä, J. (2004), Determination of flow resistance caused by non-submerged woody vegetation, *Int. J. River Basin Manage*. **2**, 1, 61–70, DOI: 10.1080/15715124.2004.9635222.

Kryniecka, K., A. Magnuszewski, and A. Radecki-Pawlik (2022), Sentinel-1 satellite radar images: A new source of information for study of river channel dynamics on the Lower Vistula River, Poland, *Remote Sens*. **14**, 5, 1056, DOI: 10.3390/rs14051056.

Liang, S., T. He, J. Huang, A. Jia, Y. Zhang, Y. Cao, X. Chen, X. Chen, J. Cheng, B. Jiang, H. Jin, A. Li, S. Li, X. Li, L. Liu, X. Liu, H. Ma, Y. Ma, D-X. Song, L. Sun, Y. Yao, W. Yuan, G. Zhang, Y. Zhang and L. Song (2024), Advancements in high-resolution land surface satellite products: A comprehensive review of inversion algorithms, products and challenges, *Sci. Remote Sens*. **10**, 100152, DOI: 10.1016/j.srs.2024.100152.

Muir, F.M.E., M.D. Hurst, L. Richardson-Foulger, A.F. Rennie, and L.A. Naylor (2024), VedgeSat: An automated, open-source toolkit for coastal change monitoring using satellite-derived vegetation edges, *Earth Surf. Process. Land*. **49**, 8, 2405–2423, DOI: 10.1002/esp.5835.

Radočaj, D., J. Obhođaš, M. Jurišić, and M. Gašparović (2020), Global open data remote sensing satellite missions for land monitoring and conservation: A review, *Land* **9**, 11, DOI: 10.3390/land9110402.

Sun, Q., and J. Li (2024), A method for extracting small water bodies based on DEM and remote sensing images, *Sci. Rep*. **14**, 1, 760, DOI: 10.1038/s41598-024-51346-7.

Xi, Z., H. Xu, Y. Xing, W. Gong, G. Chen, and S. Yang (2022), Forest canopy height mapping by synergizing ICESat-2, Sentinel-1, Sentinel-2 and topographic information based on machine learning methods, *Remote Sens.* **14**, 2, 364, DOI: 10.3390/rs14020364.

Publications of the Institute of Geophysics, Polish Academy of Sciences
Geophysical Data Bases, Processing and Instrumentation
vol. 453 (E-14), 2025, pp. 55–58
DOI: 10.25171/InstGeoph_PAS_Publs-2025-040
XLII International School of Hydraulics, Radocza, Poland, 20–23 May 2025

Comparison of 2D HEC-RAS Modeling with the Observed September 2024 Flood in Poland: A Case Study of the Bóbr River in Bolesławiec

Krzysztof ZAMIAR

Wrocław University of Science and Technology, Poland

✉ krzysztof.zamiar@pwr.edu.pl

1. INTRODUCTION

As part of the work on the Technical and Economic Analysis of the Construction of a Small Hydropower Plant in Bolesławiec, commissioned by Przedsiębiorstwo Wodociągów i Kanalizacji Sp. z o.o. Bolesławiec, a hydrodynamic model of a section of the Bóbr River was developed (Kostecki et al. 2024). This abstract highlights the key information of the research, which involved 2D modeling using HEC-RAS software to analyze flood propagation during the September 2024 flood event on the River Bóbr in Bolesławiec, Poland. The modeling results are compared with real-world conditions recorded during that period.

2. MODEL DESCRIPTION

The main purpose of the primary work was to analyze the impact of a Small Hydropower Plant in Bolesławiec, located at kilometer 145+000 of the River Bóbr. To conduct this analysis, a geodetic survey was carried out on the section between kilometer 144+700 and 145+200, covering 10 cross-sections (Short Model) as shown in Fig. 2. Additionally, a site inspection was performed, and the basic dimensions of bridges located downstream of the analyzed section were inventoried. The surveyed cross-sections were used to update the publicly available Digital Terrain Model through interpolation along the river axis, using a tool in HEC-RAS. The characteristic flows and flows with specified probabilities of occurrence were determined based on data from the "Dąbrowa Bolesławiecka" gauging station, located 7 kilometers downstream of the study area (Kostecki et al. 2024).

For model calibration, Flood Hazard Maps were utilized, particularly data from three points within the analyzed section. Due to challenges in obtaining reliable results, multiple calibration tests were conducted. One of the proposed solutions involved extending the model's range from approximately kilometer 143+800 to kilometer 148+000 (Full Model) as shown in Fig. 1. The

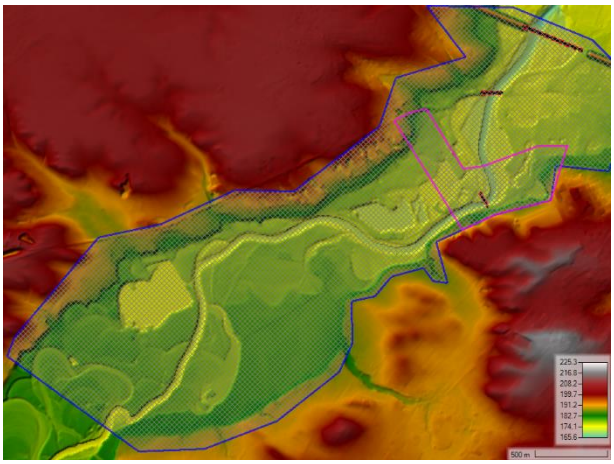

Fig. 1. Model map. Short Model – pinkcontour, Full Model – blue contour.

Fig. 2. Short Model map. Short Model – pink contour, black lines – locations of measured cross-sections, orange dots – locations of calibration points.

river bathymetry for the additional sections was extrapolated with the assumption that results for this portion may be less reliable. Implementing this solution allowed for the inclusion of two bridges located downstream of the analyzed section. The upstream boundary condition was defined as a "flow hydrograph" and the downstream boundary condition was defined as "normal depth" (the boundary condition where the energy slope is set). Two different sets of equations were tested: Diffusion Wave Equations (DWE) and Shallow Water Equation (SWE). Calibration results for Q1%, based on the Flood Hazard Map (ISOK 2025), are presented in Table 1. The bed friction was set as Manning *n* value: 0.035 for river bed, and 0.120 for floodplains. The grid size of the model ranged from 2 m by 2 m in the main channel to 15 m by 15 m in the floodplain areas.

3. CALIBRATION RESULTS

Table 1
Calibration results

	Location (kilometer of the River Bóbr)			144+916	145+177	145+204	
Model variants	Calibration tests			Water surface elevation [m a.s.l.]			Δ [m]
0	ISOK flood hazard map Q1%			174.38	174.87	174.99	–
1	Short Model	DWE	Downstream normal depth 0.002	173.669	174.314	174.926	0.52
2	Short Model	DWE	Downstream normal depth 0.001	174.343	174.728	175.033	0.09
3	Short Model	SWE	Downstream normal depth 0.002	173.663	174.696	175.075	0.43
4	Short Model	SWE	Downstream normal depth 0.001	174.354	174.941	175.190	0.12
5	Full Model	DWE	Downstream normal depth 0.002	174.408	174.768	175.080	0.08
6	Full Model	DWE	Downstream normal depth 0.001	174.400	174.764	175.038	0.07
7	Full Model	SWE	Downstream normal depth 0.002	175.254	175.538	175.746	0.77

where:

$$\Delta_{\mathrm{k}} = \sqrt{\frac{1}{n}\sum_{i=1}^{n=3}\left(WSE_{k,i} - WSE_{ISOK,i}\right)^2} \quad (1)$$

WSE – water surface elevation [m a.s.l.], *k* – variant number, *i* – location.

The results from variants 1 to 4 show significant changes in water levels when the normal depth was adjusted from 0.001 to 0.002. Since the actual value of the normal depth is difficult to determine precisely, the Full Model was considered significantly more reliable due to the distinctly smaller differences between variants 5 and 6. The application of the Shallow Water Equation (SWE) yielded less accurate results, particularly for the Full Model (variant 7). Additionally, SWE proved to be six times more computationally demanding than the Diffusion Wave Equations (DWE).

In conclusion, the Full Model DWE was deemed the most suitable approach as it provides satisfactory accuracy compared to ISOK, is not sensitive to changes in the boundary conditions, and is less computationally expensive than the SWE model.

4. FLOOD EVENT

In September 2024, a flood caused by the Genoa low-pressure system resulted in catastrophic consequences, leading to the declaration of a state of natural disaster (Rozporządzenie RM 2024). The River Bóbr experienced exceptionally high water levels, significantly impacting the town of Bolesławiec, which is represented in the numerical model. Using data from the Polish Institute of Meteorology and Water Management (IMGW) gauging station at Dąbrowa Bolesławiecka (Hydro IMGW-PIB 2025), the model was validated against the actual flood situation. The flow rates were input to reflect the real conditions without introducing any additional modifications

The obtained results satisfactorily align with the actual situation. Figure 3 shows that the flood-affected area in the model closely matches the real-world extent. This is particularly evident in the western region, where a large building with a red roof was impacted by the flood, while neighboring buildings situated slightly higher remained outside the inundation zone.

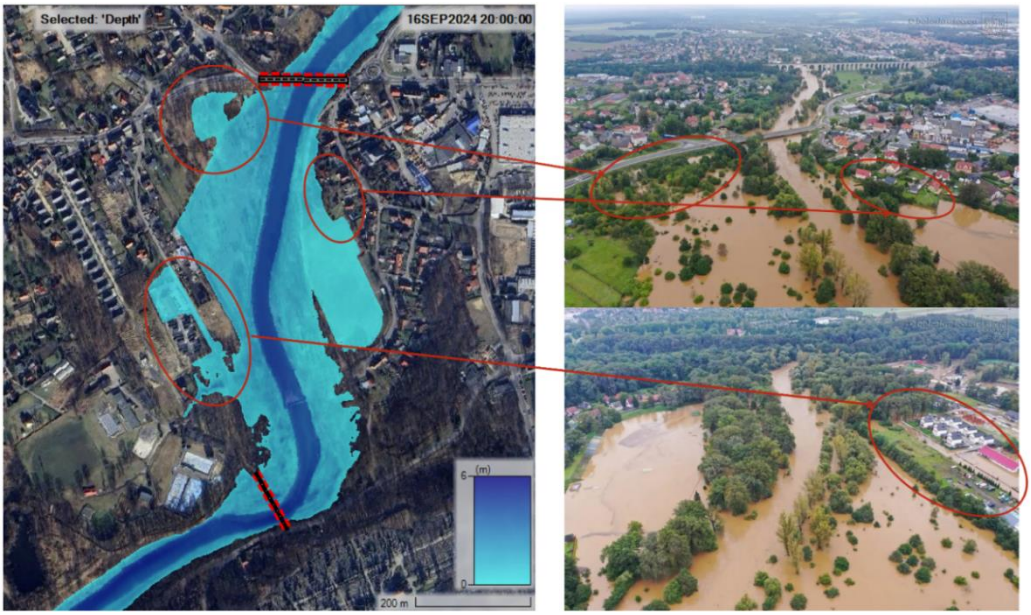

Fig. 3. Comparison of the results for the September 2024 flood, performed using the Full Model DWE, with the actual flood situation shown in the photos presented in Miasto Bolesławiec (2024).

5. CONCLUSION

The presented model successfully passed verification against the September flood, confirming the effectiveness of this tool. The calibration technique employed, based on results from the ISOK Flood Hazard Maps and the extrapolation of riverbed geometry data, proved effective and reduced the uncertainty associated with assuming a single normal depth value for the downstream boundary condition. Satisfactory results were achieved, even in areas extending beyond the more accurately modeled section of the river.

References

Miasto Bolesławiec (2024), Bolesławiec walczy z wodą (photos showing the city of Boleslawiec during the floods), Facebook, published at 17:20, available from: https://www.facebook.com/share/p/18A6fi9vC9/ (accessed: 16 September 2024).

Kostecki, S., J. Machajski, and K. Zamiar (2024), Analiza techniczno-ekonomiczna budowy małej elektrowni wodnej w Bolesławcu w km 145+000 biegu rzeki Bóbr, Raport series SPR no. 62/2024, Wrocław University of Science and Technology, Wrocław.

ISOK (2025), Mapa zagrożenia powodziowego z głębokością wody Q1%, Państwowe Gospodarstwo Wodne Wody Polskie, Informatyczny System Osłony Kraju, available from: https://wody.isok.gov.pl/ imap_kzgw/?gpmap=gpMZP.

Hydro IMGW-PIB (2025), Gauging station at Dąbrowa Bolesławiecka, Polish Institute of Meteorology and Water Management IMGW, available from: https://hydro.imgw.pl/#/station/hydro/151150140?h=1009.

Rozporządzenie RM (2024), Rozporządzenie Rady Ministrów z dnia 16 września 2024 r. w sprawie wprowadzenia stanu klęski żywiołowej na obszarze części województwa dolnośląskiego, opolskiego oraz śląskiego, Dz. U. z 2024 r., poz. 1365.

Publications of the Institute of Geophysics, Polish Academy of Sciences
Geophysical Data Bases, Processing and Instrumentation
vol. 453 (E-14), 2025, pp. 59–59
DOI: 10.25171/InstGeoph_PAS_Publs-2025-041
XLII International School of Hydraulics, Radocza, Poland, 20–23 May 2025

Hydraulics, Water Quality, Biodiversity and Policy Research to Support Nature-based Water Management using Vegetated Floodplains

Kaisa VÄSTILÄ

Aalto University, Aalto, Finland

✉ kaisa.vastila@aalto.fi

A b s t r a c t

There are increasing needs to bring more of the lost riparian ecosystem functions back to human-impacted streams. Nature-based solutions (NbS), such as vegetated floodplains, aim at improving the state of the ecosystem while addressing the water management needs of the society. However, there are substantial knowledge gaps on how to efficiently implement and up-scale NbS considering e.g. the complex societal boundary conditions and the multi-faceted impacts of vegetation on the physico-chemico-biological environment. This contribution aims at describing research developments by the author and a large number of colleagues on floodplain vegetation as well as linking the findings with the mainstreaming of NbS with vegetated floodplains. Firstly, I will describe findings on the impacts of flexible woody vegetation on flow processes as well as some proposed modeling approaches. Secondly, I will present two-stage channels with vegetated floodplains as an example of a NbS for agricultural streams. I will cover recent findings on the performance of two-stage channels from the viewpoints of fine sediment transport, water quality, and biodiversity. Thirdly, I will show examples of how the research on natural sciences and engineering can be complemented with considerations of costs, benefits, financing, governance, and capacity. In conclusion, the combination of these various aspects enables making changes in the associated water and river management practices and policies.

Publications of the Institute of Geophysics, Polish Academy of Sciences
Geophysical Data Bases, Processing and Instrumentation
vol. 453 (E-14), 2025, pp. 61–64
DOI: 10.25171/InstGeoph_PAS_Publs-2025-042
XLII International School of Hydraulics, Radocza, Poland, 20–23 May 2025

Velocity Fields around Single and Interacting Particles Sinking in Mucus-rich Water

Magdalena MROKOWSKA[1,✉], Arkadiusz ANTONOWICZ[2], Anna KRZTOŃ-MAZIOPA[3], Sylwia RÓŻAŃSKA[4], Ewelina WARMBIER-WYTYKOWSKA[4], and Peter FISCHER[5]

[1]Institute of Geophysics, Polish Academy of Sciences, Warsaw, Poland

[2]Eurotek International Sp. z o.o., Warsaw, Poland

[3]Warsaw University of Technology, Faculty of Chemistry, Warsaw, Poland

[4]Poznań University of Technology, Faculty of Chemical Technology, Poznań, Poland

[5] ETH Zürich, IFNH Food Process Engineering Group, Zürich, Switzerland

✉ m.mrokowska@igf.edu.pl

Abstract

Exopolymers dispersed in water create mucus-rich environments that can modify sedimentation dynamics when secreted in excess by microorganisms. Here we use PIV measurements combined with shear and extensional rheology to demonstrate non-Newtonian effects of mucus-rich water including extended flow, negative wake, and aggregation of solid spheres in test solutions. The methodology designed in this study allows the future development of analogue experiments to model the sinking dynamics of microplastic pollutants and mineral grains and organic aggregates in algal bloom-afflicted regions or wastewater treatment plants.

1. INTRODUCTION

Natural waters gain non-Newtonian properties when exopolymers (EPS) are excessively secreted by algae and bacteria (Jenkinson 1986), which affects the sinking dynamics of particles, e.g., microplastics (Mrokowska and Krztoń-Maziopa 2024). However, the influence of mucus on the flow field around sinking particles remains elusive.

Aqueous solutions of polysaccharides, which dominate mucus as EPS display shear-thinning and viscoelastic properties. These non-Newtonian systems can induce distinct flow behaviour, such as forming extended or negative wakes behind sinking particles. Moreover, particles sinking on top of one another in shear-thinning thixotropic liquids may experience mutual attraction (Zenit and Feng 2018). Nevertheless, the specific effects of mucus-rich environments on particle dynamics are still unclear. The present study aims to identify velocity field patterns around particles sinking in such conditions. Here we used xanthan gum as a proxy for EPSs to address the flow field around solid spheres in mucus-rich aqueous environments.

2. MATERIALS AND METHODS

Two solutions of XG (Sigma Aldrich) in distilled water with concentrations of 0.75 gL^{-1} (XG 0.75) and 1.25 gL^{-1} (XG 1.25) were studied. The density of solutions, ρ_f, was measured using DMA 4100 M densimeter (Anton Paar), shear rheology with a Physica MCR 301 rheometer with coaxial cylinders measuring geometry (0.714 mm gap), and extensional rheology using Extensional Capillary Breakup Extensional Rheometer (CaBER, ThermoFisher). Three types of test spheres were made of POM (polyoxymethylene) – diameters, d = 5.00 mm (S1), and 4.00 mm (S2), density, ρ_p = 1.37 g cm^{-3}, and made of Si_3N_4, d = 2.38 mm (S3), ρ_p = 3.20 g cm^{-3}.

The test liquid in a transparent settling tank was seeded with fluorescent PMMA particles (1–20 μm). A vertical laser sheet (green light, Nd:YAG double-pulsed laser) was aligned with the trajectory of a falling sphere. Camera images (2448×2048 pixel, 124 Hz) were processed using Dantec Dynamic Studio and custom scripts in Matlab®. Adaptive PIV analysis was applied to compute instantaneous velocity vector fields. The average sinking velocity of spheres, U, was estimated from time-resolved particle position data derived from PIV images.

3. RESULTS

Test liquids demonstrated shear-thinning behaviour, with a power-law region corresponding to shear rates, $\dot{\gamma}$, typical for sinking test particles (32–200 s^{-1}) along with slight thixotropy (Fig. 1a). Moreover, the liquids showed stretching characterised by extensional viscosity (Fig. 1b), with the Trouton ratio (extensional viscosity, η_E (Fig. 1b) to shear viscosity, η (Fig. 1a)) for sinking particles ranging from 18 to 57. Both viscosities were higher for XG1.25 due to a more entangled network in the dispersion of larger polymer content.

The flow field around spheres sinking with modified Reynolds number ($\rho_f Ud/\eta$) between 9 and 80 displayed non-Newtonian characteristics (Fig. 2a). Velocity profiles in front of a sphere (Fig. 2b) were similar for the three test particles, with distances z/d = 3.5 for XG0.75 and 4.5

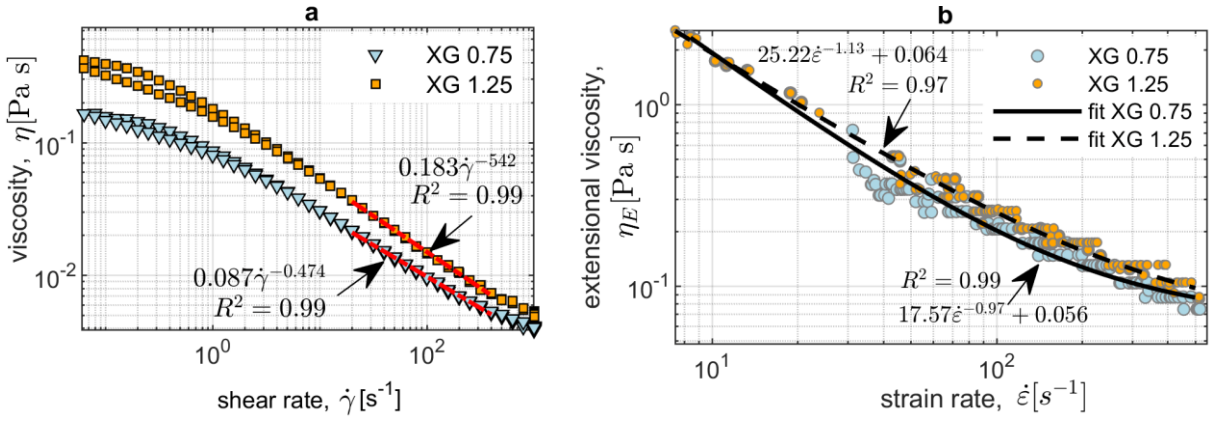

Fig. 1. Viscosities of xanthan-based liquids: a) shear viscosity curves with slight thixotropy and power-law fitted region indicated by red lines; b) extensional viscosity curves with power function fitting.

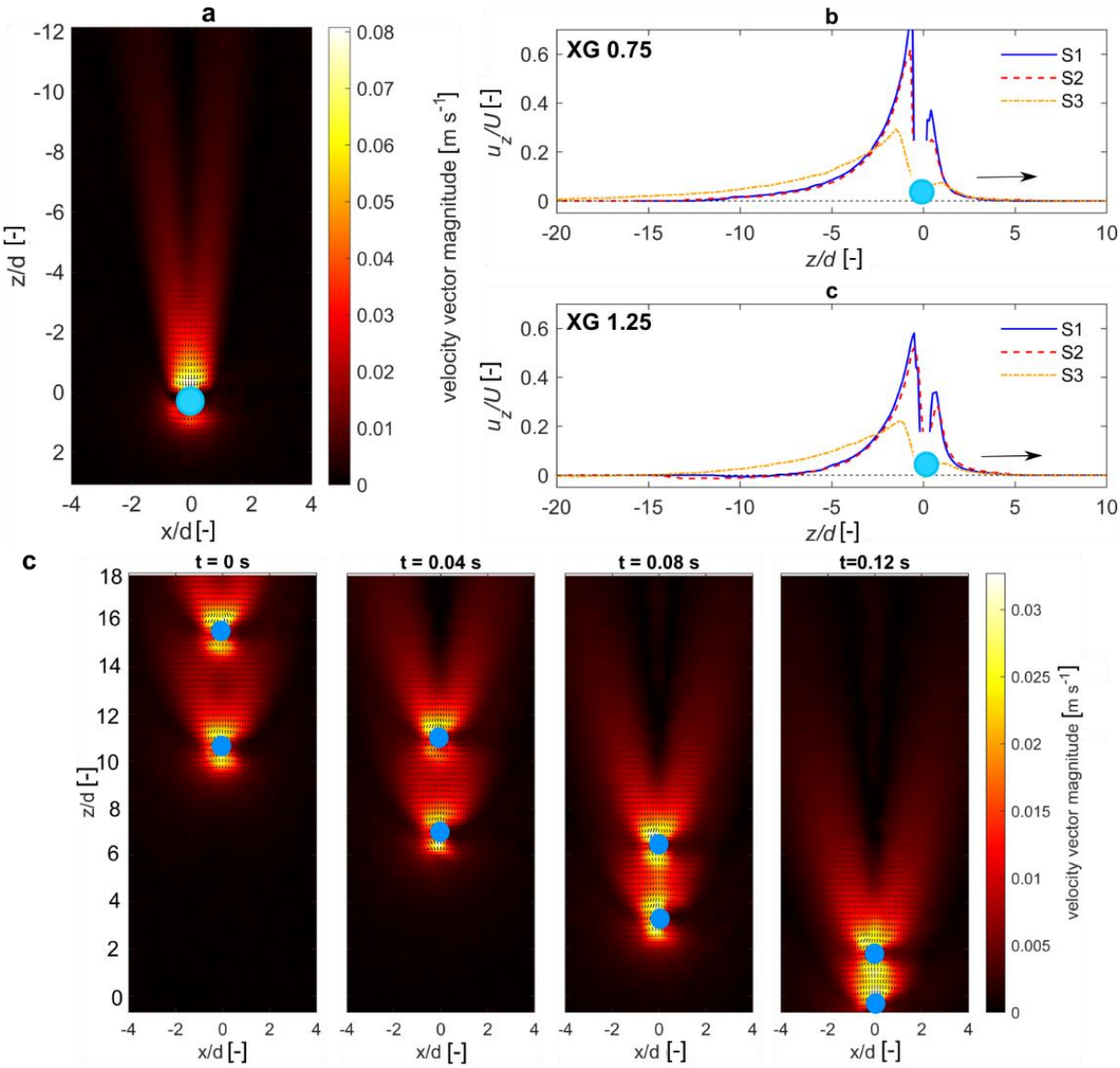

Fig. 2. Instantaneous velocity field around sinking spheres: a) S1 sinking in XG0.75; b) non-dimensional fluid velocity at the vertical centerline of spheres in XG0.75 and XG1.25, arrow indicates sinking direction; c) velocity fields around interacting spheres sinking in XG1.25 solution, negative wake visible.

for XG1.25. The greater extent in XG1.25 can be attributed to a more structured polymeric network. The wake's shape behind a sphere varied depending on the type of solution, showing a predominantly extended wake pattern, with the onset of negative wake in XG1.25. Figure 2b shows that stagnation points formed closer to S1 and S2 than for S3 particles (e.g., $z/d = 8$ for S1, S2, and $z/d = 15$ for S3 in XG1.25). This was accompanied by an increase in wake angles from 15° in XG0.75 to 22° in XG1.25 and from 10° to 14° for S1 and S3, respectively.

Figure 2c demonstrates that particles sinking in a doublet experienced attraction in the XG1.25 solution. This was caused by a time-dependent decrease in shear viscosity behind a leading particle evidenced by thixotropy in the viscosity curve (Fig. 1a).

4. CONCLUSIONS

Our experiments demonstrated that EPSs can induce non-Newtonian properties resulting in wake patterns affecting settling dynamics and particle interactions. This study highlights the

significant role of exopolymer's concentration and network structure on modulating particle dynamics.

Acknowledgements. This work was supported by the National Science Centre, Poland grant no. 2019/35/D/ST10/01135 and partly supported by the statutory budget of the Faculty of Chemistry, Warsaw University of Technology.

References

Jenkinson, I.R. (1986), Oceanographic implications of non-Newtonian properties found in phytoplankton cultures, *Nature* **323**, 6087, 435–437, DOI:10.1038/323435a0.

Mrokowska, M.M., and A. Krztoń-Maziopa (2024), Settling of microplastics in mucus-rich water column: The role of biologically modified rheology of seawater, *Sci. Total Environ.* **912**, 168767, DOI: 10.1016/j.scitotenv.2023.168767.

Zenit, R., and J.J. Feng (2018), Hydrodynamic interactions among bubbles, drops, and particles in non-Newtonian liquids, *Ann. Rev. Fluid Mech.* **50**, 505–534, DOI: 10.1146/annurev-fluid-122316-045114.

Publications of the Institute of Geophysics, Polish Academy of Sciences
Geophysical Data Bases, Processing and Instrumentation
vol. 453 (E-14), 2025, pp. 65–67
DOI: 10.25171/InstGeoph_PAS_Publs-2025-043
XLII International School of Hydraulics, Radocza, Poland, 20–23 May 2025

Assessment of Trends in the Polish Annual Peak Flow Data

Geetika CHAUHAN and Iwona KUPTEL-MARKIEWICZ

Institute of Geophysics, Polish Academy of Sciences, Warsaw, Poland

✉ gchauhan@igf.edu.pl; iwonamar@igf.edu.pl

A b s t r a c t

The present study investigates the stationarity of annual peak flow data from 140 gauging stations in Poland. The primary criterion for selecting these stations was the availability of continuous 70-year peak flow records. The modified Mann–Kendall test is employed to identify the trend in the data series.

1. INTRODUCTION

The stationarity of the annual peak flow records has been a cornerstone of flood frequency analysis and more generally, the flood risk analysis (Villarini et al. 2009). A fundamental assumption in classical flood frequency analysis is the stationarity of annual peak flow data, i.e. the data under consideration is free of trend, shifts, or periodicity. However, anthropogenic changes in land use or land cover and the regulation of rivers through dams and reservoirs question the assumption of stationarity of annual peak flow data. The recent devastating flood in September 2024 in southwestern Poland raises the need to study the assumption of stationarity of the annual peak flows in the country. The most common way to check for the existence of non-stationarity in the annual peak time series is to check for the presence of slowly varying changes through trend analysis. Analysing the trend of the historical and present data is an important tool for obtaining a clearer understanding of what the future will hold for us (Villarini et al. 2011). Because when a trend is detected, it is likely to continue into the future (Villarini et al. 2009). In this study, we investigate the stationarity of annual peak flow data from 140 gauging stations in Poland, using the modified Mann–Kendall test at the significance level of 0.05.

2. METHOD

2.1 Data

A total of 140 gauging stations were selected for this study, based on the criterion of having continuous annual peak flow time series of 70 years. The data was provided by the Institute of Meteorology and Water Management – National Research Institute (IMGW–PIB). The selected gauging stations are evenly spread out across Poland. The rivers monitored by these stations are affected mostly by hydrotechnical structures like dams, reservoirs, weirs, run-of-river hydropower plants, and urbanization.

2.2 Trend analysis

The most commonly used tool for trend detection in hydrological time series is the Mann–Kendall (MK) test. The null hypothesis for the MK test states that the data are independent and randomly ordered, i.e., there is no trend or serial correlation among the observations. However, annual peak flow data is often related to a previous observation. The existence of positive or negative autocorrelation in a time series will interfere with the proper identification of a significant trend. Therefore, we used the modified MK test to detect the trend in the selected time series. The modification of the MK test is based on the assumption that data are autocorrelated, and therefore the autocorrelation is estimated from the data in the test procedure.

3. RESULTS

Our analysis reveals that out of the 140 selected gauging stations, only 16 stations exhibit a positive trend in the annual peak flow data. However, a statistically significant trend at the 0.05 significance level is observed only in three stations. Conversely, 124 stations demonstrate a negative trend, with 76 stations exhibiting statistical significance at the 0.05 level, as illustrated in Fig. 1. The majority of rivers in Poland show a negative trend in the annual peak flow data, which is reported by as many as 89% of the gauging stations examined, with just 11% of the stations reporting a positive trend. The type I error of incorrect rejection of the null hypothesis when there is no trend, was detected at two gauging stations. The type II error of incorrect acceptance of the null hypothesis when a trend exists, was detected at eight gauging stations due to the presence of autocorrelation in the time series.

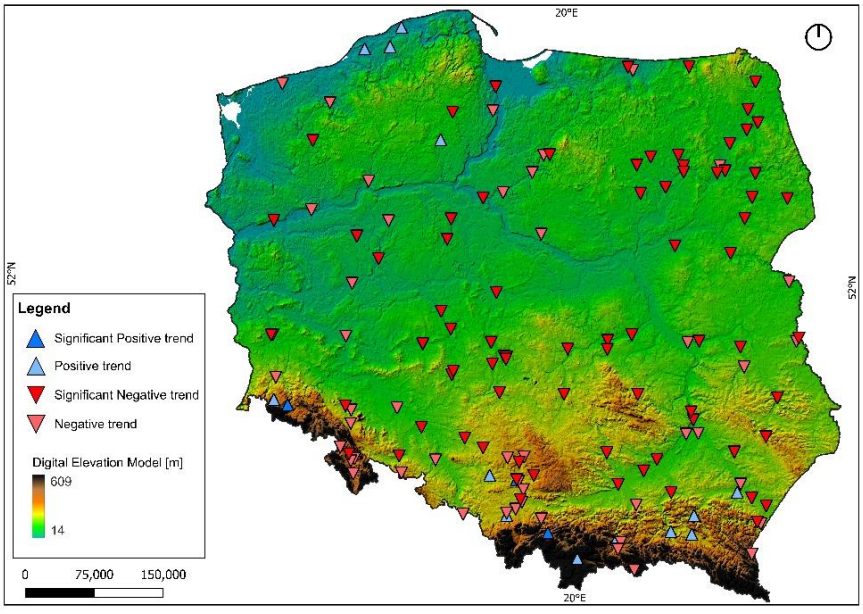

Fig. 1. Results of modified MK test analysis for 140 gauging stations in Poland.

References

Villarini, G., J.A. Smith, F. Serinaldi**,** J. Bales, P.D. Bates, and W.F. Krajewski (2009), Flood frequency analysis for nonstationary annual peak records in an urban drainage basin, *Adv. Water Resour*. **32**, 8, 1255 –1266, DOI: 10.1016/j.advwatres.2009.05.003.

Villarini, G., J.A. Smith, F. Serinaldi, and A.A. Ntelekos (2011), Analyses of seasonal and annual maximum daily discharge records for central Europe, *J. Hydrol*. **399**, 3–4, 299–312, DOI: 10.1016/j.jhydrol.2011.01.007.

Publications of the Institute of Geophysics, Polish Academy of Sciences
Geophysical Data Bases, Processing and Instrumentation
vol. 453 (E-14), 2025, pp. 69–72
DOI: 10.25171/InstGeoph_PAS_Publs-2025-044
XLII International School of Hydraulics, Radocza, Poland, 20–23 May 2025

Adaptation of Dams and Reservoirs to Climate Change and Environmental Flows

Anastasios I. STAMOU

Laboratory of Applied Hydraulics, School of Civil Engineering,
National Technical University of Athens (NTUA), Athens, Greece

✉ stamou@mail.ntua.gr

Abstract

Dams and Reservoirs (D&R) are vulnerable to climate hazards; thus, they need to be adapted to climate change. In this adaptation procedure D&R systems are broken into components, the impacts of the climate hazards on each component are determined, the vulnerable components whose risks are high are identified, and adaptation measures are proposed to reduce these risks. One of the most important components of D&R systems is the environmental flow (E-FLOW). In the literature, there exist more than 200 methods for assessing E-FLOW that can be categorized as hydrological, hydrodynamic habitat modelling (HHM), and holistic methods combining the first two methods. In this work the HHM method is presented using indicative examples and the effects of climate change on E-FLOW are briefly discussed.

1. INTRODUCTION

Dams and Reservoirs (D&R) are essential water infrastructure systems that serve multiple purposes, such as water storage, flood control, hydroelectric power generation, irrigation, and recreation. During their long history D&R systems suffered from hundreds of failures that caused severe and often catastrophic consequences, such as loss of life, injuries, and damage to infrastructure. The mechanisms of these failures can be accelerated by climate change and climate hazards, the most important of which can be categorized into three groups that are: (1) mean air temperature increase and extreme heat; (2) mean precipitation decrease, aridity and droughts; and (3) extreme precipitation and flooding (Stamou et al. 2025). The effects of climate change on D&R systems are usually assessed via a Climate Risk and Vulnerability Assessment. According to one of these methodologies (Stamou et al. 2024), which is based on literature and the EC guidelines technical guidelines on climate-proofing infrastructure, D&R systems are broken into components, the impacts of the climate hazards on each component are determined, the vulnerable components whose risks are high are identified, and adaptation measures are

proposed to reduce these risks. The main components of D&R systems can be categorized into five groups: (1) inflows, (2) functions (storage, flood control, hydropower, and recreation), (3) assets (embankment, spillway, auxiliaries, and buildings), (4) outflows (water supply, hydropower production, and environmental flow), and (5) supporting infrastructure (power supply, communications, transportation, and personnel). One of the most important components of D&R systems is the environmental flow (E-FLOW) that is the flow regime necessary to maintain river ecosystems. In the literature, there exist more than 200 methods for assessing E-FLOW that can be categorized as: (1) hydrological, (2) hydrodynamic habitat modelling (HHM), and (3) holistic methods combining the first two methods; HHM involves a hydrodynamic model and a habitat model for the species of interest. In the last ten years research has been performed in the NTUA on the determination of E-FLOW using HHM; this research, which was initiated in the Technical University of Munich (Prof. Peter Rutschman) and continued within a TUM-NTUA cooperation, resulted in a significant number of publications that described various versions and applications of the HMM method for assessing E-FLOW. In this work the main steps of the HHM method are presented using indicative examples and the effects of climate change on E-FLOW are briefly discussed.

2. METHODOLOGY

The main steps of the HMM method to assess E-FLOW the following:

1. Determination of the river reach and the species of interest, and the environmental parameters (or conditions) that affect E-FLOW. Usually, the river reach is located downstream of the technical work that interrupts river continuity, i.e. the D&R system, while the environmental parameters include hydraulic characteristics, such as flow velocity (V) and water depth (D); however, they may also include water temperature (T), conductivity (C), pH, substrate type (S), and concentrations of water quality parameters, such as dissolved oxygen (DO).
2. Construction of the 3D geometry of the river reach (usually via a topographic survey) that is used as input in the hydrodynamic model.
3. Performance of field measurements for water depths and flow velocities, at various sections of the river reach, which are used for: (i) the development of the stage – discharge (rating) curves, and (ii) the calibration and validation of the hydrodynamic model.
4. Selection, formulation, calibration, and verification of the hydrodynamic model. Typically, a 2D hydrodynamic model is selected, such as TELEMAC-2D or RIVER2D, that determines V and D; then the model is formulated using the 3D geometry of the reach (see 2), calibrated to determine the values of roughness coefficient and verified using the hydrodynamic data (see 3).
5. Development of the habitat model that is virtually the Habitat Suitability Curves (HSCs); these are constructed based on collected microhabitat data in the river reach. HSCs quantify the suitability of the hydraulic conditions (i.e. V and D), which is typically expressed as Suitability Index (SI_D for D and SI_V for V) and measured on a scale from 0 (unsuitable) to 1 (optimal). In Fig. 1 the HSCs for small and large chub are shown for D and V, respectively (Stamou et al. 2018).
6. Application of the HMM that involves the application of the hydrodynamic and the habitat model to calculate the 2D distributions of V, D, SI_D and SI_V, and the Weighted Useable Area (WUA) for various values of discharges (Q); WUA is an indicator of habitat quality and quantity equal to the sum of the areas weighed by the inferred suitability within the entire domain of the hydrodynamic model. In Fig. 2 indicative WUA-Q curves are shown for the small and the large chub, expressed in m^2 (left) and m^2/1000 m length of river (right).

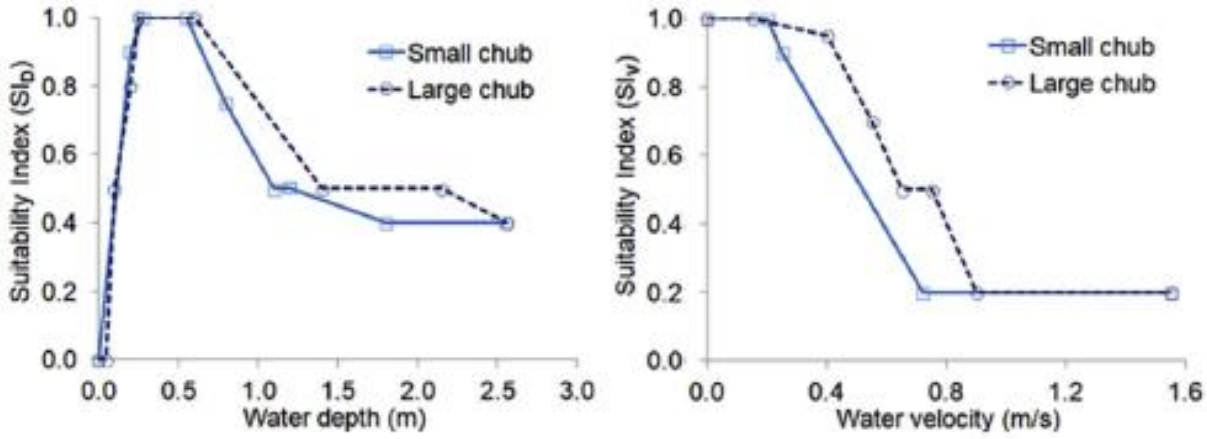

Fig. 1. Indicative HSCs for D and V (Stamou et al. 2018).

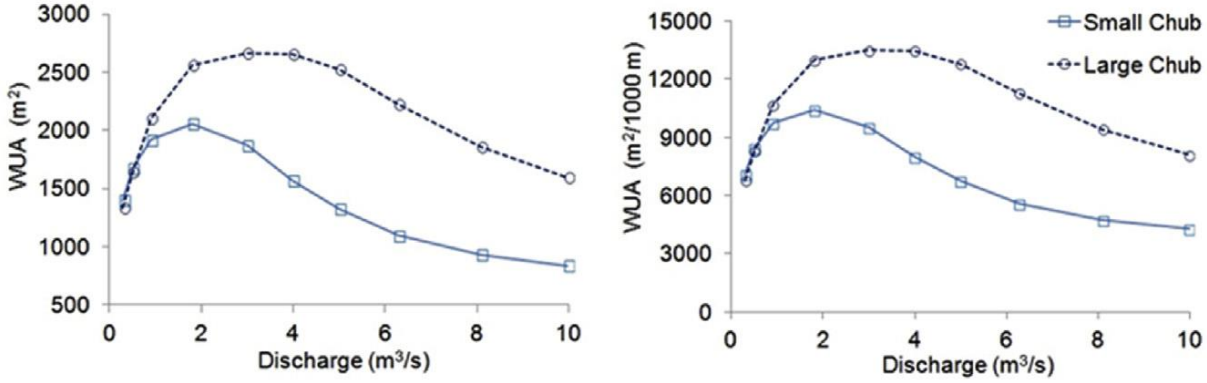

Fig. 2. Indicative WUA-Q curve (Stamou et al. 2018).

3. DISCUSSION AND CONCLUSIONS

Figure 2 indicates that the optimum range of E-FLOW is 2–4 m^3/s for large chub and 1–3 m^3/s for small chub, i.e. E-FLOW is ideally in the range 2–3 m^3/s; higher or lower discharges are expected to have a negative impact on suitable habitat availability. Climate hazards may affect E-FLOW. For example, mean air temperature increase and extreme heat increase T, decrease DO, and increase the pollution of the reservoir, while mean precipitation decrease, aridity, and droughts increase the concentrations of pollutants and sediments in the reservoir; thus, both groups of hazards reduce the water quality of the reservoir and thus of the downstream flow, increase the demand for higher E-FLOW that creates management conflicts for multi-purpose reservoirs. Extreme precipitation and flooding increase the downstream flow, create flooding and pollution, and deterioration of S. These effects on the E-FLOW can be taken into account via including in the HHM the relevant environmental parameters, such as T, DO, and S.

Acknowledgements. The present work was performed within the project “Support the upgrading of the operation of the National Network on Climate Change (CLIMPACT)” of the General Secretariat of Research and Technology under Grant “2023NA11900001”.

References

Stamou, A.I., A. Polydera, G. Papadonikolaki, F. Martínez-Capel, R. Muñoz-Mas, Ch. Papadaki, S. Zogaris, M.-D. Bui, P. Rutschmann, and E. Dimitriou (2018), Determination of environmental flows in rivers using an integrated hydrological-hydrodynamic-habitat modelling approach, *J. Environ. Manage.* **209**, 273–285, DOI: 10.1016/j.jenvman.2017.12.038.

Stamou, A.I., G. Mitsopoulos, and A. Koutroulis (2024), Proposed methodology for climate change adaptation of water infrastructures in the Mediterranean region, *Environ. Process.* **11**, 12, DOI: 10.1007/s40710-024-00691-w.

Stamou, A.I., G. Mitsopoulos, A. Sfetsos, A.T. Stamou, S. Sideris, K.V. Varotsos, C. Giannakopoulos, and A. Koutroulis (2025),Vulnerability assessment of dams and reservoirs to climate change in the Mediterranean region: The case of Almopeos Dam in Northern Greece, Preprints 2025031362, DOI: 10.20944/preprints202503.1362.v1.

Publications of the Institute of Geophysics, Polish Academy of Sciences
Geophysical Data Bases, Processing and Instrumentation
vol. 453 (E-14), 2025, pp. 73–76
DOI: 10.25171/InstGeoph_PAS_Publs-2025-045
XLII International School of Hydraulics, Radocza, Poland, 20–23 May 2025

The Influence of Vegetation on the Spatial Distribution of Water Velocity in a Regulated Lowland River – Preliminary Results

Andrzej STRUŻYŃSKI, Maciej WYRĘBEK, and Leszek KSIĄŻEK

University of Agriculture in Kraków, Kraków, Poland

✉ rmstruzy@cyf-kr.edu.pl; Maciej.Wyrebek@urk.edu.pl; Leszek.Ksiazek@urk.edu.pl

A b s t r a c t

The paper deals with the study of the influence of vegetation (*Sparganiaceae, Batrachium, Ceratophyllaceae, Elodea Michx.*) on the hydraulic conditions of water flow in a lowland river. The paper presents the results of measuring the spatial distribution of water table and water velocity in the Nida River. The studied section of the Nida is regulated, with a straight course however, the influence of regulation disappears. Banks and bed of the river are partially overgrown in summer seasons. Rigid vegetation grows on the banks of the Nida, but also covers the bottom with tufts of soft vegetation.

Measurements were taken in the summer period during low discharge in Nida (9.15 $m^3 s^{-1}$). Analyses of distribution in hydraulic parameters; water velocities in stream lines or in verticals and the depth variation as a preliminary analysis were presented.

1. DESCRIPTION OF THE OBJECT AND PURPOSE OF THE WORK

The research object is located in the Świętokrzyskie Province (Poland) (Fig. 1). The total length of the river euqals 153 km and a catchment area exceeds 3.8 thousand km^2. The Nida is a lowland river with sandy bottom. The measurements were carried out in the middle course of the Nida near the localities of Kije and Umianowice. Studied section has been regulated however river banks were not reinforced. The current of flowing water is so slow that both, banks and bed of the river during spring and summer are overgrown by aquatic vegetation which influences the distribution of flowing water (Bartnik et al. 2004; Dąbkowski and Pachuta 1996). On the banks, mainly stiff vegetation develops (mainly *Sparganiaceae*, sometimes *Batrachium*), growing vertically in compact habitats, while in the current, soft vegetation developing in clusters appear (*Ceratophyllaceae, Elodea Michx.*). The velocity profile of the water flowing

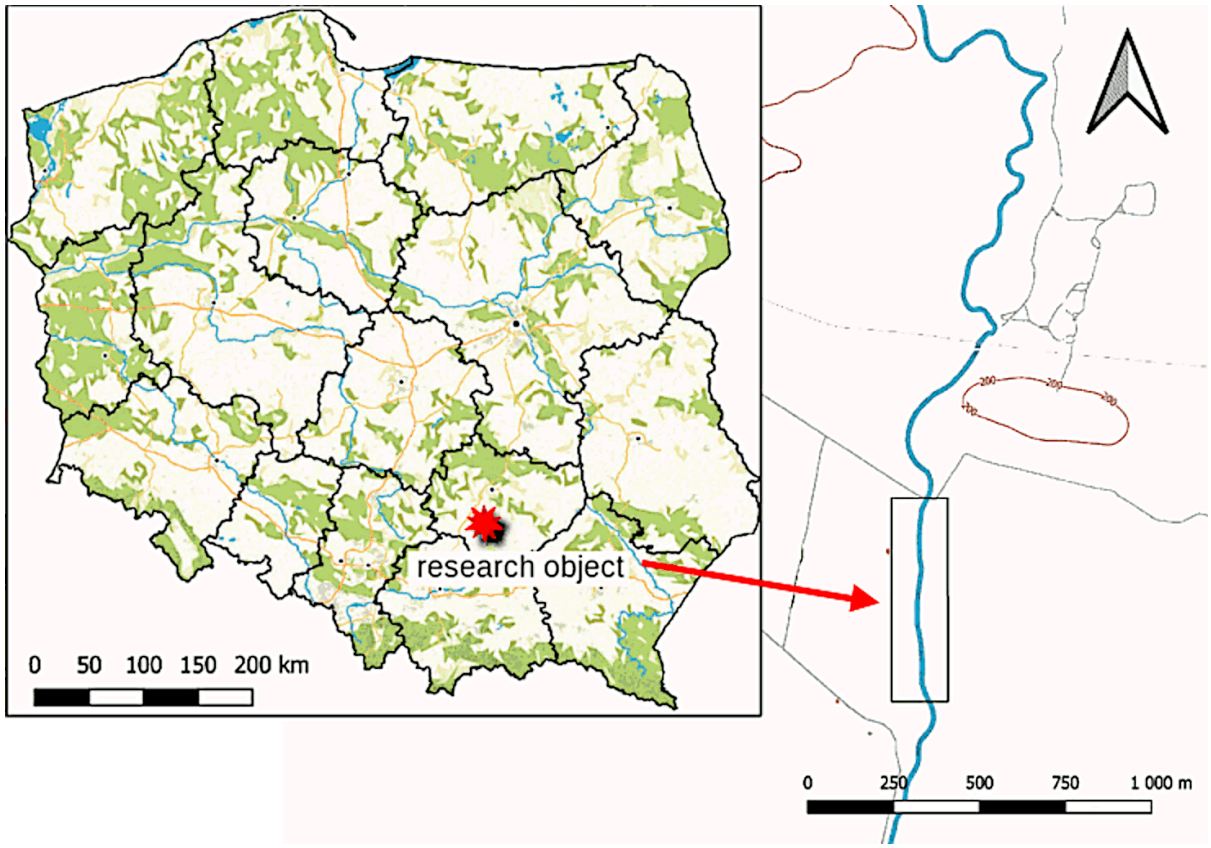

Fig. 1. Location of the study area in the map of Poland.

around and over these clusters is different from the logarithmic one (Chalfen et al. 2010, Kozioł et al. 2016). Its faster growth is favoured by low water levels that usually appear in the summer. The aim of the work is to compare water flow parameters in sections covered with and without vegetation.

2. RESEARCH METHODOLOGY, RESULTS, AND SUMMARY

Measurements of the depth and velocity of water flowing in the Nida River were carried out using the SONTEK S5 acoustic profiling probe (ADCP).

The water surface elevation was measured using the GPS-RTK TITAN TR7 device. ADCP measurements were taken on September 21, 2020 in the length of over 270 m. Obtained model of the riverbed was combined with a digital terrain model downloaded from the geoportal.gov.pl website. Additionally, an unmanned aerial plane equipped with an RGB Full HD camera was used to fly. Acquired photos of vegetated part of the reach were processed to obtain a georeferenced image in the PL1992 (EPSG 2180) system. The performed flight covers a section of the river over 70 m long.

These data were used, on the one hand, to create a longitudinal profile of the water surface in Nida and to create a model of the Nida channel, and on the other hand, a visualization of the average velocity and water table elevation in cross-sections. These measurements were made to describe the effects of slow overgrowing of the riverbed with vegetation during the growing season. On basis of the georeferenced images, polygons reflecting bed vegetation distribution were drawn (Fig. 2).

The velocity cross-sections presented at Fig. 2 indicate a close relationship between the distribution of the flowing water velocity and the growth vegetation. The lack of vegetation results in a uniform cross-sectional profile of the mean velocity in the riverbed. Also, soft vegetation

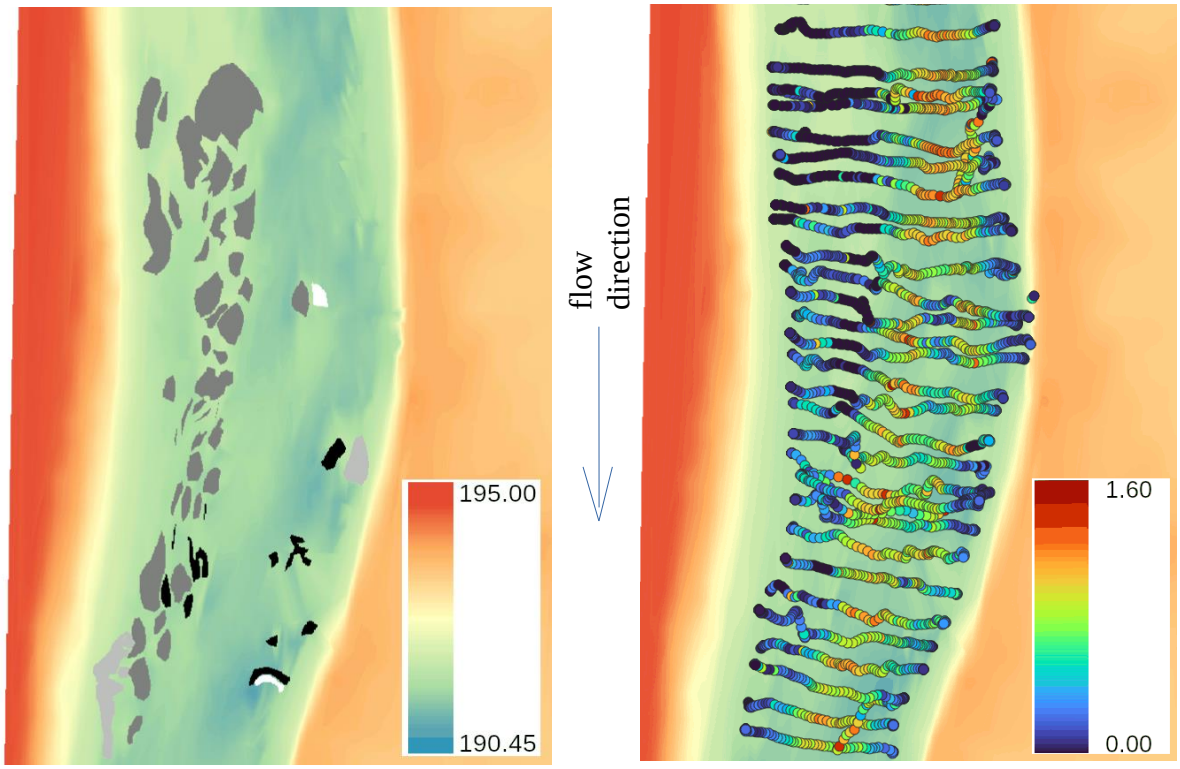

Fig. 2. The Nida River within the investigated reach. The left figure shows a sketch of the location of plants growing on the bottom (on the legend there is data presented elevations in the PL-KRON86-NH altitude system). The right figure shows measurement cross-sections with the value of the average velocity in the hydrometric verticals (on the legend there is data presented velocities in m s^{-1}).

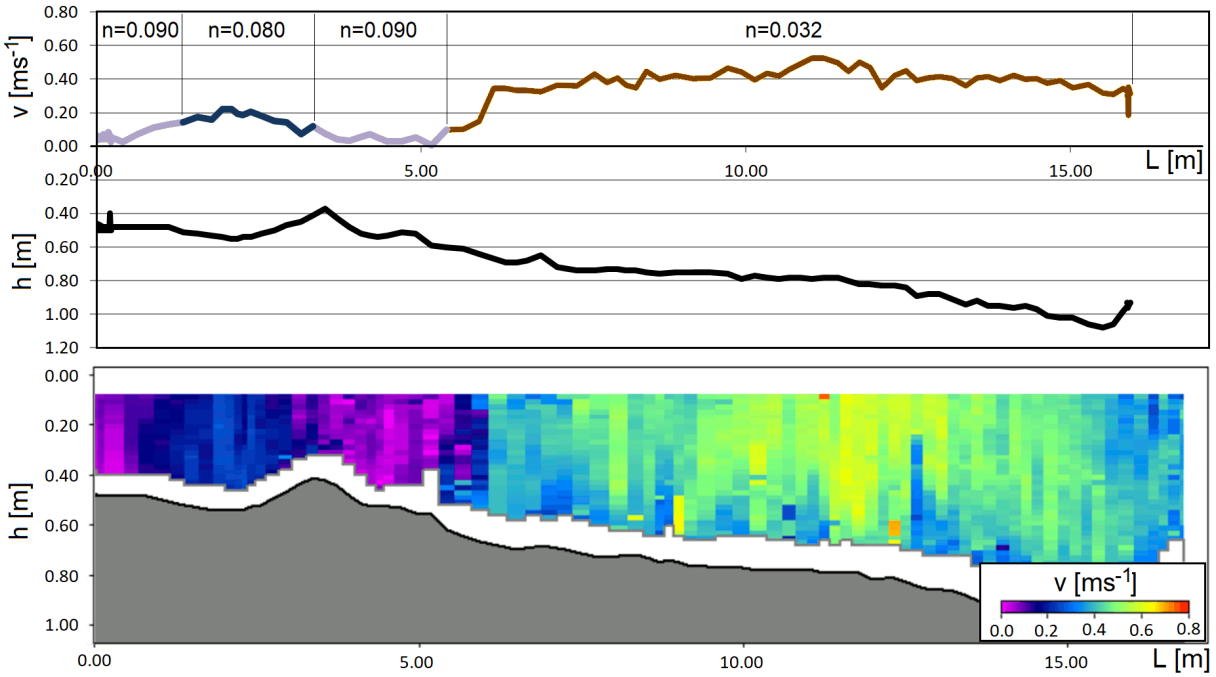

Fig. 3. Visualization of measurement data in chosen cross-section. The upper graph presents velocity averaged in verticals; in brown is an open channel flow marked, in grey and blue the vegetated regions are presented. The lower graph presents the typical picture prepared by ADCP dedicated software. The graph presents temporar velocities captured during measurement.

reaching the water surface can significantly reduce the capacity of the riverbed. Further analyses shell be conducted to determine the clogging effect of vegetation grow within variable flows conditions in the riverbed. At Fig. 3 presented is the chosen one of a cross-sections made in location covered with vegetation. The results are presented by a graph of the average velocity as well as assumed Manning roughness with marked locations of differentiated plant growth (Fig. 3, upper graph). The lower graph of Fig. 3 presents visualization of hydrometric verticals recorded by the ADCP device (Fig. 3, lower graph). There, the area of reduced water flow velocity is clearly marked in violet and blue colour zone.

Acknowledgements. The measurements were performed as part of the Life4Delta project "Renaturalisation of inland delta of Nida River" no. LIFE17 NAT/PL/000018. The authors of the article would like to thank Wojciech Sołtysiak (Zespół Świętokrzyskich i Nadnidziańskich Parków Krajobrazowych in Kielce) for performing the unmanned aerial vehicle flight and Paweł Adamski (Institute of Nature Conservation in Kraków, Polish Academy of Sciences) for georeferencing of the taken photographic images.

References

Bartnik, W., J. Florek, F. Schöberl, and A. Strużyński (2004), Flow velocity fluctuations over rough bed covered with lighneous water plants, *Zesz. Nauk. AR we Wrocławiu, Ser. Konferencje XXXVII* **481**, 143–153.

Chalfen, M., T. Molski, and T. Tymiński (2010), Wpływ roślin na zmianę profilu prędkości przepływu w małym cieku [The influence of vegetation on velocity profiles in small river], *Infrastruc. Ecol. Rural Areas* **8**, 1, 153–164 (in Polish with English summary).

Dąbkowski, Sz.L., and K. Pachuta (1996), *Roślinność i Hydraulika Koryt Zarośniętych*, Wyd. IMUZ, Falenty, 152 pp. (in Polish).

Kozioł, A., J. Kubrak, E. Kubrak, M. Krukowski, and A. Kiczko (2016), Rozkłady prędkości w korycie rzecznym o złożonym przekroju poprzecznym z roślinnością wysoką w terenach zalewowych, *Acta. Sci. Pol. Formatio Circumiectus* **15**, 4, 227–241.

Publications of the Institute of Geophysics, Polish Academy of Sciences
Geophysical Data Bases, Processing and Instrumentation
vol. 453 (E-14), 2025, pp. 77–79
DOI: 10.25171/InstGeoph_PAS_Publs-2025-046
XLII International School of Hydraulics, Radocza, Poland, 20–23 May 2025

The Negative Phenomenon of Anthropogenically Induced Hydropeacs – Process and Damage

Leszek KSIĄŻEK, Jacek FLOREK, Maciej WYRĘBEK, and Andrzej STRUŻYŃSKI

University of Agriculture in Krakow, Kraków, Poland

✉ leszek.ksiazek@urk.edu.pl; jacek.florek@urk.edu.pl;
maciej.wyrebek@urk.edu.pl; andrzej.struzynski@urk.edu.pl

Abstract

The dynamics of hydropeaks significantly deviates from the same processes in nature by the short time and the number of events. These hydropeaks do not exceed the range of natural floods however, their frequency impacts environment negatively. This creates entirely new conditions for the riverbed morphology. Banks nearly vertical mainly above 6 m height. Narrow river channel regularly less than 40 m wide. More frequent elevated flows lead to stronger erosion, changes in the riverbed structure, and negative impacts on the river's environment. During a flood, animals seek shelter and when the flow decreases they return to the main channel of the river. This process leads to biological losses of fish, larvae, and eggs and applies to all species inhabiting the river. Every high enough water event is therefore a natural risk. Increasing the frequency of the event increases the likelihood of losses. A series of such events were observed and analysed by numerical modelling. We were able to establish an unprecedented frequency and short event time of the phenomenon as compare to the natural conditions. During the disappearance of the flow, as well in river as in model we found variable, rapidly, repeatedly changing and misleading directions of the water outflow. The human-induced narrow eroded channel structure proved to be more susceptible to dynamic changes escalating the negative process and has demonstrated by examples of fish population losses.

1. INTRODUCTION

Very little research on hydropeacs has been done in Poland (Bipa et al. 2024). In 2024, were carried out an analysis of the impact conditions on the section of the The Vistula River bed below the Przewóz Barrage, measurements of water flow, longitudinal profile, water surface level and photogrammetric documentation. Our research consisted of numerical simulation of flow phenomena of the mid-channel forms at the downstream location of the Przewóz Barrage

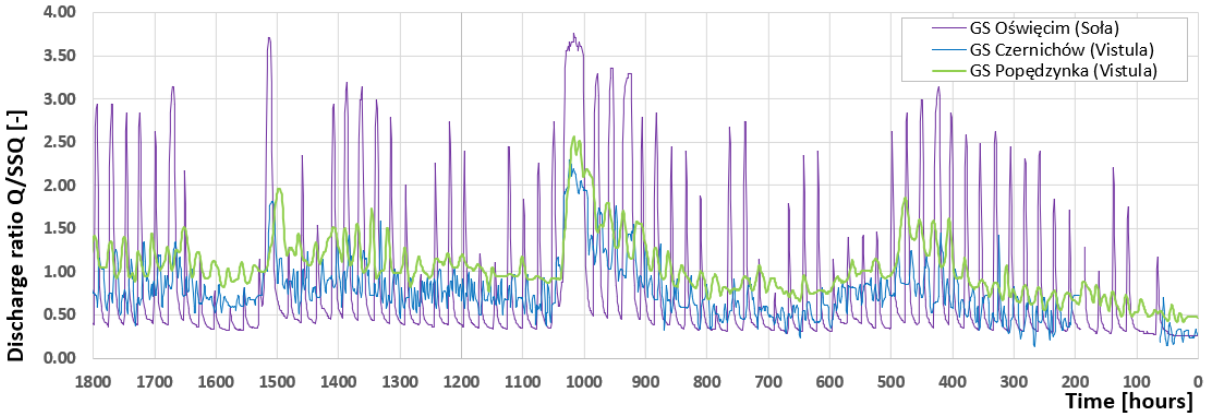

Fig. 1. Flow in relation to SSQ discharge at the Oświęcim (The Soła River), Czernichów, and Popędzynka (The Vistula River) water gauging stations.

and analysis of hydraulic conditions of water flow. The data obtained from the IMGW–PIB made it possible to determine the dynamics of the hydropeaks (Fig. 1).

2. CHANGES THE WATER SURFACE LEVEL AT THE PRZEWÓZ BARRAGE

The insufficient capacity of the regulated and narrowed Vistula riverbed below the Przewóz Barrage cannot effectively handle significant flow changes caused by the development of the Upper Vistula Waterway. As a result, water levels fluctuate dramatically in a short period. These fluctuations significantly exceed the near-natural hydromorphological and hydrological conditions of the Vistula River in the studied section. The recorded water level changes indicate that fluctuations upstream can occur in 15 minutes or less, ranging from 0.21 to 0.20 m. At the downstream position of the Przewóz Barrage, fluctuations can also occur within 15 minutes or less, reaching up to 30 cm and down to 106 cm (Fig. 2).

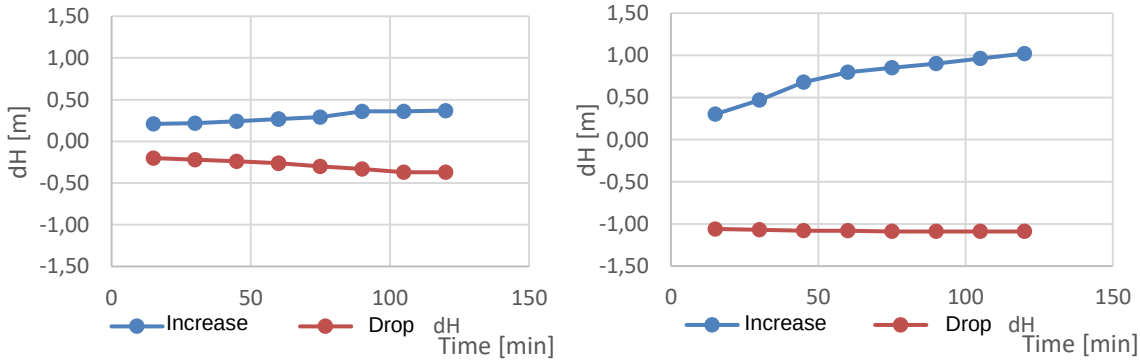

Fig. 2. Highest recorded fluctuation of water surface level in the period August–November 2023 from 15 to 120 minutes, The Vistula River, upstream (left) and downstream (right) of The Przewóz Barrage.

3. SPATIAL VELOCITY DISTRIBUTION

The riverbed features a deep cut with steep banks, and there is almost no fine sediment present, which poses challenges for the river's biological ecosystem. Using 2D numerical modelling, we intend to demonstrate the rapid, short-term nature of hydrodynamics and the transient currents that occur along the riverbed. While fluctuations in water levels are a natural occurrence, the significant number of human-made events can have destructive consequences (Hayes et al. 2021). Numerical simulation was carried out using depth averaged 2D model for unsteady flow

Table 1
Model parameters

Time [min]	Discharge [m^3s^{-1}]	WSL [m a.s.l.]	ΔH [cm]	Δt [min]	Δh [cm/min]
0	140.0	189.54	–	–	–
30	117.5	189.49	5	30	0.17
60	95.0	189.26	23	30	0.77
90	72.5	189.07	19	30	0.63
110	57.5	188.82	25	20	1.25
120	50.0	188.58	24	10	2.40

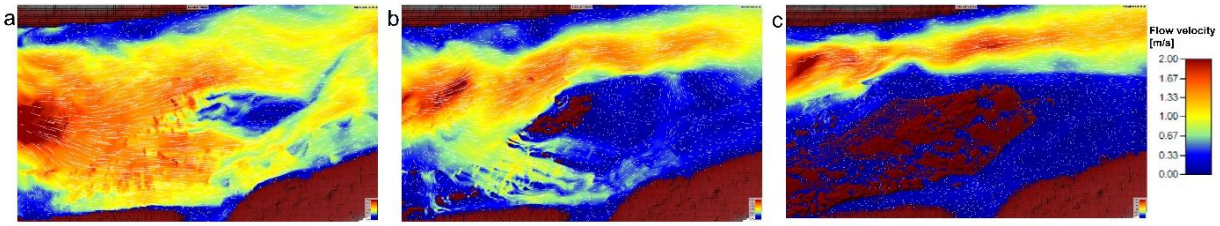

Fig. 3. Spatial velocity distribution around a gravel bar downstream the barrage: a) Q = 140 m^3s^{-1}, t = 0 min; b) Q = 72.50 m^3s^{-1}, t = 90 min; c) Q = 50 m^3s^{-1}, t = 120 min.

conditions (Table 1 and Fig. 3). The results reveal the decay of the attracting current in the channel separating the mid-channel form from the banks. This site becomes as a trap for living aquatic organisms.

Acceptable flow rate changes are guided by changes in the water surface level. Assuming a maximum allowable water levels drop of 3 $cm \cdot min^{-1}$ (Greimel et al. 2018) an operating time of up to 2 hours was obtained for the water stage closure. This is 8 times longer than the recorded data. The operating principles of the control devices require significant adjustment.

Acknowledgements. The work was supported by The State Water Holding Polish Waters, Regional Water Management Authority in Krakow, Poland.

References

Bipa, N.J., G. Stradiotti, M. Righetti, and G.R. Pisaturo (2024), Impacts of hydropeaking: A systematic review, *Sci. Total Environ*. **912**, 169251, DOI: 10.1016/j.scitotenv.2023.169251.

Greimel, F., L. Schülting, W. Graf, E. Bondar-Kunze, S. Auer, B. Zeiringer, and C. Hauer (2018), Hydropeaking impacts and mitigation. **In:** S. Schmutz, and J. Sendzimir (eds.), *Riverine Ecosystem Management*, Aquatic Ecology Series, Vol. 8, Springer, Cham, 91–110, DOI: 10.1007/978-3-319-73250-3_5.

Hayes, D.S., E. Lautsch, G. Unfer, F. Greimel, B. Zeiringer, N. Höller, and S. Schmutz (2021), Response of European grayling, Thymallus thymallus, to multiple stressors in hydropeaking rivers, *J. Environ. Manage*. **292**, 112737, DOI: 10.1016/j.jenvman.2021.112737.

Publications of the Institute of Geophysics, Polish Academy of Sciences
Geophysical Data Bases, Processing and Instrumentation
vol. 453 (E-14), 2025, pp. 81–83
DOI: 10.25171/InstGeoph_PAS_Publs-2025-047
XLII International School of Hydraulics, Radocza, Poland, 20–23 May 2025

Method for Measuring High Tracer Concentrations in River Mixing Studies

Filip BOJDECKI and Monika KALINOWSKA

Institute of Geophysics, Polish Academy of Sciences, Warsaw, Poland

✉ fbojdecki@igf.edu.pl; mkalinow@igf.edu.pl

A b s t r a c t

Tracer experiments are a well-established technique for investigating mixing processes in rivers. A critical aspect of these experiments is ensuring the use of an appropriate amount of fluorescent tracer so that its concentration can be accurately measured with the available equipment. However, determining the optimal amount of tracer beforehand is often challenging. Furthermore, tracer concentrations can vary significantly during mixing processes, making accurate measurements at cross-sections near the injection point, as well as at more distant river cross-sections, particularly difficult. To overcome these challenges, a method was developed to retrieve valuable data when tracer concentrations exceed the measurement capabilities of the equipment. This approach utilizes the optical properties of the tracer solution in the presence of scattering particles within the fluid. By combining turbidity and fluorescence intensity readings, the method enables calibration of the turbidity–concentration relationship. This allows for the determination of tracer concentrations even when the fluorescence intensity–concentration relationship exceeds the linear regime.

1. INTRODUCTION

Fluorometers excite the tracer molecules with short wavelength light. During subsequent relaxation, longer wavelength fluorescence light is emitted. For low tracer concentrations, fluorescence light intensity is proportional to the tracer concentration. However, for high tracer concentrations proportionality fails (Wilson et al. 1986). It is caused mainly by absorption of fluorescence by tracer and self-quenching (excited tracer molecules relax without fluorescence emission due to interactions with each other). Those effects make fluorescence unsuited for measurements of high tracer concentrations. But for high tracer concentration absorption can be used to determine its value.

2. RESULTS

The Submersible Fluorometer from Turner Designs (SCUFA), enables simultaneous measurement of turbidity and fluorescence of tracer. This device utilises the same light beam for fluorescence excitation and for measuring light scattered by suspended particles in water – in order to estimate turbidity. Assuming constant amount of scattering particles in a solution, turbidity readings are mainly influenced by the absorption – determined by the tracer concentration. This enables calibration of turbidity–concentration relation.

A series of rhodamine WT water solution samples with a constant amount of suspended particles (kaolin powder) was prepared to test our approach. Tracer concentrations and turbidities readings were recorded for series of samples. The result of this experiment is presented in Fig. 1. As expected for very high tracer concentrations, the concentration readings recorded by SCUFA is dropping. At the same time turbidity readings decrease.

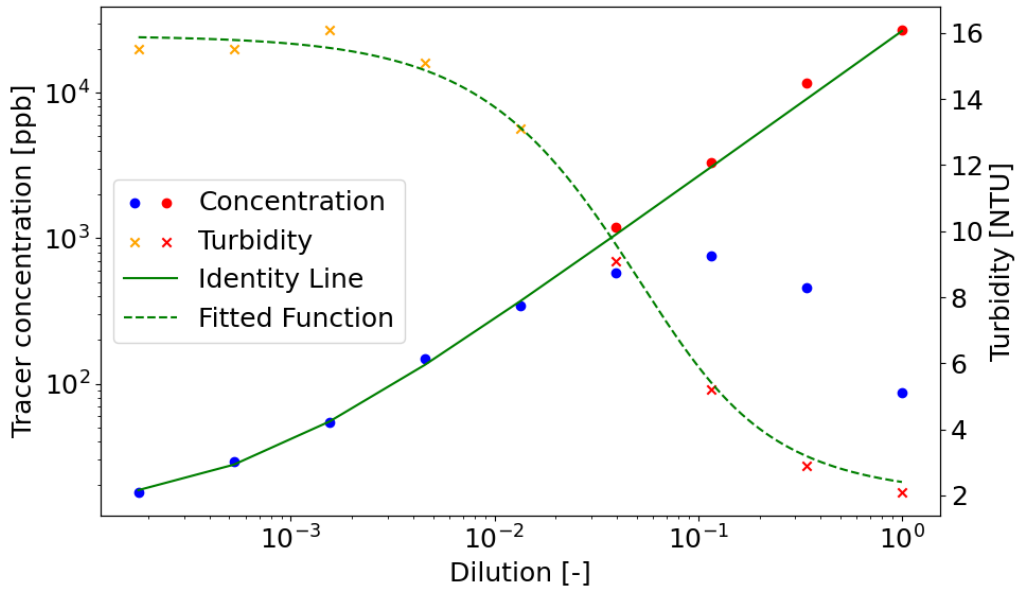

Fig. 1. Recorded tracer concentration and turbidity for dilution series of rhodamine WT. Blue dots represent direct fluorometer readings, while red dots indicate tracer concentrations recovered from turbidity data. Crosses denote turbidity readings. The dashed line represents the fitted turbidity–concentration relation. Only data represented as yellow crosses was used to perform the fit. Turbidity readings marked as red crosses were used to recover tracer concentration data (red dots) and were skipped. Identity line is a linear relation fitted to the five lowest tracer concentration points. Tracer concentration was treated as dependent variable and dilution as independent variable. Apparent curvature is due to log-log scale.

The relation between turbidity read and tracer concentration read was fitted. In the fitting procedure, only five lowest tracer concentration data points were used. This decision was motivated by the fact that this way we simulate a real-world scenario in which true tracer concentration outside linear region remains unknown.

To determine the proper form of the fitted function, a simple physical model was introduced. We assume that the amount of scattered lights reaching the detector per unit volume, denoted as ρ, is constant within a given space. Thus, the detector optical power I can be expressed as:

$$I = \int_V \rho dV. \tag{1}$$

Considering that scattered light is absorbed by the tracer and assuming that the path length of a scattered light ray is proportional to its distance from the detector window, we modify this equation using the Beer–Lambert law:

$$I = \int_V \rho e^{-\mu x c} dV, \tag{2}$$

where x is distance to the detector window, c is tracer concentration, and μ is a constant that encapsulates information about the extinction coefficient and the relationship between x and the actual path length along the ray. This integral can be computed for a specific scattering region geometry. For simplicity, we assume the scattering region to be a cuboid with dimensions $L_x \times L_y \times L_z$. Under this assumption the integral simplifies to:

$$I = \frac{L_y L_z \rho}{\mu c}(e^{-\mu L_x c} - 1). \tag{3}$$

This equation can be reparametrized to form:

$$I(c) = \frac{P_1}{c}(e^{-P_2 c} - 1) + P_3, \tag{4}$$

where P_1 and P_2 account for constants in Eq. 3 and P_3 was introduced to account for residual signal. During fit we assumed a priori knowledge of P_3 parameter. Taking into account that the turbidity reading is proportional to the optical power detected (Davies-Colley and Smith 2001), a function of this form can be fitted to the turbidity–concentration relationship.

Equation 4 was numerically inverted to retrieve tracer concentration data. Recovered points align very well in line with directly measured tracer concentration (see Fig. 1), which confirms that concentration was successfully recovered.

3. CONCLUSIONS

This study presents a method for estimating high tracer concentrations using turbidity measurements, addressing the challenges of measuring high concentrations when dilution or other alternative methods are not feasible. The approach was experimentally validated, showing good agreement between recovered and directly measured concentrations.

A key limitation is that the instrument must rely on light wavelength absorbed by the tracer. Initial tests in natural river environments have been conducted and preliminarily confirm the validity of the approach. However, further research is planned to drive final conclusions.

Acknowledgements. This research was funded by the National Science Centre, Poland, grant number 2024/53/B/ST10/01460. We are grateful to Professor Ian Guymer for providing access to essential resources that contributed to this research.

References

Davies-Colley, R.J., and D.G. Smith (2001), Turbidity suspended sediment, and water clarity: A review, *JAWRA J. Am. Water Resour. Assoc*. **37**, 5, 1085–1101, DOI: 10.1111/j.1752-1688.2001.tb03624.x.

Wilson, J.F., E.D. Cobb, and F.A. Kilpatrick (1986), Fluorometric procedures for dye tracing, *Tech. Water-Resour. Invest.* 03-A12, DOI: 10.3133/twri03A12.

Publications of the Institute of Geophysics, Polish Academy of Sciences
Geophysical Data Bases, Processing and Instrumentation
vol. 453 (E-14), 2025, pp. 85–88
DOI: 10.25171/InstGeoph_PAS_Publs-2025-048
XLII International School of Hydraulics, Radocza, Poland, 20–23 May 2025

Plastic Journey of Pathogens in a Mountain River: How Hydrological Conditions and Riverbed Morphology Influence Their Transport?

Agnieszka RAJWA-KULIGIEWICZ[1], Anna BOJARCZUK[1],
Anna LENART-BOROŃ[2], Oktawia KAFLIŃSKA[1], and Wiktoria SUWALSKA[1]

[1]Jagiellonian University in Kraków, Faculty of Geography and Geology,
Institute of Geography and Spatial Management, Kraków, Poland

[2]University of Agriculture in Kraków, Faculty of Agriculture and Economics,
Department of Microbiology and Biomonitoring, Kraków, Poland

✉ agnieszka.rajwa@uj.edu.pl; anna.bojarczuk@uj.edu.pl; anna.lenart-boron@urk.edu.pl;
oktawia.kaflinska@student.uj.edu.pl; wiktoria.suwalska@student.uj.edu.pl

Abstract

Riverine litter poses a significant environmental challenge, with plastics being particularly problematic due to their persistence, potential to degrade into microplastics, and ability to act as vectors for pathogens, facilitating the spread of harmful bacteria in river ecosystems. This study investigated the types of litter deposited in a mountain gravel-bed river, the pathogens colonising these materials, and the influence of riverbed morphology and flow conditions on macroplastic transport and deposition. This research employed field mapping, tracer experiments with PET bottles, and microbiological analysis, and utilised probabilistic methods to describe bottle transport and deposition. Field mapping revealed that plastics were the most frequently deposited materials in the riverbed (up to 86%), with plastic foils comprising about 50% of all plastic materials. Microbiological analysis showed that the litter biofilm was colonised by fecal indicator bacteria and pathogenic bacteria. Tracer experiments indicated that PET bottle deposition was strongly influenced by discharge, river depth, and channel morphology, varying across different river sections. As flow rates decreased, the probability of bottle passage diminished, while the cumulative hazard of retention increased.

1. INTRODUCTION

Litter in rivers is a significant environmental challenge, impacting ecosystems, human health, and the economy (van Emmerik and Schwarz 2020). Plastics are especially concerning due to their durability and their tendency to break down into microplastics, which enter the water and are consumed by animals. Additionally, plastic waste can host pathogens, facilitating the spread of harmful bacteria within river ecosystems (Pow et al. 2025). This study investigated the types of litter deposited in a mountain gravel-bed river, the pathogens colonising these materials, and the influence of riverbed morphology and flow conditions on macroplastic transport and deposition. Specifically, we aim to link the deposition and transport behaviour of plastics with their potential role in the spread of harmful pathogens within river ecosystems.

2. STUDY SITE AND METHODS

The study was conducted in the braided channel of the Białka River, which sources in the High Tatras (Fig. 1). The designated river section is located in the town of Białka Tatrzańska and is 95 m long and has an average width of 9.4 m. The riverbed consists of granite cobbles, ranging from 16 to 32 cm in size. The study reach was divided into five sections based on channel geometry and morphological features. The channel contains woody debris, gravel bars, riffles, pools, and riparian vegetation.

The research consisted of field mapping of litter (including mesoplastic and macroplastic), microbiological analysis on selective media of swabs taken from selected waste items and two tracer experiments with PET bottles in natural river channel. The experiment was conducted under low (Q = 0.63 m^3s^{-1}) and average discharges (Q = 1.24 m^3s^{-1}) and aimed to determine the likelihood of bottle passage and trap in different sections of the river channel. Each experiment consisted of 10 trials with the point injection of 20 bottles. The transport and deposition of the bottles were analysed using probabilistic methods, including Kaplan–Meier survival analysis and cumulative hazard functions (Kaplan and Meier 1958). A pairwise Chi–Square test was used to compare cumulative trapping probabilities, identifying significant differences in trapping rates across sections. The survival probabilities of bottles under average and low flow conditions were compared using the Mantel–Cox test to evaluate the impact of flow conditions on bottle passage (Bland and Altman 2004).

Fig. 1. Study site location.

3. RESULTS

3.1 Litter mapping

The field mapping revealed that the plastics (e.g., PET, PVC, PUR, PE, PP) were the most frequently (up to 86%) deposited materials followed by metal, textiles, and glass. The study showed that plastic foils (PE, PP) accounted for approximately 50% of all plastic materials in the riverbed. These items were often found in riffles, frequently within the main current, while other types of litter tended to accumulate along the outer bank of river bend, often on woody debris.

3.2 Microbiological analyses

Microbiological analysis revealed that the litter was covered with a biofilm hosting numerous bacteria. The most prevalent species were fecal *streptococci* (*Enterococcus faecalis* and *E. faecium*). Additionally, the presence of *E. coli*, *Staphylococcus* spp., and *Klebsiella* spp. was confirmed. Bacteria within the biofilm have the potential to act as carriers of antibiotic resistance, as demonstrated by the growth of bacterial colonies on selective media designed for isolating *ESBL-positive bacteria* and *methicillin-resistant staphylococci*. The swabs collected from biofilms on materials such as foams, foils, rigid plastics (PET) and pebble (for comparison) revealed that *Enterococcus* and *E. coli* were found on all tested materials, *Staphylococcus* spp. was present on most surfaces, except foam; *Klebsiella* spp. appeared on harder surfaces (PET and pebble); *Staphylococcus aureus* was detected only on foil and foam.

3.3 Tracer experiment

Tracer experiments showed that the cumulative probability of bottle passage was decreasing with decreasing flow while the cumulative hazard increased significantly under low flow conditions, especially in downstream sections (Fig. 2). The cumulative trapping probabilities var-

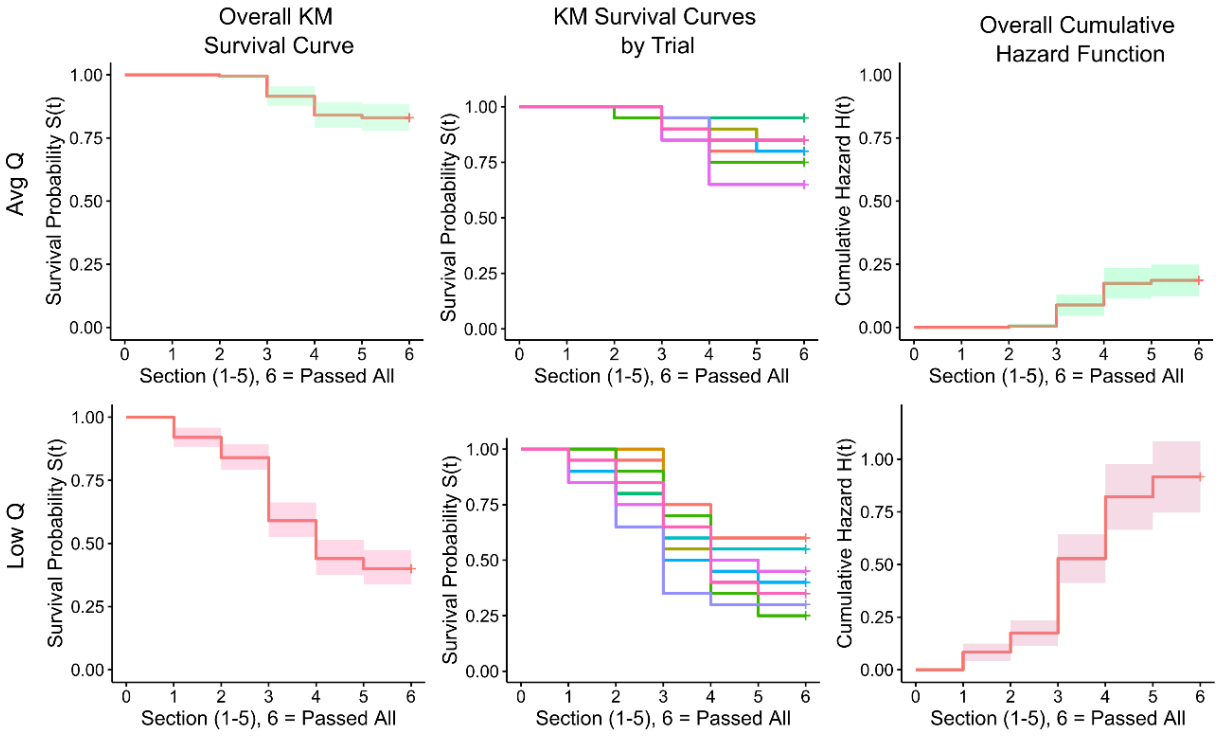

Fig. 2. Kaplan–Meier survival curves and cumulative hazard functions for average and low discharges. The x-axis is labeled with river sections (1–5), with 0 marking the start and 6 representing the final endpoint.

ied significantly across river sections, closely linked to the distribution and characteristics of channel morphological features. At average flow, most bottles accumulated in the middle and downstream sections of the river bend, while at low flow, deposition was more evenly spread across sections. In both scenarios, the highest number of bottles was deposited on either gravel bars or protruding cobbles, followed by woody debris. The Mantel–Cox test revealed significant difference in the survival probability curves obtained for average and low discharges, suggesting that the flow conditions have a substantial effect on the passage of bottles in the river.

4. CONCLUSIONS

The tracer experiments demonstrate that PET bottle deposition is significantly influenced by discharge and riverbed features, with the highest trapping occurring on gravel bars and woody debris. The microbiological findings highlight the potential health risks posed by biofilms on litter, which harbour bacteria, including antibiotic-resistant strains. Additionally, the study suggests that bacterial colonisation varies by material type, with harder surfaces supporting a more diverse microbiome. These results highlight the importance of addressing both the physical and microbiological impacts of plastic pollution in rivers to develop effective environmental management strategies.

Acknowledgements. This work was supported by the National Science Foundation (Poland) grant 2024/08/X/ST10/01264.

References

Bland, J.M., and D.G. Altman (2004), The logrank test, *BMJ* **328**, 7447, 1073, DOI: 10.1136/bmj.328.7447.1073.

Kaplan, E.L., and P. Meier (1958), Nonparametric estimation from incomplete observations, *J. Am. Stat. Assoc.* **53**, 282, 457–481, DOI: 10.1080/01621459.1958.10501452.

Pow, C.J., R. Fellows, H.L. White, L. Woodford, and R.S. Quilliam (2025), Fluvial flooding and plastic pollution – The delivery of potential human pathogenic bacteria into agricultural fields, *Environ. Poll.* **366**, 125518, DOI: 10.1016/j.envpol.2024.125518.

van Emmerik, T., and A. Schwarz (2020), Plastic debris in rivers, *WIREs Water* **7**, 1, e1398, DOI: 10.1002/wat2.1398.

Publications of the Institute of Geophysics, Polish Academy of Sciences
Geophysical Data Bases, Processing and Instrumentation
vol. 453 (E-14), 2025, pp. 89–92
DOI: 10.25171/InstGeoph_PAS_Publs-2025-049
XLII International School of Hydraulics, Radocza, Poland, 20–23 May 2025

Construction of an Automatic Flushing System for Retention Tanks, Including Rainwater Retention Tanks in Urban Stormwater Drainage Systems using Sluice Gate Devices

Marcin KRUKOWSKI[1], Piotr SIWICKI[1], and Ewa SIEDLEC[2]

[1]Institute of Environmental Engineering, Warsaw University of Life Sciences, Warsaw, Poland
✉ marcin_krukowski@sggw.edu.pl; piotr_siwicki@sggw.edu.pl

[2]Delinee Consulting Sp. z o.o., Infinite Fund, Warsaw, Poland
✉ e.siedlec@delineeconsulting.com

Abstract

Application of an autonomous flushing system for retention tanks using sluice gate systems that enable automated release of the stored energy of the water column in the impoundment chamber to achieve highly effective flushing of sedimentary contaminants accumulated in the tank during operation. The system operates automatically through sluice gate arrangements equipped with pneumatic drives and liquid level sensors, allowing precise control of the process. Compared to traditional methods (tilting gates, ejectors, pumps), the proposed system is characterized by low energy consumption, approximately 0.05 kWh per flushing cycle, and a simple configuration consisting of channel sluice gates and their drives, which reduces the risk of failure and simplifies routine maintenance of the tank. Additionally, the proposed solution is cost-effective in operation, with readily available spare parts on the domestic market. The flushing system consisted of valves installed on the front wall of the water damming tank. The facilities, including the installation, were verified by conducting tests to determine the hydraulic and technological conditions (sediment leaching efficiency) during the tank flushing process.

1. INTRODUCTION

The discharge of rainwater through the sewer system, especially the so-called intensive (short-term) ones, causes its flow to be overloaded. Due to the limited possibilities of designing cross-sections of pipes for such incidental events, when they occur, the system is overloaded and flooding occurs (Edel 2009). Given the existing and ongoing climate change (Wibig 2000; Słyś 2008), such situations are on the rise, which makes the use of technical solutions to reduce the

occurrence of flooding as well as floods by lowering maximum rainfall flows even necessary. Therefore, a key solution in rainwater drainage systems, but also in combined sewer systems, is the need for technical solutions in the form of retention tanks for periodic collection and retention of rainwater. This allows for proper water management, reduction of flood risk (during intense rainfall), use of stored water for economic purposes (irrigation of green areas) and the indirect function of reducing water pollution (mechanical pretreatment from suspended solids) (Królikowska and Królikowski 2012) or their gradual discharge into the sewer system or directly into a receiver (e.g., a watercourse) (Kaca and Kubrak 2020).

2. TECHNOLOGICAL TESTS OF THE RETENTION TANK

Rainwater flowing into the reservoir contains highly variable values of suspended solids concentrations over time. Therefore, it becomes very difficult to establish a suspended solids (granular) composition that can be unambiguously taken as a reference composition and used in modeling studies. Knowledge on this subject is not systematized. Therefore, after analyzing the necessary literature study and available research (Królikowska 2011; Ociepa 2011), a suitable granulometric composition was adopted and a mixture called substrate in the description was prepared to mimic the sludge in the retention tank under test (see, Fig. 1). The prepared substrate mixture was spread over the length of the reservoir $L = 17$ m and the width from the wall to the installed supports in the tank $B = 2.91$ m. As a result, the total area (A = area of the assumed substrate deposit) was about 46 m^2 per tank track), where the substrate was spread to a height (thickness) of about $m = 0.015$ m. For each part of the tank (per tank track), 750 kg of substrate was used. For the flushing process (one test), there was 1500 kg of substrate in the entire tank. Next, experiments were performed for the adopted criteria, namely: the flushing process with three valves installed per tank track, without walls and with walls separating the tank tracks (Fig. 1), for two actual fills in the damming tank $T_{max} = 2.4$ m, $T_{min} = 1.5$ m, and with a fixed opening of the valves $a = 0.1$ m and opening $a = 0.2$ m. Technological studies from the flushing process shown in Fig. 2 (selected material illustrating the effect of the flushing process), which illustrates the stages of the test performed. Decomposed substrate with the valves closed and thus accumulated flushing water in the flushing chamber $T = 2.4$ m and the subsequent programmed raising of the gates $a = 0.2$ m and the moving flushing wave can be seen, as well as the completely washed out deposited substrate in the next shot (Fig. 2). On the basis of the experiments carried out at the site, the efficiency of removal of sediment-mimicking

Fig. 1. A reservoir with a system of installed sluice gates to flush the tank. Visible line of installed supports for wide tanks (without walls). On the right, installed walls separating the recipient track from the supports.

Fig. 2. Effectiveness of substrate leaching on the real model at the preset filling T = 2.4 m in the reservoir damming chamber and the assumed opening of the sluice gates a = 0.2 m. Sediment flushed out at 100%. View of one track without applied walls.

substrate in fixed amounts and over the adopted area was determined using a quantitative method (see Table 1). Comparing the amount lined on the bottom to the amount of substrate remaining after the leaching process, collected and measured.

Table 1

Results of the calculated leakage efficiency of the decomposed substrate on the bottom of the retention tank model (weight per test for two tracks is 1500 kg). Flushing wave efficiency

Lp.	Flow q [m^3/ms]	Water level in tank T [m]	Opening of the sluice gates a [m]	Determined parameters to determine the effect of the flushing wave	
				Substrate volume Ms [kg]	Flushing wave efficiency EF [%]
Without the use of walls					
1	0.79	2.4	0.2	**16.59**	**99**
2	0.41	2.4	0.1	**219.51**	**85**
3	0.62	1.5	0.2	**599.05**	**60**
4	0.32	1.5	0.1	**755.12**	**50**

3. SUMMARY

The obtained results of the leaching efficiency on the real facility summarized above in Table 1, evidently show that the increase in the damming vessel T (height of the water column) is very important and affects the effect of gravitational flushing (leaching) of the accumulated deposit (prepared substrate). The selected opening of the sluice gates $a = 0.2$ m at the analyzed water fill T in the damming tank also allowed to obtain the most favorable technological parameters during the process of flushing the tank. The conducted experiments showed that the use of three sluice gates is the right for the flushing process in the tank.

References

Edel R. (2009), *Odwodnienie Dróg*, Wydawnictwa Komunikacji i Łączności, Warszawa, 411 pp. (in Polish).

Kaca, E., and J. Kubrak (eds.) (2020), *Budowle i Urządzenia do Pomiaru Przepływu Wody w Kanałach Melioracyjnych*, Bogucki Wydawnictwo Naukowe, Poznań, 264 pp. (in Polish).

Królikowska, J. (2011), Urządzenia inżynierskie z ruchem wirowym stosowane na sieci kanalizacyjnej do zmniejszenia ładunku zawiesiny w ściekach deszczowych, *Inż. Ekol*. **26**, 156–170 (in Polish).

Królikowska, J., and A.J. Królikowski (2012), *Wody Opadowe: Odprowadzanie, Zagospodarowanie, Podczyszczanie i Wykorzystanie*, Wydawnictwo Seidel-Przywecki, Warszawa, 368 pp. (in Polish).

Ociepa, E. (2011), Ocena zanieczyszczenia ścieków deszczowych trafiających do systemów kanalizacyjnych, *Inż. Ochr. Środow.* **14**, 4, 357–364 (in Polish).

Słyś, D. (2008), *Retencja i Infiltracja Wód Deszczowych*, Oficyna Wydawnicza Politechniki Rzeszowskiej, Rzeszów, 145–146 (in Polish).

Wibig, J. (2000), Współczesne zmiany klimatu – obserwacje, przyczyny, prognozy. **In:** K. Prandecki and M. Burchard-Dziubińska (eds.), *Zmiana Klimatu – Skutki dla Polskiego Społeczeństwa i Gospodarki*, Wyd. Komitet Prognoz „Polska 2000 Plus" przy Prezydium PAN, Warszawa, 213–246 (in Polish).

Publications of the Institute of Geophysics, Polish Academy of Sciences
Geophysical Data Bases, Processing and Instrumentation
vol. 453 (E-14), 2025, pp. 93–93
DOI: 10.25171/InstGeoph_PAS_Publs-2025-050
XLII International School of Hydraulics, Radocza, Poland, 20–23 May 2025

Sedimentation Conditions in Small Anthropogenic Pond Estimated by Fast Field Measurements with the Use of Unmanned Vehicles

Tomasz LEWICKI[1,✉], Artur MAGNUSZEWSKI[2,✉], and Piotr SZWARCZEWSKI[2]

[1]Water Survey Tech, Warszawa, Poland
✉ tomasz.lewicki@watersurveytech.pl

[2]Faculty of Geography and Regional Studies, University of Warsaw, Warsaw, Poland
✉ asmagnus@uw.edu.pl

A b s t r a c t

Zapadliska Lake is situated approximately 1 km from the Zegrze Reservoir, near the confluence of the Narew and Rządza rivers. The terrain where it is located is the Holocene overflood terrace and Vistulian glaciation dune terrace. The pleistocene dune terrace at the contact with the Holocene terrace was dissected forming elongated valleys filled with the organic material. The lake was formed due to a rise in the groundwater table following the construction of the Zegrze Reservoir in 1963. Zapadliska Lake has an area of 18,900 m^2 and its catchment is 102,000 m^2. The catchment area is covered by the pine forest and is not connected to the river system. Lake has a stable water level controlled by the level of Zegrze Reservoir which is stabilized at 79.02 m a.s.l.

Publications of the Institute of Geophysics, Polish Academy of Sciences
Geophysical Data Bases, Processing and Instrumentation
vol. 453 (E-14), 2025, pp. 95–98
DOI: 10.25171/InstGeoph_PAS_Publs-2025-051
XLII International School of Hydraulics, Radocza, Poland, 20–23 May 2025

Beaver Dams in the Context of a Factor Shaping the Hydromorphological and Hydrological Conditions of Small Lowland Streams

Stanisław ZABOROWSKI, Tomasz KAŁUŻA, Maciej PAWLAK
and Mateusz HAMMERLING

Poznań University of Life Sciences, Poznań, Poland

✉ stanislaw.zaborowski@up.poznan.pl; tomasz.kaluza@up.poznan.pl;
maciej.pawlak@up.poznan.pl; mateusz.hammerling@up.poznan.pl

Abstract

Beavers are responsible for creating temporary water reservoirs, that significantly impact the environment and local river hydrology. This study focused on the possibility of determining the impact of beaver (Castor spp.) dams as a method to support water retention in the environment. Studies carried out on three small lowland streams in central Poland revealed that beaver dams, even in modified riverbeds, aid the creation of shallow floodplains and ponds by improving instream retention. Innovative analyses considered the construction materials of the dams and their impact on river hydromorphology and sediment transport. The results highlight the importance of beavers in water retention processes, stabilisation of water levels during low flows and protection of biodiversity. The study demonstrated that beaver dams locally, these structures influence hydrology, improve ground moisture, extend water retention times and create habitats for many new species improving biodiversity. The collected data highlights the potential of beaver dams as a tool to help manage water resources in the context of climate change. Further research may provide guidance for the sustainable utilisation of beavers in conservation strategies and landscape planning.

1. METHODOLOGY AND MATERIALS

Analyses of the influence of natural damming on hydromorphological, hydrological, and environmental conditions were carried out on the example of selected lowland rivers located in the Wielkopolska region, Poland. The studied streams inhabited by beavers include the Kończak River (Stobniczka), Mogilnica, and Cybina.

The water table configuration in the riverbed near the beaver dams was determined based on elevation measurements conducted during fieldwork. Detailed measurements of the riverbed were conducted, taking into account the geometry of the riverbed and the water table level. Data for analysis and calculations were obtained from field studies conducted between 2020 and 2023. Geodetic equipment such as an optical level and RTK GPS were used for elevation measurements. Water flow velocity in river channels was measured using a Valeport Model 801 electromagnetic. To determine the discharge of water, the results of velocity measurements were utilised. In each cross-section, several hydrometric verticals were identified, located both downstream and upstream of the structure.

The determination of the material used to construct the beaver dams (Scamardo at al. 2022; Butler 2012) was carried out based on field studies and measurements of the diameters of the branches that made up the structure of the dam. The measurements were made using a digital calliper with an accuracy of 0.5 mm. The granulometric composition of the sediment samples was determined using the sieving method, according to the standard procedure described in the national standard PN-EN 933-1.

For hydrological analyses, the SCALGO Live software was used, which is considered a very useful tool for determining surface runoff paths and a better understanding of the impact of land use on hydrological conditions in the catchment area. SCALGO is based on a digital terrain model obtained through Airborne Laser Scanning (ALS). According to the available information, the models take into account the detailed microrelief of the terrain, including buildings, road embankments, and drainage ditches. A Digital Elevation Model (DEM) was used to create a three-dimensional representation of fragments of the studied catchments. The terrain model was built with a raster resolution of 1×1 meters. The program was used, among other things, to determine the surface area and volume of the beaver ponds and the extent of the backwater, which was verified by field measurements.

2. RESULTS

Measurements of the type and properties of the dam material have been made based on 103 samples. The largest percentage of all measured samples consisted of branches with a diameter of Ø 5 cm (22.14%). Branches with a diameter of Ø 4 cm accounted for 19.08%. Branches with diameters ranging from 2 to 5 cm accounted for as much as 74.05% of all branches used in the construction of the dams. The dam, in addition to the wooden material, was also constructed with mud (which sealed the structure) and was partially covered with herbaceous vegetation. The construction material consisted of willow shrubs (Salix alba L. and Salix fragilis) and branches of black alder (Alnus glutinosa (L.) Gaertn.), with trunks and gnaw marks identified on the banks of the stream.

The SCALGO program was used to estimate the volume of beaver ponds and to represent the areas that will be covered by water as a result of the rise in the water table in the stream. Due to the capabilities of the software, these results were presented assuming a constant water level elevation. The estimated increase in retention volume was calculated based on the increase in the cross-sectional area of the stream resulting from the rise in the water level (considering the water level before the beaver dam and after the beaver dam, treating the latter as the pre-dam construction level) and the length determined using the Digital Elevation Model (DEM) of the backwater formed as a result. Due to the decrease in the water level as a result of the cessation of the backwater effect created by the beaver dams, it was assumed that the backwater would decrease uniformly along its length, halving the estimated increased retention volume.

Based on field measurements of the rise in water level resulting from the construction of beaver dams, the change in the water level elevation was estimated. Figure 1a shows the extent of the backwater associated with the rise in the water level on the Kończak River. The impact

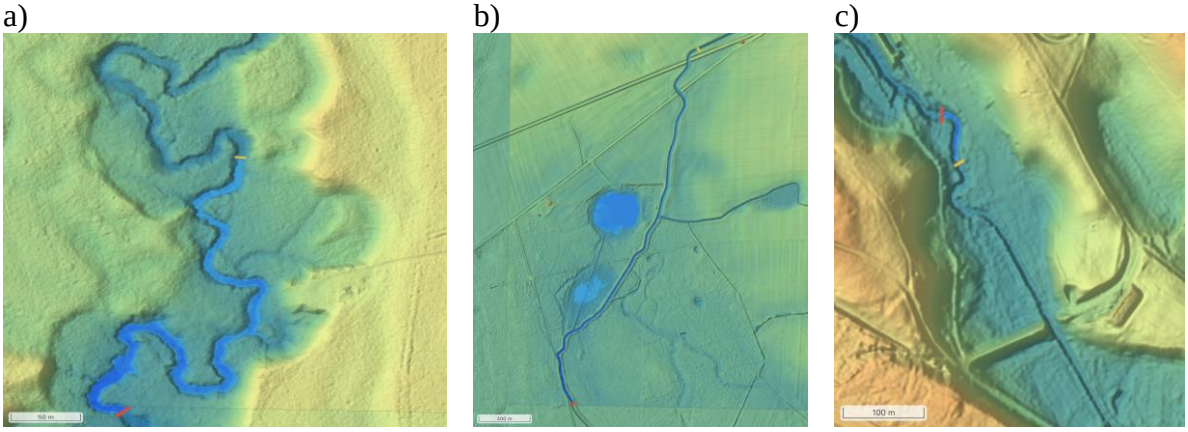

Fig. 1. The extent of backflow due to the construction of the Beaver Dam on the: a) Kończak River (WL 54.22 m a.s.l. – damming 0.31 m); b) Mogilnica River (WL 76.16 m a.s.l. – damming 0.74 m); c) Cybina River (WL 60.52 m a.s.l. – damming 0.37 m) (The red line represents the location of the beaver dam, and the yellow line indicates the extent of the backflow at the specified water level elevation).

of the backwater in this case is 510 m. Figure 1b shows the extent of the backwater associated with the rise in water levels on the Mogilnica River, which reaches as much as 1.8 km. Additionally, as a result of the rise in the water level, two depressions in the terrain were filled with water, forming two ponds. The additional retention volume of these two ponds is approximately 6,500 m³, with a water level elevation of 76.16 m above sea level. In Figure 1c, the reach of the backwater effect related to the rise in the water table on the Cybina River is shown. In this case, due to the terrain surrounding the river and the slope of the riverbed, the reach of the backwater effect was approximately 80 m.

3. CONCLUSIONS

Studies conducted on three small lowland watercourses located in central Poland have shown beaver's influence on shaping local watercourse hydromorphology and water retention. Even in the case of transformed, narrow troughs (e.g. on the Mogilnica River, where channel retention was relatively low and the valley layout did not directly affect the formation of beaver ponds) the extent of beaver dam accumulation allowed the formation of shallow floodplains and ponds in field depressions hydraulically connected to the main watercourse. The novelty of the research is the detailed analysis of dam construction material and the study of the impact of beaver dams on river hydromorphology, including changes in the grain size of the debris. Precise data on the size of dams and their impact on water retention and sediment transport have been obtained, enriching knowledge of the role of beavers in ecosystems. Despite the numerous ecological benefits, there are still research gaps regarding the comparison of beaver dams with other anthropogenic water bodies. This includes their impact on farming and forestry. The results also underscore the potential importance of beaver dams as a tool in water management in the context of climate change. The magnitudes of flows during low periods clearly indicate that only the additional effect of beaver damming in the channel allows the water table to remain relatively stable.

Further research into their activities could provide valuable insights into the effective use of beavers in sustainable development.

References

Butler, D.R. (2012), Characteristics of beaver ponds on deltas in a mountain environment, *Earth Surf. Process. Landf.* **37**, 8, 876–882, DOI: 10.1002/esp.3218.

Scamardo, J.E., S. Marshall, and E. Wohl (2022), Estimating widespread beaver dam loss: Habitat decline and surface storage loss at a regional scale, *Ecosphere* **13**, 3, e3962, DOI: 10.1002/ecs2.3962.

Publications of the Institute of Geophysics, Polish Academy of Sciences
Geophysical Data Bases, Processing and Instrumentation
vol. 453 (E-14), 2025, pp. 99–99
DOI: 10.25171/InstGeoph_PAS_Publs-2025-052
XLII International School of Hydraulics, Radocza, Poland, 20–23 May 2025

Critical Submergence for Horizontal Intake Structures under Symmetrical Approach Flow Conditions

Serkan GOKMENER[1,✉], Mustafa GOGUS[2], and Dalal Al-OBAIDI[2]

[1]Hydraulics Laboratory, Department of Civil Engineering, Middle East Technical University, Ankara, Turkey

[2]Department of Civil Engineering, Çankaya University, Ankara, Turkey

✉ gokmener@metu.edu.tr; sgokmener11@gmail.com

A b s t r a c t

Air-entraining vortices at intake structures pose significant challenges to the operation of water intake systems, leading to efficiency losses and potential damage to hydraulic equipment. This study focuses on predicting critical submergence depth, S_c, the vertical distance required to prevent air-entrainment vortices, for horizontal intakes under symmetrical approach flow conditions. Dimensional analysis is employed, analyzing the effect of intake geometry, Froude number, Reynolds number, and Weber number. 409 experimental data observations were reanalyzed from different studies to derive more general and accurate empirical equations predicting dimensionless critical submergence, S_c/D_i. The analysis revealed that the intake Froude number $(Fr)_i$ and the geometric parameter, $2b/D_i$, are the dominant factors influencing S_c/D_i. Moreover, it is stated that narrower sidewall clearances are more prone to the formation of air-entraining vortices at $(Fr)_i$ values smaller than 3.5 while wider ones are at $(Fr)_i$ values greater than 3.5. Empirical equations derived exhibit strong statistical performance, with R^2 values up to 0.988. The most accurate empirical equations are obtained while considering all the flow and geometric parameters to predict S_c/D_i. On the contrary, the accuracy of the empirical equations considering only $(Fr)_i$ gives moderate results in predicting S_c/D_i.

Publications of the Institute of Geophysics, Polish Academy of Sciences
Geophysical Data Bases, Processing and Instrumentation
vol. 453 (E-14), 2025, pp. 101–104
DOI: 10.25171/InstGeoph_PAS_Publs-2025-053
XLII International School of Hydraulics, Radocza, Poland, 20–23 May 2025

Ecosystem Services to Enhance the Resilience of Coastal Regions and Communities to Flood Risks in a Catchment to Sea Perspective

María BERMÚDEZ[1], Maurizio BROCCHINI[2], Rui GASPAR[3], Michael NONES[4], Sebastian VILLASANTE[5], and Mario FRANCA[6]

[1]University of Granada, Granada, Spain
✉ mariabermudez@ugr.es

[2]Marche Polytechnic University, Ancona, Italy
✉ m.brocchini@staff.univpm.it

[3]HEI-Lab-Human-Environment Interaction Lab, Lusófona University, Lisbon, Portugal
✉ rui.gaspar@ulusofona.pt

[4]Institute of Geophysics, Polish Academy of Sciences, Warsaw, Poland
✉ mnones@igf.edu.pl

[5]CRETUS-EqualSea Lab, University of Santiago de Compostela, Compostela, Spain
✉ sebastian.villasante@usc.es

[6]Karlsruhe Institute of Technology, Karlsruhe, Germany
✉ mario.franca@kit.edu

A b s t r a c t

An overview of the recently financed Water4All Joint Transnational Call 2023 project "Ecosystem services to enhance the resilience of coastal regions and communities to flood risks in a catchment to sea perspective (EcoC2S)" is given, highlighting innovative points, and challenges that the involved parties aim to address in the next years. EcoC2S is a joint initiative of six partners, specifically the University of Granada and the University of Santiago de Compostela (Spain), the Marche Polytechnic University (Italy), the Lusófona University (Portugal), the Institute of Geophysics PAS (Poland), and the Karlsruhe Institute of Technology (Germany).

1. THE ECOC2S PROJECT

1.1 Background

Globally, and in Europe in particular, coastal floods are one the most common natural hazards with major economic, social, and ecological impacts on communities (Vousdoukas et al. 2020). Coastal systems support biodiversity and provide critical ecosystem services (ES), including flood protection. The effects of climate change (CC) enhance hazards in such flood-prone areas and place additional physical pressure on ES, while also adding pressure to the social system, by interfering with people's socio-cultural and socio-economic valuation of such places, with potential consequences to their place identity and their motivation, emotions, cognitions, and behaviours associated with them. This creates an urging need for reliable risk assessment, management and communication methods (Parlagreco et al. 2019) and innovative community engagement approaches through stakeholders' co-design methods, towards reducing vulnerabilities, protecting what people value, and enhancing socio-physical systems adaptation towards building resilience (Gaspar et al. 2019).

The lack of reliable methods for a holistic evaluation of flood risk is hampering progress. Many catastrophic floods have a compound dimension, where the interaction of multivariate and multiscale drivers usually exacerbates their effects. This is particularly true for estuarine cities and regions (Brocchini 2024) and calls for a holistic approach to flood risk management, combining both physical and ecological drivers and feedback.

1.2 Objective and methods

To address the above-mentioned knowledge gaps, EcoC2S aims to co-develop a holistic flood risk assessment approach (Fig. 1) to quantify the contribution of natural systems and blue-green infrastructure to flood protection in transitional and coastal areas and the co-creation and further implementation of resilient pathways based on ES. Such an approach will allow for:

- Reliable and affordable assessment of flood risk jointly considering geophysical and societal preconditions and relevant flood drivers, with their dependencies and interactions.
- Estimating the contribution of meteorological, eco-morphodynamic and human drivers to flood impact.
- Valuation of water flow regulation by inland and coastal ecosystems spanning the water continuum.
- Assessment of the functionality of ecosystems and blue-green infrastructure within a CC context, including coastal ecosystems' resilience and geomorphic adaptation under SLR.
- Assessment of the socio-cultural and socio-economic value of ES for local communities, the determinants of such valuation (behavioural, motivational, affective, and cognitive), and if perceived past, present and future changes in ES, change its perceived value and predict (non)acceptance of ES solutions.
- Engagement of local communities and stakeholders in the co-identification of research gaps and needs, and the co-design and co-implementation of ES, with a focus on overcoming barriers to these.
- Promoting resilience pathways towards sustainable development under CC, which are based on ES and are multifunctional, flexible, gender-responsive and adaptive to account for multiple uncertainties.

The project will focus on five different topics:

1) Co-identification of knowledge gaps and ecosystem services valuation, following a participatory approach. Use of counterfactual analysis to assess the key flood drivers and their contribution to flood risk based on previous flood events, and to understand human preferences and perceptions of ES, and their value.

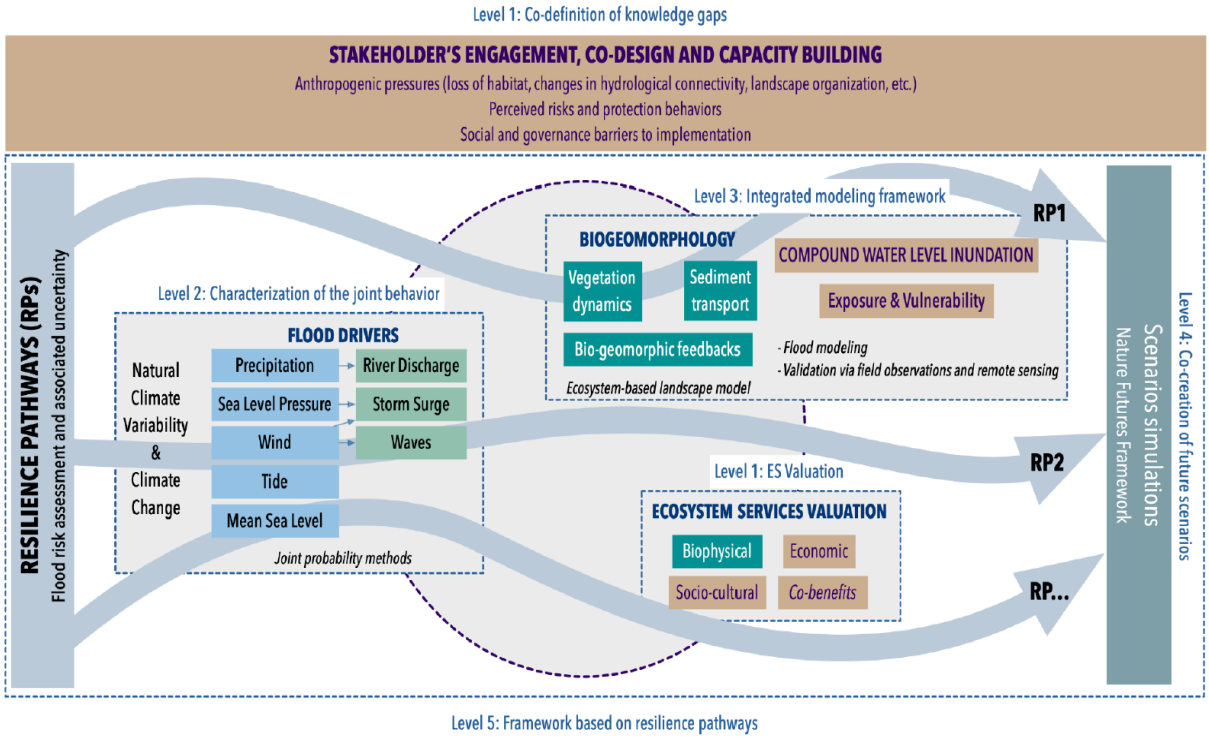

Fig. Conceptual framework of the EcoC2S project.

2) Characterization of the joint behaviour of the geophysical preconditions of the catchment with the atmospheric and marine drivers at the coast, considering the combination of multiple and concomitant variables to define the probability of occurrence of compound extreme events.
3) Integrated modelling framework that includes eco-morphodynamic effects on compound flood hazard. Physically based formulations will be implemented to consider the effect of vegetation on the flow field in areas such as tidal marshes. The long-term eco-morphological evolution, driven by the interactions between vegetation dynamics, water flow, and sediment transport (bio-geomorphic feedbacks), will be analysed with a combination of remote sensing, field measurements and numerical simulations.
4) Co-creation of plausible future scenarios for sustainable and resilient ES, bringing together different actors into dialogue and reflexive learning, to co-create and co-realize solution-oriented pathways.
5) Establishment of a framework that guides the development of long-term mitigation measures and management strategies that enhance the resilience of human and natural coastal systems to extreme events. Rather than deterministic approaches, the definition of resilience pathways allows adaptive measures considering the stochastic nature of the geophysical factors, the evolution of natural systems, and how humans interact and value the ecosystems where they live and that they use.

The methodology will be tested in two pilot case studies at the river basin level: i) Cádiz Bay in Spain, and ii) Senigallia in Italy, as both are coastal systems with compound flooding potential and highly intervened by human activity. They are characteristic of European archetypes (namely, structured approaches to classify, understand, and address compound flooding) in terms of the different contributions of the flooding drivers, ES potential, and catchment, and coastal typologies. Those case studies will be used as a framework to identify and categorize common flooding patterns and get a first estimation of the likelihood and severity of flood

events. Moreover, they will be ideal to help in the process of communication between experts, policymakers, and the public in the co-development of resilience pathways, and ultimately to facilitate the transfer to other sites.

Acknowledgements. The EcoC2S project is funded by the Joint Transnational Call 2023 "Aquatic Ecosystem Services" of the Water4All Partnership. Each consortium participant is funded by the Funding Organisation from its country/region, as follows: University of Granada and University of Santiago de Compostela (Spain) by AEI – Agencia Estatal de Investigación, Università Politecnica delle Marche (Italy) by MUR – Ministry of Universities and Research, COFAC-Universidade Lusófona (Portugal) by FCT – Fundação para a Ciência e a Tecnologia, Institute of Geophysics Polish Academy of Sciences by NCBR – The National Centre for Research and Development.

References

Brocchini, M. (2024), Sea-river interactions within microtidal systems: field observations, modeling and applications. **In:** *Keynote Lecture at 38th Int. Conf. Coastal Engineering, 8–14 September 2024, Rome, Italy*, available from: https://icce2024.com/keynote-lectures/.

Gaspar R., Z. Yan, and S. Domingos (2019), Extreme natural and man-made events and human adaptive responses mediated by information and communication technologies' use: A systematic literature review, *Technol. Forecast. Soc. Change* **145**, 125–135, DOI: 10.1016/j.techfore.2019.04.029.

Parlagreco, L., L. Melito, S. Devoti, E. Perugini, L. Soldini, G. Zitti, and M. Brocchini (2019), Monitoring for coastal resilience: Preliminary data from five Italian sandy beaches. *Sensors* **19**, 8, 1854, DOI: 10.3390/s19081854.

Vousdoukas, M.I., L. Mentaschi, J. Hinkel, P.J. Ward, I. Mongelli, J.C. Ciscar, and L. Feyen (2020), Economic motivation for raising coastal flood defenses in Europe, *Nat. Commun.* **11**, 1, 2119, DOI: 10.1038/s41467-020-15665-3.

Publications of the Institute of Geophysics, Polish Academy of Sciences
Geophysical Data Bases, Processing and Instrumentation
vol. 453 (E-14), 2025, pp. 105–105
DOI: 10.25171/InstGeoph_PAS_Publs-2025-054
XLII International School of Hydraulics, Radocza, Poland, 20–23 May 2025

Phytoplankton Blooms Localized by Sentinel-2 Images and Hydrodynamic Modelling – Sulejów Reservoir, Pilica River, Poland

Peshang Hama KARIM[1], Monika B. KALINOWSKA[2],
Aleksandra ZIEMIŃSKA-STOLARSKA[3], and Artur MAGNUSZEWSKI[4,✉]

[1]Doctoral School of Exact and Natural Sciences,
Discipline of Earth and Related Environmental Sciences,
University of Warsaw, Warsaw

[2]Institute of Geophysics, Polish Academy of Sciences, Warsaw

[3]Faculty of Process and Environmental Engineering, Technical University of Lodz, Łódź

[4]Faculty of Geography and Regional Studies, University of Warsaw, Warsaw

✉ asmagnus@uw.edu.pl

A b s t r a c t

Reservoirs created by damming rivers significantly modify the abiotic and biotic elements of the environment. One of the problems is the storage of nutrients and organic matter in reservoirs, resulting in the lowering of water quality due to eutrophication. The Sulejów Reservoir in Central Poland was the subject of the research presented in this article; it focused on gaining a better understanding of the balance of nutrients and the use of Sentinel-2 remote sensing data to detect phytoplankton blooms, and on finding the pattern of wind-driven surface currents using the CCHE2D – a depth-averaged hydrodynamic model. Hydraulic conditions such as average in cross-section velocities have been shown using HEC-RAS model. The calculation of the total phosphorus load has shown that the reservoir mainly acts as a place for nutrient storage. Still, during low flow and intensive phytoplankton blooms, it can be a source of nutrients. The distribution of phytoplankton blooms on the Sulejów Reservoir was documented using eight Sentinel-2 satellite images from the vegetation season of 2020 and the Normalized Difference Chlorophyll Index (NDCl). Coupling remote sensing data and 2D numerical modelling helps to interpret the hydrodynamic model results and understand nutrients and sediment dynamics within the reservoir.

Publications of the Institute of Geophysics, Polish Academy of Sciences
Geophysical Data Bases, Processing and Instrumentation
vol. 453 (E-14), 2025, pp. 107–110
DOI: 10.25171/InstGeoph_PAS_Publs-2025-055
XLII International School of Hydraulics, Radocza, Poland, 20–23 May 2025

Forecasting the Flood in 2024 in SW Poland on Virtual Stations of Altimetry Satellites Based on the AltHydro System

Michał HALICKI✉ and Tomasz NIEDZIELSKI

Department of Geoinformatics and Cartography,
Faculty of Earth Sciences and Environmental Management, University of Wrocław,
Wrocław, Poland

✉ michal.halicki@uwr.edu.pl

Abstract

This study describes the AltHydro system, which is the first approach to calculate water level predictions at virtual stations (VS) of altimetry satellites. It has been developed for the middle Odra River basin, where 8 VS of the Sentinel-3A satellite have been selected. The system is based on a Vector Autoregressive Model, which is utilized to issue water level prognoses for gauge stations. The forecasts are later transferred to the neighbouring VS using (1) linear regression (vertical shift) updated whenever a new satellite measurement is available, as well as (2) flow velocity estimates (temporal shift), calculated hourly for each prediction. The system operates in real-time and its results are presented on the AltHydro map portal (http://althydro.uwr.edu.pl/). The accuracy assessment can only be based on nadir (Sentinel-3A) and wide-swath (SWOT) altimetry observations, as these are the only water level measurements available for the virtual stations. In this study we used the system to forecast water levels during the flood in September 2024 in SW Poland. A good accuracy of the AltHydro progoses was observed, with absolute error values ranging from 4 to 45 cm for forecasts with a lead time of 24 hours.

1. INTRODUCTION

Satellite altimetry is a technique of measuring elevation, that has been providing regular water level measurements over the recent decades. Although originally designed to monitor ocean dynamics, recent altimetry missions have proven to be suitable for monitoring inland waters, including medium and small rivers less than 100 m wide. Due to the nadir-looking nature of radar altimetry (unlike satellite imagery), water level observations are only obtainable at virtual stations (VS), specifically located where the ground track of the satellite intersects a river

course. However, these observations cannot be used directly to predict water levels due to the poor temporal resolution of the measurements (e.g. 27 days for the Sentinel-3 satellites). On the other hand, given the decreasing number of gauging stations worldwide (Hannah et al. 2011) and the increasing accuracy and availability of satellite observations, the incorporation of remote sensing data into hydrological models seems to be a scientific goal of growing importance.

The goal of this paper is to present the AltHydro water level prediction system (http://althydro.uwr.edu.pl/) that has been developed at the University of Wrocław. AltHydro provides real-time forecasts of water levels at 8 VS of the Sentinel-3A satellite on the middle Odra River (Table 1). A short assessment of the accuracy of the AltHydro system during the flood in 2024 in SW Poland will also be presented.

2. DATA AND METHODS

The main idea of AltHydro is to calculate water level predictions for gauge stations and then transfer them to the neighbouring VS. For each hour, the system downloads the most recent gauge measurements. These observations are then analysed for potential outliers using the Isolation Forest algorithm (Liu et al. 2008) and interpolated with the LinAR method (Niedzielski and Halicki 2023). Altimetry observations are downloaded from the DAHITI database (Schwatke et al. 2015) and corrected for the river slope bias (Halicki et al. 2023) using the high-resolution water surface slopes calculated by Schwatke et al. (2024).

For each hour, the AltHydro system calculates water level predictions (based on gauge data only) in a 72-hour horizon for six gauge stations (Table 1) using a Vector Autoregressive Model (Halicki and Niedzielski 2024). To transfer the predictions to the neighbouring VS, two aspects have to be considered: (1) the vertical, and (2) the temporal shift. To account for the vertical difference between the stations, we calculate linear regression equations based on paired gauge and satellite observations. Each time a new satellite observation is available, i.e. every 27 days, the regression coefficients are recalculated and updated.

Second, to estimate the time needed for the water to flow from the upstream gauge to the neighbouring VS, we apply a statistical approach to determine the water velocity based on the time lag between two gauging stations (Halicki and Niedzielski 2022). Finally, the water level predictions for the upstream gauge are shifted in time and recalculated with the most current regression coefficients.

Table 1
Virtual stations included in the AltHydro system

VS name	Latitude	Longitude	Gauge upstream	Distance to gauge [km]
VS1 Lubusz	52.44061	14.57103	Słubice	11.880
VS2 Kunice	52.26289	14.65722	Biała Góra	24.748
VS3 Bieganów	52.19821	14.68858	Biała Góra	14.634
VS4 Pomorsko	52.0443	15.4924	Cigacice	8.453
VS5 Zabór	51.97289	15.73154	Nowa Sól	26.769
VS6 Dąbrowa	51.9007	15.7661	Nowa Sól	13.769
VS7 Bytom Odrzański	51.72609	15.84947	Głogów	21.668
VS8 Wyszanów	51.68025	16.2548	Ścinawa	45.628

3. RESULTS AND DISCUSSION

Since there are no *in situ* measurements at VS, the only data for assessing the prediction accuracy were the satellite observations themselves, including those from Sentinel-3A and SWOT. Here, we have analyzed only a short period between September and October 2024, when the flood in SW Poland occurred. In general, the absolute errors of predictions with a lead time of 24 hours ranged from 4 cm (VS4) to 45 cm (VS6) with a mean value of 19 cm. Longer predictions were characterized by greater errors, exceeding 1 m for the 72-hour predictions. The accuracy of the AltHydro forecasts at VS1 with lead time of 24 hours are presented in Fig. 1. A generally good agreement between forecasts and water level estimations at VS can be observed, although discrepancies occur at the most dynamic rise of the hydrograph. On the other hand, the very good accuracy of altimetry observations should be noted, both from the nadir (Sentinel-3A) and wide-swath (SWOT) altimetry mission.

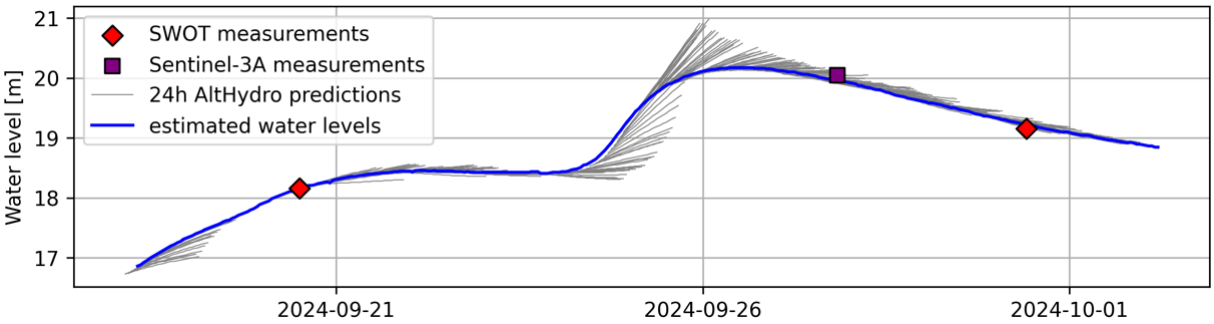

Fig. 1. Water level predictions with a lead time of 24 hours for the VS1 (Lubusz) during the flood in 2024 in SW Poland.

AltHydro is the first approach to forecast water levels at VS of altimetry satellites. It operates in real time and, for each hour, it provides predictions for 8 VS on the middle Odra River (http://althydro.uwr.edu.pl/). It allows to densify the network of water level forecasts, which can be valuable especially in sparsely monitored basins.

Acknowledgements. The research presented in this paper has been carried out in frame of the project no. 2020/38/E/ST10/00295 within the Sonata BIS programme of the National Science Centre, Poland. The research has also been supported by the Bekker Programme of the Polish National Agency for Academic Exchange, as well as by the program "Excellence Initiative – Research University".

References

Halicki, M., and T. Niedzielski (2022), The accuracy of the Sentinel-3A altimetry over Polish rivers, *J. Hydrol*. **606**, 127355, DOI: 10.1016/j.jhydrol.2021.127355.

Halicki, M., and T. Niedzielski (2024), A new approach for hydrograph data interpolation and outlier removal for vector autoregressive modelling: a case study from the Odra/Oder River, *Stoch. Environ. Res. Risk Assess*. **38**, 2781–2796, DOI: 10.1007/s00477-024-02711-5.

Halicki, M., C. Schwatke, and T. Niedzielski (2023), The impact of the satellite ground track shift on the accuracy of altimetric measurements on rivers: A case study of the Sentinel-3 altimetry on the Odra/Oder River, *J. Hydrol.* **617**, A, 128761, DOI: 10.1016/j.jhydrol.2022.128761.

Hannah, D.M., S. Demuth, H.A.J. van Lanen, U. Looser, C. Prudhomme, G. Rees, K. Stahl, and L.M. Tallaksen (2011), Large-scale river flow archives: importance, current status and future needs, *Hydrol. Process*. **25**, 7, 1191–1200, DOI: 10.1002/hyp.7794.

Liu, F.T., K.M. Ting, and Z.-H. Zhou (2008), Isolation forest. **In:** *2008 Eighth IEEE Int. Conf. Data Mining*, IEEE, 413–422, DOI: 10.1109/ICDM.2008.17.

Niedzielski, T., and M. Halicki (2023), Improving linear interpolation of missing hydrological data by applying integrated autoregressive models, *Water Resour. Manage.* **37**, 5707–5724, DOI: 10.1007/s11269-023-03625-7.

Schwatke, C., D. Dettmering, W. Bosch, and F.Seitz (2015), DAHITI – an innovative approach for estimating water level time series over inland waters using multi-mission satellite altimetry, *Hydrol. Earth Syst. Sci*. **19**, 4345–4364, DOI: 10.5194/hess-19-4345-2015.

Schwatke, C., M. Halicki, and D. Scherer (2024), Generation of high-resolution water surface slopes from multi-mission satellite altimetry, *Water Resour. Res.* **60**, 5, e2023WR034907, DOI: 10.1029/2023WR034907.

Publications of the Institute of Geophysics, Polish Academy of Sciences
Geophysical Data Bases, Processing and Instrumentation
vol. 453 (E-14), 2025, pp. 111–114
DOI: 10.25171/InstGeoph_PAS_Publs-2025-056
XLII International School of Hydraulics, Radocza, Poland, 20–23 May 2025

OBIA Classification of Riverine Vegetation in a Small Open Channel Using RGB Drone Imagery

Adrian BRÓŻ, Monika KALINOWSKA, and Emilia KARAMUZ

Institute of Geophysics, Polish Academy of Sciences, Warsaw, Poland

✉ adrian.broz@igf.edu.pl; monika.kalinowska@igf.edu.pl; emikar@igf.edu.pl

Abstract

In temperate areas, small watercourses, especially agricultural ditches, are typically surrounded by seasonally changing vegetation, which significantly influences hydrodynamic and ecological processes within and around the channel. However, research on how different vegetation maintenance practices affect flow and mixing processes at the reach scale remains limited. Addressing this knowledge gap requires a series of field experiments conducted under varying flow and vegetation conditions, along with a simple and accessible method for vegetation characterisation. This study evaluates the efficiency of RGB drone imagery in mapping riverine vegetation using OBIA classifiers. For low vegetation coverage, SVM combined with Haralick textural features provided the best results, while for high vegetation, SVM combined with DEM delivered the best classification outcomes.

1. INTRODUCTION

Fluvial vegetation plays a crucial role in the wellbeing of lotic ecosystems by creating habitats for aquatic fauna, reducing pollutant and nutrients loads, and, importantly, influencing hydrodynamics. Fluvial vegetation includes both riparian and riverine vegetation. However, most studies focus primarily on riparian vegetation, while riverine vegetation, especially in small channels, plays a key role in modifying flow dynamics. Regular mowing of vegetation for flood prevention remains common, yet its impact on fluvial ecosystems is poorly studied. Although the need for alternative solutions is often emphasised, it has not been thoroughly investigated. (Kalinowska et al. 2023). To fill the gap, a series of field experiments are planned to investigate the impact of riverine vegetation on flow and mixing processes in small watercourses with natural vegetation. Assessing seasonal changes in vegetation coverage (V_C) will be essential. Therefore, developing an efficient, objective, and reproducible method for evaluating aquatic vegetation coverage is crucial. The primary objective of this study is to explore the feasibility of using RGB drone imagery alone for river vegetation assessment in small rivers.

2. METHODS

The images were captured using a DJI Phantom 4 UAV equipped with an RGB camera in Warszawicki Channel, located within the Vistula Basin in eastern Poland (Kalinowska et al. 2023). The mission was conducted twice: firstly under full vegetation conditions (high V_C) and after mowing (low V_C). The collected images were processed in Agisoft Metashape using the Structure from Motion technique to generate orthomosaics and Digital Elevation Models (DEMs). The orthomosaics for both low and high V_C were then segmented using the Mean Shift algorithm. Training sample layers were generated with a relatively small number of samples to maintain a similar number of polygons (20–30 per class) and comparable area for both classes in two vegetation cases.

The segmented images and training layers were then used to perform supervised classification using all four supervised object-based image classification (OBIA) algorithms available in ArcGIS Pro: Maximum Likelihood (ML), Random Trees (RT), Support Vector Machine (SVM), and K-Nearest Neighbors (KNN). OBIA was chosen because, in contrast to pixel-based image classification, it groups adjacent pixels into meaningful objects and classifies them based on spectral, shape, texture, and spatial characteristics.

In order to calculate accuracy of the classification results, 250 points were generated randomly and manually labeled as either water or vegetation. Moreover, the F1 score (a metric useful when there is an imbalance between classes due to its emphasis on misclassifications) and Cohen's kappa (assesses the agreement between two classifiers, correcting for the agreement that could happen by chance) were calculated.

In this study, the use of DEM and Haralick Texture Extraction (HTE) (Haralick et al. 1973) in addition to RGB data was also investigated. HTE was performed using the Orfeo Toolbox (OTB) plugin in QGIS. Three Haralick texture features were selected: Entropy (distinguishes heterogeneous vegetation from homogeneous water surfaces), IDM (measures texture homogeneity), and Inertia (highlights local intensity variations, particularly at edges and boundaries).

3. RESULTS AND CONCLUSIONS

KNN and RT produced inconsistent results due to the inherent randomness in the algorithms. RT's randomness could not be controlled in ArcPy, preventing reproducibility. The minimum accuracy for KNN ranged from 0.62 to 0.92, and for RT, it ranged from 0.47 to 0.88 in case of 60 layers for both vegetation coverages. These variations suggest that such inconsistency is unacceptable in regular field studies, where stable and reproducible results are crucial.

Very good results were achieved for areas with low V_C and good results for areas with high V_C (Fig. 1, Tables 1-2). Note that the F1 score formula does not account for True Negatives, which represent correctly classified negative instances (vegetation). This may lead to underestimation when vegetation is dominant. Calculating the F1 score with vegetation as the

Table 1
Vegetation coverage results*

	RGB [%]	RGB+HTE [%]	RGB+DEM [%]	RGB+HTE+DEM [%]
ML low V_C	6.7	19.2	16.4	16.5
SVM low V_C	22.3	**11.9**	12.5	12.5
ML high V_C	87.1	91.4	96.0	96.7
SVM high V_C	88.0	88.6	**80.7**	82.4

*The best results are bolded

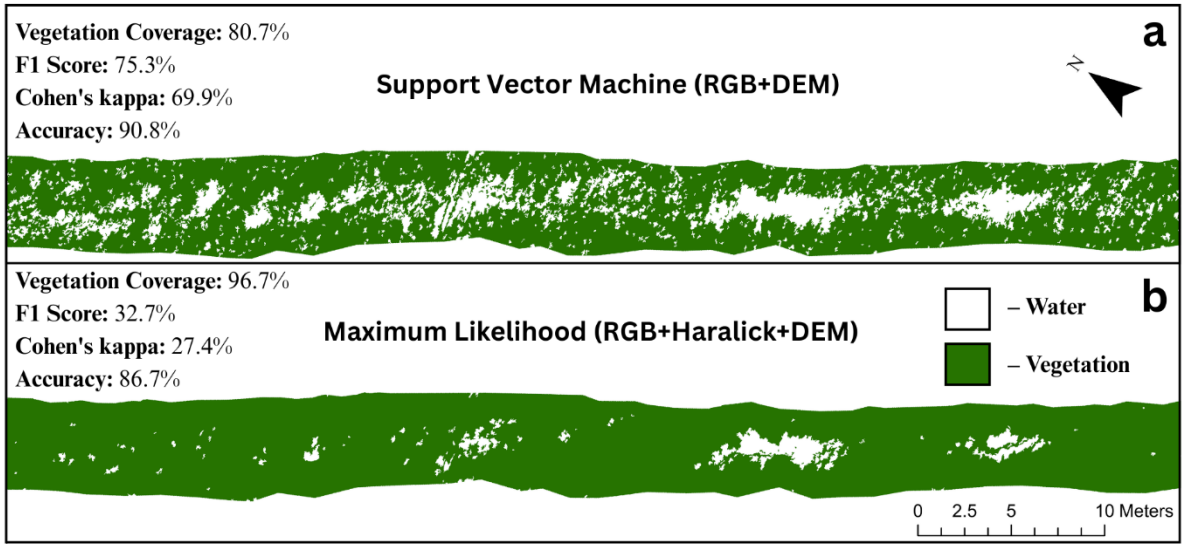

Fig. 1. Classification results showing the best (a) and worst (b) performance for high V_C.

Table 2
F_1 score results*

	RGB [%]	RGB+HTE [%]	RGB+DEM [%]	RGB+HTE+DEM [%]
ML low V_C	96.9	96.3	97.5	97.5
SVM low V_C	90.3	**98.4**	98.0	98.0
ML high V_C	65.7	61.3	36.0	32.7
SVM high V_C	50.7	57.1	**75.3**	74.4

*The best results are bolded

positive class and water as the negative class yielded a score of 94.7%. Overall, SVM performed better than ML in both cases, consistent with the findings of Pande-Chhetri et al. (2017) for wetlands and Szabó et al. (2024) for an oxbow lake.

Based on the results of this study, it can be concluded that using only an RGB camera enables satisfactory classification of aquatic vegetation in small rivers using a drone, with very good results for low vegetation cover and good results for high vegetation coverage.

Acknowledgements. This research was funded by the National Science Centre, Poland, grant number 2024/53/B/ST10/01460.

References

Haralick, R.M., K. Shanmugam, and I. Dinstein (1973), Textural features for image classification, *IEEE Trans. Syst. Man Cyb.* **SMC-3**, 6, 610–621, DOI: 10.1109/TSMC.1973.4309314.

Kalinowska, M.B., K. Västilä, M. Nones, A. Kiczko, E. Karamuz, A. Brandyk, A. Kozioł, and M. Krukowski (2023), Influence of vegetation maintenance on flow and mixing: case study comparing fully cut with high-coverage conditions, *Hydrol. Earth Syst. Sci.* **27**, 4, 953–968, DOI: 10.5194/hess-27-953-2023.

Pande-Chhetri, R., A. Abd-Elrahman, T. Liu, J. Morton, and V.L. Wilhelm (2017), Object-based classification of wetland vegetation using very high-resolution unmanned air system imagery, *Eur. J. Remote Sens*. **50**, 1, 564–576, DOI: 10.1080/22797254.2017.1373602.

Szabó, L., L. Bertalan, G. Szabó, I. Grigorszky, I. Somlyai, G. Dévai, S.A. Nagy, I.J. Holb, and S. Szabó (2024), Aquatic vegetation mapping with UAS-cameras considering phenotypes, *Ecol. Inform.* **81**, 102624, DOI: 10.1016/j.ecoinf.2024.102624.

Publications of the Institute of Geophysics, Polish Academy of Sciences
Geophysical Data Bases, Processing and Instrumentation
vol. 453 (E-14), 2025, pp. 115–117
DOI: 10.25171/InstGeoph_PAS_Publs-2025-057
XLII International School of Hydraulics, Radocza, Poland, 20–23 May 2025

Satellite-based Analysis of River Morphology and Riparian Vegetation Changes: Insights from the Vistula River Case Study

Raveena Raj NAGARAJAN and Michael NONES

Institute of Geophysics, Polish Academy of Sciences, Warsaw, Poland

✉ raveena.nagarajan@igf.edu.pl; mnones@igf.edu.pl

Abstract

Rivers continually alter their planform due to natural processes and human activities, affecting their morphology and the enclosing ecosystems. Understanding these changes is crucial for managing water resources, floods, and conservation efforts. In this study, we use satellite-derived indices, including Normalized Difference Vegetation Index (NDVI), Modified Normalized Difference Water Index (MNDWI), and Automated Water Extraction Index (AWEI), to assess sediment deposition, erosion, sinuosity variations, and riparian vegetation shifts over a 40-year period (1984–2024). Using Google Earth Engine, we analyze river morphology and vegetation changes, providing insights into environmental and anthropogenic influences on the Vistula River and its sub-reaches. This watercourse was selected for its historical significance and susceptibility to urban pressures, and to test the approach proposed here. Preliminary results reveal key trends in river morphology and vegetation dynamics, emphasizing the importance of remote sensing in large-scale river monitoring. This research contributes to broader efforts to understand climate-driven changes in river planforms, with future studies aiming to improve accuracy through higher-resolution data and field validation.

Keywords: Google Earth Engine, remote sensing, riparian vegetation, river morphology, sinuosity.

1. INTRODUCTION

The Vistula River, the largest river in Poland, has long been the subject of intensive geomorphological and hydrological research across its various valley reaches. Its dynamic fluvial system exhibits distinct morpho-dynamic patterns shaped by both natural processes and historical human interventions. Unlike many other European rivers, the Vistula has experienced a unique historical trajectory due to geopolitical influences, which continue to shape present-day fluvial processes and morphological characteristics, such as braided channels and island formations.

Traditionally, satellite imagery has been employed for tracking river morphological changes, but the advent of cloud-based geospatial analysis platforms like Google Earth Engine (GEE)

has revolutionized large-scale river system monitoring (Hansen et al. 2013). By enabling the efficient processing of extensive satellite datasets, GEE facilitates the detection of river meandering, sediment deposition, and erosion patterns across large spatial and temporal scales.

This study leverages GEE to examine river morphology changes and riparian vegetation dynamics along the Vistula River (Poland) while proposing a general framework for extending such analyses to global river systems. Using satellite-derived indices such as Normalized Difference Vegetation Index (NDVI), Modified Normalized Difference Water Index (MNDWI), and Automated Water Extraction Index (AWEI) (Tobón-Marín and Barriga 2020), the research quantifies sediment deposition, erosion patterns, and sinuosity variations over the period 1984–2024. The findings contribute to a broader understanding of river planform evolution and offer a methodological approach that can be applied to river systems worldwide.

2. MATERIALS AND METHODS

2.1 Study area and data pre-processing

The Vistula, Poland's longest river, spans around 1,047 km and drains an area of approximately 194,000 km², with more than half of its basin lying within Poland (Majewski 2013). Rising in the Carpathian Mountains at an altitude of 1,200 m a.s.l., it flows northward through major cities such as Kraków and Warsaw, ultimately emptying into the Bay of Gdańsk. This study employed Landsat (5, 7, and 8) satellite imagery from 1984 to 2024 to guarantee images for each year with extended coverage in the region. To delimit river surfaces, annual mosaics were created, combining multiple images of the same river covering the entire study period. Given that only Landsat images were used, the Simple Composite algorithm was leveraged, and the mosaics were created by taking the pixels with the lowest cloud content of all the images available in the selected period. To ensure high-quality images, a maximum cloud coverage threshold of 20% was imposed.

2.2 River delimitation and riparian vegetation

To assess river morphology and riparian vegetation dynamics, three satellite-derived indices were applied: MNDWI and AWEI for river surface delineation and NDVI for vegetation monitoring. The table below summarizes the formulas and purposes of each index.

Target	Index	Formula	Purpose	Reference
River delimitation	Modified Normalized Difference Water Index (MNDWI)	$\text{MNDWI} = \frac{\text{G} - (\text{SWIR}_1)}{\text{G} + (\text{SWIR}_1)}$	Enhances water detection by suppressing noise from built-up areas; improves contrast between water and land.	Xu 2006
	Automated Water Extraction Index (AWEI)	$\text{AWEI} = 4 \times (\text{G} - (\text{SWIR}_1)) - (0.25 \times (\text{NIR}) + 2.75 \times (\text{SWIR}_1))$	Improves water classification in shadowed/dark areas where traditional indices may underperform.	Feyisa et al. 2014
Riparian vegetation	Normalized Difference Vegetation Index (NDVI)	$\text{NDVI} = \frac{(\text{NIR} - \text{R})}{(\text{NIR} + \text{R})}$	Measures vegetation health and density. Applied only on dry, non-water pixels to assess greenness trends along riparian zones.	Petrakis et al. 2023

3. PRELIMINARY RESULTS AND FUTURE OUTLOOKS

Preliminary results indicate that satellite-derived indices are effective for monitoring long-term changes in large rivers like the Vistula. However, further validation using high-resolution satellite/aerial imagery and field data is needed. Key observations include:

- Sinuosity variations: changes in meandering intensity observed in some reaches, likely driven by hydrological shifts and climate change;
- Sediment dynamics: distinct erosion and deposition patterns have been detected, correlating with urban and agricultural developments and climate-related shifts in precipitation patterns;
- Riparian vegetation changes: NDVI trends suggest fluctuations in vegetation density, possibly due to land-use changes and climate variability.

Future work will enhance spatial accuracy using higher-resolution data, validate findings with field measurements, and expand the methodology to other global river systems. This will support the analysis of climate impacts on river sinuosity and sediment transport, contributing to adaptive river management strategies. Ultimately, we aim to develop a more comprehensive framework for understanding river planform dynamics under both natural and anthropogenic influences.

Acknowledgements. This study has been financed by NCN National Science Centre Poland – call SONATA BIS-13, Grant Number 2023/50/E/ST10/00261.

References

Feyisa, G.L., H. Meilby, R. Fensholt, and S.R. Proud (2014), Automated Water Extraction Index: A new technique for surface water mapping using Landsat imagery, *Remote Sens. Environ.* **140**, 23–35, DOI: 10.1016/j.rse.2013.08.029.

Hansen, M.C., P.V. Potapov, R. Moore, M. Hancher, S.A. Turubanova, A. Tyukavina, D. Thau, S.V. Stehman, S.J. Goetz, T.R. Loveland, A. Kommareddy, A. Egorov, L. Chini, C.O. Justice, and J.R.G. Townshend (2013), High-resolution global maps of 21st-century forest cover change, *Science* **342**, 6160, 850–853, DOI: 10.1126/science.1244693.

Majewski, W. (2013), General characteristics of the Vistula and its basin, *Acta Energetica* **2**, 6–23, DOI: 10.52710/ae.333.

Petrakis, R.E., L.M. Norman, and B.R. Middleton (2023), Riparian vegetation response amid variable climate conditions across the Upper Gila River watershed: informing Tribal restoration priorities, *Front. Environ. Sci.* **11**, DOI: 10.3389/fenvs.2023.1179328.

Tobón-Marín, A., and J. Cañón Barriga (2020), Analysis of changes in rivers planforms using Google Earth Engine, *Int. J. Remote Sens.* **41**, 22, 8654–8681, DOI: 10.1080/ 1431161. 2020.1792575.

Xu, H. (2006), Modification of normalised difference water index (NDWI) to enhance open water features in remotely sensed imagery, *Int. J. Remote Sens.* **27**, 14, 3025–3033, DOI: 10.1080/ 01431160600589179.

Publications of the Institute of Geophysics, Polish Academy of Sciences
Geophysical Data Bases, Processing and Instrumentation
vol. 453 (E-14), 2025, pp. 119–122
DOI: 10.25171/InstGeoph_PAS_Publs-2025-058
XLII International School of Hydraulics, Radocza, Poland, 20–23 May 2025

Modelling Impacts of Sediment Transport and Climate Change on Flood Hazard Zones

Tomasz DYSARZ

Poznan University of Life Sciences, Poznań, Poland

✉ tomasz.dysarz@up.poznan.pl

Abstract

The primary focus of the presented work is an analysis of the specific impacts on flood hazard maps developed for Polish conditions. Long-term sediment transport and climate change are considered. The computational methodology employed is based on geoprocessing, simulations, and automated computations. The results obtained underline the importance of both factors and indicate potential interrelations between them.

1. INTRODUCTION

The presented work is inspired by the implementation of the EU Flood Directive (EC 2007) in Poland (ISOK 2015). The flood hazard and risk maps were developed between 2011 and 2015 and between 2017 and 2020. From the first public release in 2015, the maps were examined in light of numerous uncertainties. However, other problems may be generated by non-stationarity of the natural processes. Firstly, the impact of climate change on precipitation needs to be mentioned. The second is sediment transport and associated morphodynamic changes of river beds, including deposition and erosion.

The presented work is based on two different analyses focused on the non-stationarity of flood hazard zones related to sediment transport and climate change. Although there are some differences in the time scale of the obtained results, this preliminary comparison enlightens the potential relationship between these two processes.

2. STUDY CASE: REACH OF THE WARTA RIVER

The selected reach shown in Fig. 1 is located in the lowland part of the Warta River course. The length of the reach equals 39 km. Downstream of Oborniki, there is the junction of the Warta and Wełna rivers. The gauge stations located along the Warta River are Oborniki and Wronki.

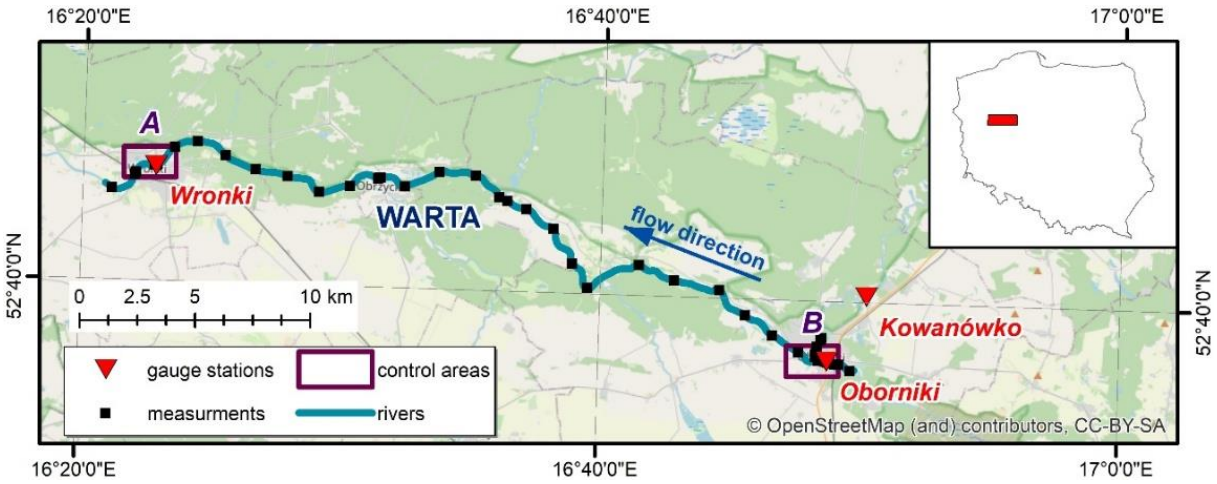

Fig. 1. Reach of the Warta River selected for tests.

In the tributary, there is Kowanowko (Fig. 1). For the presentation of the results, two control areas were chosen. These are denoted as A and B.

The risk of flooding is high in the Warta River valley and threatens mainly the three towns located along the reach: Oborniki, Obrzycko, and Wronki. The flood hazard maps were determined for the Warta River during the implementation of the EU Flood Directive (EC 2007).

3. MANAGEMENT OF SIMULATIONS

It was assumed that the applied procedures are consistent with the implementation of the EU Flood Directive. Due to this, the computations of water surface profiles in the selected reach were performed using a 1D model. In both cases, HEC-RAS was applied. Although there are different recommendations, the steady state module was used due to its simplicity. The maximum flows chosen for determining the flood hazard maps were 10-, 100-, and 500-year floods. In this case, attention is focused on a 100-year flood, reflecting a 1% probability of exceedance. Such an approach deeply depends on the elements being impacted, namely: (1) the configuration of the bed, and (2) the variability of precipitation that generates flow in the streams.

For the sediment transport simulations, two periods were assumed, 6 and 12 years, following the predicted update periods outlined in the EU Flood Directive. Thirty scenarios of each type were generated from historical data spanning the period 1971–2017. The bed sediment samples were collected along selected reaches of the Warta River to determine the average sample for simulations. Due to some stability issues detected in the computations, the number of tested transport formulas was limited to four: Meyer-Peter and Müller (MPM), Engelund-Hansen (EH), Toffaleti (Tof), and Wilcock-Crowe (WC) (Dysarz 2020). The simulations produced bed profiles applied in the computation of water surface profiles for given max flows. Based on computations, new flood hazard maps were generated and then compared with reference flood hazard maps.

The simulations of climate change are based on the Representative Concentration Pathways (RCP) of the Intergovernmental Panel on Climate Change (IPCC 2014). The historical data were used to generate nine scenarios of three different types: (1) neutral, denoted as None; (2) RCP4.5; and (3) RCP8.5 (IPCC 2014). The precipitation scenarios were processed using the SWAT + model to simulate the rainfall-runoff process. This step generated a synthetic series of data in selected gauge stations. The series were processed as real data and flood flows were calculated for each scenario. The next elements of the procedure were similar to the previous simulations. A 1D model was used to determine water surface profiles, and subsequently, flood hazard maps were developed.

4. RESULTS

In Fig. 2, the examples of obtained results are presented. The percentage of increases and decreases in the inundation areas is shown. The results are presented for the 12-year simulations of sediment transport (Fig. 2a) and climate change impacts (Fig. 2b).

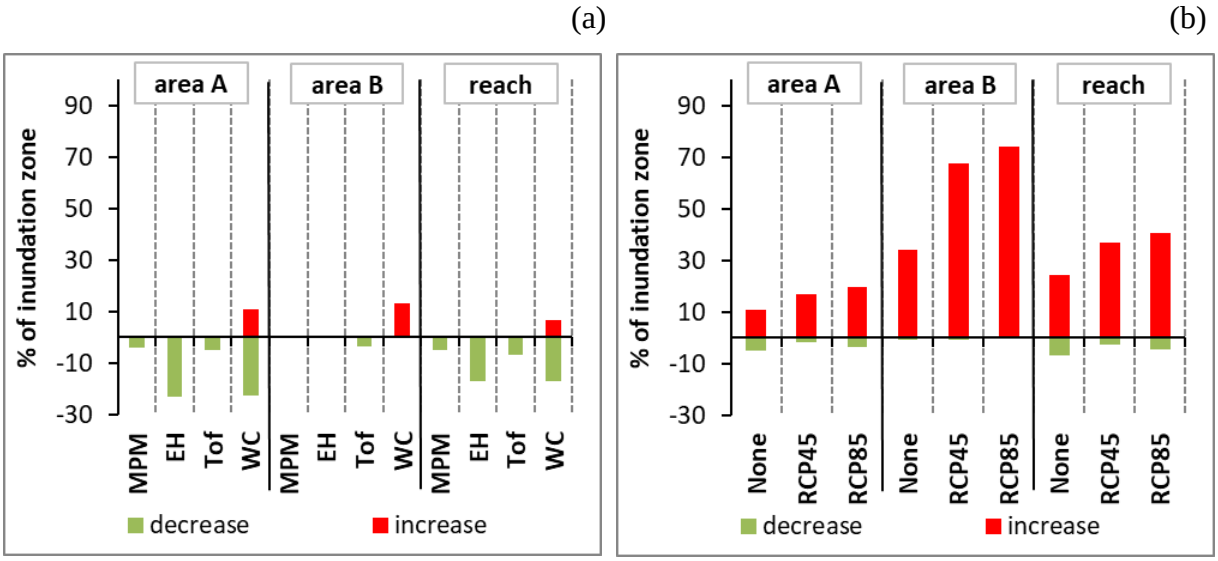

Fig. 2. Summary of sediment transport impacts on flood hazard zone in 12-year simulations (a) and climate change impacts (b). The results are shown for areas A, B, and the entire reach.

The important factor in the presented results is the range of changes. While the impact of climate change across the entire reach varies between –5% and 40%, the effect of sediment transport depends on the transport function, but generally changes between –17% and 7%. Even if the time horizons in both analyses differ, it must be taken into account that both processes occur in parallel and are interrelated.

5. CONCLUSIONS

The effects of sediment transport simulations are not unambiguous. Complex processes of channel bed transformations can cause fluctuations in the size of inundation zones. The climate change impact is clearer. In general, climate change increases the extent of the flood hazard, though decreases were observed in some scenarios. It becomes clear that sediment transport processes can significantly complicate any analysis of climate change impacts.

References

Dysarz, T. (2020), Development of methodology for assessment of long-term morphodynamic impact on flood hazard, *J. Flood Risk Manage.* **13**, 4, e12654, DOI: 10.1111/jfr3.12654.

EC (2007), Directive 2007/60/EC of the European Parliament and of the Council of 23 October 2007 on the "Assessment and management of flood risks", Official Journal of the European Communities, No. 288, Brussels.

IPCC (2014), Climate Change 2014: Synthesis Report. Contribution of Working Groups I, II and III to the Fifth Assessment Report of the Intergovernmental Panel on Climate Change [Core Writing Team; R.K. Pachauri and L.A. Meyer (eds.)], IPCC, Geneva, Switzerland, 151 pp.

ISOK (2015), IT system of the country's protection against extreme hazards, available from: http://www.isok.gov.pl/en (accessed: 10 June 2015).

Publications of the Institute of Geophysics, Polish Academy of Sciences
Geophysical Data Bases, Processing and Instrumentation
vol. 453 (E-14), 2025, pp. 123–123
DOI: 10.25171/InstGeoph_PAS_Publs-2025-059
XLII International School of Hydraulics, Radocza, Poland, 20–23 May 2025

Towards Sustainability in Water Distribution Networks

P. Amparo LÓPEZ-JIMÉNEZ

Hydraulic and Environmental Engineering Department, Valencia, Spain

✉ palopez@upv

Abstract

Today, it is crucial to fully understand the actions that water distribution network managers must take toward sustainability. Sustainable management in any activity related to the urban water cycle will be related to the responsible and efficient use and control of the network to meet current needs without compromising the ability of future generations to meet theirs. To this end, various actions are proposed to take the network from the line to the circle.

This entails shifting from linear management (where collection takes place at a specific point and wastewater is discharged at another) to management based on the circular economy, which allows the system to reuse water and (recoverable) energy through integrated resource management. This will entail optimization, sectorization, monitoring, and, above all, a path toward digitalization of the water distribution network (which, with the digital twin as the culmination of these actions, will allow managers to lead the water network toward maximum sustainability).

This vision towards more sustainable water distribution networks, particularly in the water urban circle answers to the need to confront the global water crisis and ensure a future with adequate access to water and sanitation for all. Therefore, the challenges and opportunities for achieving sustainability in these systems are immense. Many problems must be faced and solved: aging infrastructure, the impact of climate change, growing demand, and isolated management models.

To do so, the suggested actions include optimizing, sectorizing, monitoring, implementing energy actions, using renewable energy and implementing energy recovery techniques, and finally, making a strong commitment to digitalization. This is the that the managers of water distribution systems must take towards sustainability.

Publications of the Institute of Geophysics, Polish Academy of Sciences
Geophysical Data Bases, Processing and Instrumentation
vol. 453 (E-14), 2025, pp. 125–126
DOI: 10.25171/InstGeoph_PAS_Publs-2025-060
XLII International School of Hydraulics, Radocza, Poland, 20–23 May 2025

The September 2024 Flood – Hydrological Analysis, Infrastructure Performance, and Consequences

Marta BARSZCZEWSKA and Mateusz BALCEROWICZ

The State Water Holding Polish Waters, Warsaw, Poland

✉ marta.barszczewska@wody.gov.pl; mateusz.balcerowicz@wody.gov.pl

Abstract

In September 2024, southwestern Poland was struck by one of the most intense floods in recent years. The main causes of the disaster were prolonged, torrential rains that occurred between 13 and 15 September, with daily totals locally exceeding 300 mm—several times above multi-month precipitation norms. The flood primarily affected the Odra River basin, and the resulting flood wave caused alarm levels to be exceeded on numerous water-courses. Retention reservoirs and dry polders played a key role in flood mitigation, including the Racibórz Dolny reservoir, the Buków polder, and the cascade of reservoirs on the Nysa Kłodzka River, which collectively retained significant volumes of flood-water, helping to prevent more severe damage in cities such as Wrocław.

Despite these efforts, the flood had serious consequences: 9 fatalities, more than 238,000 people affected, estimated damages exceeding PLN 13 billion, and widespread destruction of infrastructure. The flood had fluvial and pluvial characteristics and was accompanied by failures of hydrotechnical infrastructure. In most cases, the extent of flooded areas corresponded to zones outlined on flood hazard maps; however, in some locations (e.g., Głuchołazy, Stronie Śląskie), events occurred beyond previously anticipated scenarios. The findings from this analysis will inform the update of the flood risk assessment as part of the third planning cycle.

1. INTRODUCTION

In September 2024, southwestern Poland was affected by one of the most extensive and intense flood events in recent years. The phenomenon included fluvial, pluvial, and partly technogenic flooding due to failures of hydrotechnical structures. This event constitutes an important reference point for future flood risk assessments in Poland and demonstrates both the capabilities and limitations of the current flood protection infrastructure under extreme conditions.

2. METEOROLOGICAL AND HYDROLOGICAL CONDITIONS

The flood was caused by torrential rainfall associated with Mediterranean low-pressure systems that brought extreme daily precipitation totals between 13 and 15 September, locally exceeding 200 mm. Monthly precipitation norms were exceeded several times in many locations – e.g., by over 450% in Jelenia Góra. As a result, water levels on rivers rose rapidly, triggering multiple instances of alarm level exceedances and fast-moving flood waves across the Odra and Vistula basins.

2.1 Flood dynamics

The peak of the flood activity occurred between 14 and 18 September. On 16 September, a record number of alarm level exceedances was recorded (81 locations in the Odra basin). The flood wave then propagated downstream, reaching successive towns and causing local inundations and damage. Notably, the peak flow of the Odra River did not coincide with the peaks of its tributaries, which helped reduce the flood risk in the Wrocław area.

3. ROLE OF FLOOD PROTECTION INFRASTRUCTURE

Flood protection reservoirs played a key role in mitigating the impact. The Racibórz Dolny reservoir retained 147 million m³ of water (197 million m^3 of water including the Buków reservoir), while the cascade of reservoirs on the Nysa Kłodzka (Topola, Kozielno, Otmuchów, Nysa) collectively stored about 155 million m³. Additional support came from dry reservoirs (e.g., Buków, Stronie Śląskie) and six polder systems (e.g., Blizanowice-Trestno, Oławka). The coordinated operation of this infrastructure significantly limited the impact of the flood wave and reduced the threat to downstream urban areas.

4. IMPACTS AND DAMAGE

According to government estimates, total losses exceeded PLN 13 billion. The flood claimed 9 lives, affected more than 238,000 people, and led to the evacuation of nearly 4,500 residents. A total of 10,522 residential buildings and 814 socially significant facilities were inundated. Over 3,600 km of roads, 229 bridges and 1,823 culverts were damaged. Failures were also reported in the hydrotechnical infrastructure, particularly in the Stronie Śląskie and Topola reservoirs.

5. THE 2024 FLOOD AND FLOOD HAZARD MAPS

A comparative analysis of the actual flood extent versus existing flood hazard maps showed high predictive accuracy – in most cases, the inundated areas corresponded to 1% (1-in-100-year) or 0.2% (1-in-500-year) probability scenarios. Deviations were observed mainly in areas affected by infrastructure failures (e.g., Morawka, Biała Lądecka) or exceptional rainfall (e.g., Głuchołazy, Jelenia Góra).

6. CONCLUSIONS

The September 2024 flood revealed both the effectiveness and the limitations of current flood protection systems in Poland. The data and observations from this event are crucial for updating the Preliminary Flood Risk Assessment (PFRA), flood hazard and risk maps (FHRM), and for developing improved emergency management scenarios. The flood confirmed the urgent need for further modernization of hydrotechnical infrastructure, enhancement of early warning systems, and strengthening of community flood resilience.

Publications of the Institute of Geophysics, Polish Academy of Sciences
Geophysical Data Bases, Processing and Instrumentation
vol. 453 (E-14), 2025, pp. 127–129
DOI: 10.25171/InstGeoph_PAS_Publs-2025-061
XLII International School of Hydraulics, Radocza, Poland, 20–23 May 2025

Urban Resilience to Floods: Real Challenges and Misleading Myths

Corrado GISONNI

Dipartimento di Ingegneria – Università della Campania "Luigi Vanvitelli", Aversa (CE), Italy

✉ corrado.gisonni@unicampania.it

A b s t r a c t

Flooding is one of the most challenging weather-induced risks in urban areas, due both to the typically high exposures in terms of people, buildings and infrastructures, and to the uncertainties lying in the modelling of the involved physical processes.

In the last decades, European cities are increasingly facing challenges associated with urban sustainability and urban water issues.

Floods are normally a consequence of extreme rainfall events, but they can also happen because of infrastructure failures. Climate change also leads to flood risk increase, due to hydrological alterations, including changing patterns of precipitation and rising sea levels.

Hazard and risk assessment is an essential issue in the reduction of adverse effects of extreme events. Here, the term "hazard" refers to the occurrence probability of a potentially damaging event, while the term "risk" refers to the extent of consequent damages and losses. Several procedures, less or more detailed, are available in scientific literature for the assessment of hazard and risk maps, in most cases designed to provide maps or charts from the combination of probabilistic analysis of historical records and geographic information knowledge. In many countries, standard procedures are also available, mainly for planning purposes.

The European Directive 2007/60/EC (Flood Directive) establishes the framework for the assessment and the management of flood risks. A crucial tool for the achievement of these objectives is the preparation of flood hazard and flood risk maps. This activity calls for an active involvement of all the stakeholders in developing flood risk management plans.

1. INTRODUCTION

Catastrophic floods and devastating hydrological phenomena have been systematically hitting the Old Continent in recent decades, causing enormous impacts in terms of number of victims and financial losses.

The European Union (EEA 2022) states that hydrometeorological events are responsible for approximately two-thirds of the damage caused by natural disasters since the 1980s.

The numbers are impressive when we concentrate on Floods and Mudflows, as confirmed by the records available from the International Disaster Database (Centre for Research on the Epidemiology of Disasters, CRED, Université Catholique de Louvain – UCL, Brussels, Belgium; http://www.emdat.be):

- during the last century, the total amount of estimated economic losses is larger than five hundred billion Euro;
- during the same period, almost thirty million persons have been affected by destructive hydrological events, with more than twenty-nine thousand fatalities;
- a definite trend shows a significant increase of the number of events per year over the last decades.

On October 23, 2007, the European Parliament approved the so-called "Floods Directive" 2007/60/CE (hereafter referred to as the FD), aiming to regulate the procedures for the Hydraulic Risk assessment within the borders of the EU member States. The implementation process of the FD involves 27 Countries and 110 River Basin Districts (RBDs), including 40 transnational and eight extra-continental districts.

2. RISK ASSESSMENT

According to the UNISDR (2017), Risk *R* is the probability that a negative outcome will affect people, systems, or assets. The risk results from the combination of Hazard *H*, Exposure *E*, Vulnerability *V*, and capacity *C*, according to the following relationship:

$$R = \frac{H \times E \times V}{C} \tag{1}$$

where:

- *H* is the probability of occurrence of a potential source of harm, such as an extreme hydrological event;
- *E* consists of possible threats in terms of people, infrastructure, and other assets;
- *V* is the likelihood of an element being harmed by an event of a certain intensity;
- *C* represents how well a system or community can withstand a hazard.

The adverse impacts of hazards, especially for hydrogeological events, are often not fully prevented, but their severity can be significantly reduced by various strategies and actions. Engineering techniques and hazard-resistant construction are among the measures that can be implemented to prevent damage; these measures are as important as the improvement of environmental and social policies and raising public awareness. In general, the term "mitigation" is extensively used in climate change policy, and refers typically to the reduction of greenhouse gas emissions that are the source of climate change; for the case of the urban flood risk, the term "adaptation" measures is certainly more appropriate.

The assessment of flood risk in urban areas cannot neglect the so-called the "underlying risk drivers" (i.e. increasing levels of exposure and vulnerability and/or decreasing capacity) that may significantly influence the level of disaster risk (Fig. 1a).

Indeed, several dangerous situations persist due to either uncontrolled urbanization (Fig. 1b) or wrong design of urban hydraulic infrastructure. The destructive effects of these anthropogenic factors can be demonstrated through some study cases.

Actually, the state of implementation of the FD is quite heterogeneous among the various the EU member states, often presenting different methodologies and approaches to assess hazard levels, with particular reference to urban areas.

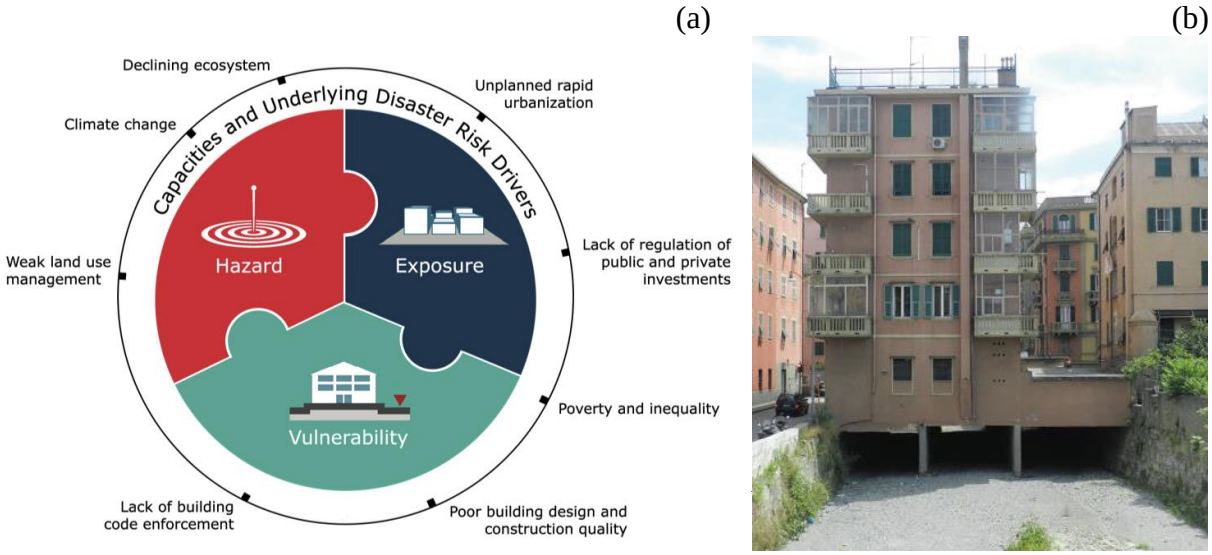

Fig. 1: (a) Components concurring to flood risk assessment (UNISDR 2017); (b) Building obstructing the Chiaravagna Torrent and provoking severe urban flooding in the city od Sestri Ponente (Liguria, Italy) on October 4, 2010.

3. HYDRAULIC HAZARD IN URBAN CONTEXTS

In urban areas, the highest levels of hazard are due to the impact of a flood stream on people, according to two different categories: (i) *direct* exposure, i.e. instability of a person impacted by the flow, and (ii) *indirect* exposure, i.e. effects of drifters (such as vehicles or urban/household furniture) washed away by large floods and investing persons or provoking blockages at bridges, culverts, and urban drainage infrastructures.

This invited lecture aims to propose the state of the art of different criteria, based on recent research findings, that should be considered to evaluate the hydraulic hazard/risk in anthropized environment.

Nowadays, there is still a lack of standardization between countries in terms of assessing flood hazard in urban contexts. Moreover, the procedures for flood hazard assessment for pedestrians are not updated to the latest available methods; in some cases, this aspect is even completely ignored.

Based on the available data, it is possible to conclude that the recent increase of urban flooding events is *probably* determined by the evolution of the climate, but it *certainly* depends on anthropogenic factors directly or indirectly linked to the use of land and water.

References

EEA (2022), Economic losses from weather- and climate-related extremes in Europe, European Environment Agency, available from: https://www.eea.europa.eu/ims/economic-losses-from-climate-related.

UNISDR (2017), National disaster risk assessment, United Nations Office for Disaster Risk Reduction, available from: https://www.unisdr.org/files/52828_nationaldisasterriskassessmentwiagu.pdf.

Publications of the Institute of Geophysics, Polish Academy of Sciences
Geophysical Data Bases, Processing and Instrumentation
vol. 453 (E-14), 2025, pp. 131–131
DOI: 10.25171/InstGeoph_PAS_Publs-2025-062
XLII International School of Hydraulics, Radocza, Poland, 20–23 May 2025

Is the River Health Concept Useful for Water Management Purposes?

Tomasz OKRUSZKO

Warsaw University of Life Sciences, Warszawa, Poland

✉ Tomasz_Okruszko@sggw.edu.pl

A b s t r a c t

The term "river health" was introduced at the end of the second millennium and applied to assessing river conditions. It was seen as analogous to human health, offering the general public a better understanding of ecological challenges in freshwater systems. However, it was unclear how rivers' physical, chemical, and biological characteristics may be integrated into conservation or restoration measures. In this respect, other definitions closer to water management purposes sound more appealing, e.g., a healthy river ecosystem is one "that is sustainable and resilient, maintaining its ecological structure and function over time while continuing to meet societal needs and expectations". In the EU context, the similarity, in a sense, but focused on the river term "good ecological status", has been defined and forms a central point of the Water Framework Directive.

For water management purposes, the ecological concepts and water-related services are broken down into indicators to assess and compare different rivers, showing their status and need for conservation or improvement. In most cases, ecologists divide river assessment methods into indicator species or comprehensive index methods. Indicator species methods include fish, phytoplankton, and macroinvertebrates as target objects to assess the quality of a river ecosystem. Comprehensive index methods use indicators combining river physical, chemical, and biological characteristics with socio-economic data. This reflects the river habitat and biota condition, the social and/or economic function, or pressures on the system.

There is a standard agreement that indicators have a fundamental technical basis in science, supporting their usage in decision-making. However, the criteria used in interpreting indicator values (good, bad, acceptable, unacceptable, etc.) are likely to go beyond scientific grounds and, in many cases, are ultimately socially determined. As water management professionals, we are challenged by a lack of acceptance or obstruction for scientifically based good ecological or sustainable resource targets. It means that for communication purposes, this intuitively easy-to-quantify term (healthy river, unhealthy river, etc.) has great potential and can be adopted for water management planning or operating hydraulic structures.

Publications of the Institute of Geophysics, Polish Academy of Sciences
Geophysical Data Bases, Processing and Instrumentation
vol. 453 (E-14), 2025, pp. 133–133
DOI: 10.25171/InstGeoph_PAS_Publs-2025-063
XLII International School of Hydraulics, Radocza, Poland, 20–23 May 2025

Workhorse Proteus ADCP
Your Instrument for the Changing Ocean

Mikołaj WYDRYCH

Teledyne RD Instruments, Warsaw, Poland

✉ mikolaj.wydrych@teledyne.com

A b s t r a c t

Acoustic Doppler Current Profilers (ADCPs) measure the relative velocity between the instrument and a group of scatterers in the water column by transmitting acoustic pulses along multiple beams that point in different directions and measure the Doppler shift of the acoustic signal that is scattered back towards the instrument in each beam. There exists a large and diverse set of applications for ADCPs—each of the applications can benefit from different instrument configurations and tradeoffs; this tradespace can, at a high level, be partitioned into the following variables: size, power, range, variance, resolution, accuracy, and features. A new Doppler-sonar platform called Proteus has been developed, with the objective to expand the existing ADCP tradespace. Several new improvements and features have been introduced in this platform, including reduced size, reduced power consumption, configurable transmit power, frequency agility, linear IQ data, and an integrated attitude and heading reference system (AHRS), to name a few. A new Workhorse Proteus line of ADCPs, built on the Proteus platform, inherit the data-quality, reliability, and many other aspects of the trusted legacy Workhorse while leveraging the latest in technology. Test results are available, demonstrating the improvements and new features of the 300 kHz Workhorse Proteus ADCP.

Publications of the Institute of Geophysics, Polish Academy of Sciences
Geophysical Data Bases, Processing and Instrumentation
vol. 453 (E-14), 2025, pp. 135–135
DOI: 10.25171/InstGeoph_PAS_Publs-2025-064
XLII International School of Hydraulics, Radocza, Poland, 20–23 May 2025

Preliminary Laboratory Studies to Quantify the Effect of Plant Branches on Longitudinal Dispersion

Finna FITRIANA, Virginia STOVIN, and Ian GUYMER

University of Sheffield, Sheffield, UK

✉ ffitriana1@sheffield.ac.uk; v.stovin@sheffield.ac.uk; i.guymer@sheffield.ac.uk

Abstract

Many studies investigating hydrodynamics and mixing in vegetated channels simplify vegetation by modelling stems (e.g., reeds) as arrays of cylinders. This study explores more realistic plant geometries, which include stems, branches, and leaves, through solute tracing experiments. Experiments were conducted in a 12.5 m long, 300 mm wide flume using various plant configurations (Fig. 1), and longitudinal dispersion coefficients (D_x) were determined over a range of velocities (u) (Fig. 2). The results confirm the linear relationship between D_x and u and quantify the increase in dispersion caused by the plant branches.

(a) (b) (c) (d) (e)

Fig. 1. Plant models used in the experiments: (a) 6 branches, (b) 4 branches, (c) 2 branches, (d) single stem (d), and (e) 8 mm cylinder.

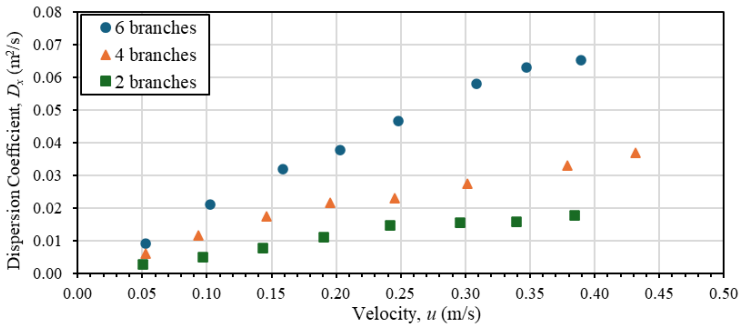

Fig. 2. Variation of the longitudinal dispersion coefficient with velocity for different plant models.

Publications of the Institute of Geophysics, Polish Academy of Sciences
Geophysical Data Bases, Processing and Instrumentation
vol. 453 (E-14), 2025, pp. 137–137
DOI: 10.25171/InstGeoph_PAS_Publs-2025-065
XLII International School of Hydraulics, Radocza, Poland, 20–23 May 2025

The Effect of the Choice of Model Calibration Procedure on the Projection of Lake Surface Water Temperatures for Future Climatic Conditions

Jarosław J. NAPIÓRKOWSKI, Adam P. PIOTROWSKI, Marzena OSUCH, and Emilia KARAMUZ

Institute of Geophysics, Polish Academy of Sciences, Warsaw, Poland

✉ jnn@igf.edu.pl; adampp@igf.edu.pl; marz@igf.edu.pl; emikar@igf.edu.pl

Abstract

This study investigates the influence of the calibration procedure on projections of surface water temperature in lowland lakes using the air2water model, which relies exclusively on daily air temperature as input. The analysis encompasses 22 Polish lowland lakes in the temperate climate zone, with surface areas ranging from 1.5 km^2 to 115 km^2, and maximum depths ranging from 2.5 m to 70 m. Projections were derived using 14 EURO-CORDEX climate models and 12 optimization algorithms.

Lake surface water temperature and daily air temperature observations for the period 1987–2016 were used for model calibration and validation. Future air temperature time series (2006–2100) from 14 climate models were applied to project future lake surface water temperatures under the RCP8.5 emission scenario.

Results indicate that the projected lake water temperatures highly depend on the calibration method used for a specific model. The differences in mean monthly surface water temperatures under future climate conditions can exceed 1.5°C for small, deep lakes, while for shallow and relatively large lakes, differences are typically lower than 0.6°C for each month. The most pronounced differences occur in winter and in early summer periods that are crucial for aquatic biota. Among the optimization algorithms that resulted in the most significant differences were those that fit historical data well and those that did not reproduce historical data adequately. Therefore, high performance of historical data does not guarantee reliable predictions of future conditions.

"Publications of the Institute of Geophysics, Polish Academy of Sciences: Geophysical Data Bases, Processing and Instrumentation" appears in the following series:

A – Physics of the Earth's Interior

B – Seismology

C – Geomagnetism

D – Physics of the Atmosphere

E – Hydrology (formerly Water Resources)

P – Polar Research

M – Miscellanea

Every volume has two numbers: the first one is the consecutive number of the journal and the second one (in brackets) is the current number in the series.